COLLEGE OF NATURAL AND COMPUTETIONAL SCIENCES

CENTER FOR ENVIRONMENTAL SCIENCE

DEVELOPMENT OF MICROFLUIDIC PAPER BASED ANALYTICAL DEVICES (μ-PAD) FOR THE DETERMINATION OF ORGANOPHOSPHATE AND CARBAMATE PESTICIDES FROM ENVIRONMENTAL SAMPLES

PhD DISSERTATION

BY

SHELEME BESHANA TESEMMA

JUNE, 2023

ADDIS ABABA, ETHIOPIA

DEVELOPMENT OF MICROFLUIDIC PAPER BASED ANALYTICAL DEVICES (μ-PAD) FOR THE DETERMINATION OF ORGANOPHOSPHATE AND CARBAMATE PESTICIDES FROM ENVIRONMENTAL SAMPLES

A DISSERTATION SUBMITTED TO THE CENTER FOR ENVIRONMENTAL SCIENCE COLLEGE OF NATURAL AND COMPUTATIONAL SCIENCES ADDIS ABABA UNIVERSITY IN PARTIAL FULFILLMENT OF THE REQUIREMENTS FOR THE DEGREE OF DOCTOR OF PHILOSOPHY IN ENVIRONMENTAL SCIENCE

By

SHELEME BESHANA TESEMMA

JUNE, 2023

ADDIS ABABA, ETHIOPIA

Addis Ababa University

College of Natural and Computational Sciences

Center for Environmental Sciences

As members of the Examining Board of the final PhD open defense, we certify that we have read and evaluated the Dissertation prepared by Sheleme Beshana Tesemma entitled:

"**DEVELOPMENT OF MICROFLUIDIC PAPER BASED ANALYTICAL DEVICES (μ-PAD) FOR THE DETERMINATION OF ORGANOPHOSPHATE AND CARBAMATE PESTICIDES FROM ENVIRONMENTAL SAMPLES"** and recommend that it be accepted as fulfilling the Dissertation requirement for the Degree of Philosophy in Environmental Science, complies with the regulation of the university and meets the accepted standards with respect to originality and quality.

Dr. Ahmed Hussen (PhD, Assoc. Prof)	_____	27/02/2023
Major Advisor	Signature	Date
Prof. Seyoum Leta (PhD)	_____	27/02/2023
Co-advisor	Signature	Date
Prof. Takashi Kaneta (PhD)	_____	27/02/2023
Co-advisor	Signature	Date
Dr. Abera Gure Tufa (PhD, Assoc.Prof)	_____	27/02/2023
External Examiner	Signature	Date
Prof. Dejene Ayele (PhD)	_____	27/02/2023
Internal Examiner	Signature	Date

STATEMENT OF THE AUTHER

This dissertation is my original work and all sources and materials used for this dissertation have been duly acknowledged. The dissertation has been submitted as a fulfillment of a PhD Degree at Addis Ababa University, College of Natural and Computational Science, Center for Environmental Sciences and is deposited at the University's Library to be made available to borrowers under rules of the Library. This work has not been submitted, in whole or in part, in any previous application for the award of any academic degree, diploma, or certificate.

Name: Sheleme Beshana Tesemma

Signature_____

College of Natural and Computational Sciences, Center for Environmental Sciences

Date of Submission: _____

ABSTRACT

This thesis focuses on the development of microfluidic paper-based analytical devices (μ-PADs) and sample preparation techniques, namely dispersive liquid-liquid microextraction (DLLME) and the combination of QuEChERS (quick, easy, cheap, effective, rugged, and safe) with DLLME for colorimetric determination of organophosphate (OP) and carbamate (CM) pesticides from water and lettuce samples. In the colorimetric quantification, the yellow color is generated by the interaction between acetylcholinesterase (AChE), acetylthiocholine iodide (ATChI), and 5, 5- dit hiobis- (2-nitrobenzoic acid) (DTNB). The digital image of the yellow color was captured and analyzed using a Canon scanner and ImageJ software, respectively. Key experimental conditions (concentrations and volumes of AChE, ATChI, and DTNB, incubation time, storage stability, and image capturing time) were systematically optimized using a univariate approach. Under optimized conditions, the method showed a wide linear range (1-16 mg L^{-1}), repeatability (3-5% RSD), and intermediate precision (7-10% RSD), and robustness (≤ 1.85% RSD), with $R^2 \geq 0.9945$. Limits of detection (LOD) were in the range of 0.24-0.33 mg L^{-1}. An acceptable mean recovery (87-94%) was observed at a 1 mg L^{-1} fortification level. Following that, the μ-PAD operational parameters (reagent concentrations and volumes) were optimized using multivariate techniques based on the Box-Behnken design (BBD). The analysis of variance revealed that high regression and fitting values were obtained between the experimental and predicted responses at a 95% confidence level. Satisfactory linearity ($R^2 \geq 0.9990$) in the range of 0.5-16 mg L^{-1}, LOD (0.12-0.17 mg L^{-1}), repeatability (3.75-7.98% RSD), intermediate precision (7.15-10.98% RSD), and accuracy (78-97%) were achieved. The results of the univariate and multivariate optimization were compared and found that the multivariate optimization requires a much lower concentration of the reagents and improved LOD values of the univariates by 29-64% for the studied pesticides.

Therefore, the multivariate approach has been demonstrated to be more efficient and effective than the univariate approach. For further improving sensitivity, the µ-PAD was coupled with an enrichment method called DLLM. The experimental parameters (volume of hexane and acetone, extraction time, and salt amount) were optimized using response surface methodology (RSM). The enrichment factors (EF) and LOD values were found in the range of 317-1471 and 0.17-0.41 µg L^{-1}, respectively, which is below the maximum residue limits of EU for drinking water. The matrix-matched calibration curve showed a wide linear range (0.625-40 µg L^{-1}) with $R^2 \geq 0.9968$. The obtained extraction recovery varied from 79-97% with repeatability (2.21-6.01% RSD) and intermediate precision (5.60-10.41% RSD). Thus, the proposed method is low cost, easy to operate, efficient, and sensitive, showing great potential for the determination of pesticides in water samples. Finally, the combination of QuEChERS, DLLME, and a µ-PAD was developed for the extraction, preconcentration and quantification of target analytes from lettuce samples, respectively. RSM using Plackett-Burman and central composite design were used for the screening and optimization of significant factors, respectively. The matrix-matched calibration curves held excellent linearity ($R^2 \geq 0.9988$) in the range of 0.01-0.64 mg kg^{-1}. The EFs and LODs were 21-31 fold and 0.006-0.009 mg kg^{-1}, respectively. The recoveries were in the range of 79-97% and good precision was obtained with RSD below 11%. Thus, the experimental results revealed that the QuEChERS-DLLME method is suitable for the routine pesticides analysis from lettuce vegetables in terms of high accuracy, precision, and efficiency.

Keywords: Acetylcholinesterase, Pesticides, Mean color intensity, Microfluidic paper-based anal ytical devices, Dispersive liquid- liquid microextraction, Box-Behnken design, Inhibition percent, Response surface methodology, QuEChERS

ACKNOWLEDGMENTS

The pursuit of a Ph.D is one of the most ambitious goals I have ever undertaken. The past several years have been a period of intense scientific, intellectual, and personal growth for me; I have learned in equal measures new technical skillsets, how to conduct scientific research, and much about who I am as a person and who I want to be. Through this endeavor I have had the pleasure to meet and work with a number of outstanding people who have contributed both to my success and enjoyment within the program.

The first and foremost person to be acknowledged would be my supervisor, Dr. Ahmed Hussen for giving me this opportunity to do research under his guidance on the microfluidic paper-based analytical device. He was a constant source of inspiration and encouragement throughout my Ph.D study. He gave me enough freedom and supported me throughout the research and academic endeavors, I have taken during these years, which helped me to expand my skills and experiences. Special thanks to my second supervisor Prof. Seyoum Leta and third supervisor Prof. Takashi Kaneta for the opportunity given to work with them and for their constant support through discussions and suggestions. I would also like to express my thanks to Dr. Teshome Tolcha for the help and support he has given me during these years.

I would like to thank Addis Ababa University for financial support through a thematic research project, entitled “Developing Innovative Microfluidic Paper-Based Analytical Devices: Viable solution for Environmental Monitoring in Ethiopia” (Project No. VPRTT/PY-021/2018/10). My sincere thanks go to North Shewa Zone Administration (Oromia) for the financial support to pursue post-graduate studies.

I also would like to thank all staff members of the Center for Environmental Science, and all of my friends for their unreserved knowledge sharing, cooperation, and encouragement. My sincere gratitude should also go to Prof. Teshome Soromessa, Dr. Andualem Mekonnon, Dr. Tadesse Alemu, Mr. Temesgen Aragaw, Mrs. Mingizem Tesfaye, Mrs. Kidist Shiferaw, Mrs. Eyerusalem Shewarega, Mr. Dejene Tsegaye, and Mrs. Ayelech Gemechu.

My acknowledgement also goes to Dr. Tekletsadik Reba, Mr. Solomon Mekonnon, Mr. Tamam Hussen, Mrs. Mezgebe Abebe, Dr. Feyisa Girma, Dr. Eshetu Lema, Mr. Tamrat Selamu, Mr. Tesfaye H/Mariam, Mr. Tewodros Amsalu, Mr. Hirpha Tesema, Mrs. Israel Habtu, Mr. Habtamu Bekele, and Mr. Habtamu Giddisa for their encouragement throughout this work.

Lastly, I would like to express my deepest gratitude and appreciation to my beloved parents. So for my family, I want to say I love you so much and thank you for encouraging me in all of my pursuits and inspiring me to follow my dreams. My dear parent; Mrs. Abesha Tesema, my sisters and brothers; Mrs. Tsehay Beshana, Mrs. Zewuditu Beshana, and Baharu Beshana are much acknowledged. Special thanks to my wife; Abebech Demise and my son Eban Sheleme, without your love and support I would not be the person I am today. I love you very much.

TABLE OF CONTENTS

CONTENTS

LISTS OF TABLE

LISTS OF FIGURES

LIST OF ANNEX

Annex **Page**

LIST OF ABBREVIATIONS AND ACRONYMS

AChE	Acetylcholinesterase
AKD	Alkyl ketene dimer
ANOVA	Analysis of variance
ATChI	Acetylthiocholine iodide
BBD	Box-Behnken design
BSA	Bovine serum albumin
CCD	Central composite design
CE	Capillary electrophoresis
CL	Chemiluminescence
CM	Carbamate pesticide
CMYK	Cyan, Magenta, Yellow, Key
CR	Cross reactivity
DARPA	Defense advanced research projects agency
DI-SDME	Direct immersion single-drop microextraction
DI-SPME	Direct immersion solid-phase microextraction
DLLME	Dispersive liquid–liquid microextraction
DMPC	Dynamic mask photo curing
DOE	Design of experiment
dSPE	Dispersed solid phase extraction
DTNB	5, 5 dithiobis-(2-nitrobenzoic acid)
EC	European Commission

EF	Enrichment factor
ELISAs	Enzyme-linked immunosorbent assays
EU	European union
GC	Gas chromatograph
GCB	Graphitized carbon black
GC-MS	Gas chromatography-mass spectrometry
HF-LPME	Hollow fiber liquid-phase microextraction
HPLC	High-performance liquid chromatography
HS-SPME	Head space solid-phase microextraction
HSV	Hue, Saturation, Value
JPEP	Joint photographic experts group
LC	Liquid chromatography
LC-TMS	Liquid chromatography-tandem mass spectrometry
LLE	Liquid-liquid extraction
LOD	Limit of detection
LPME	Liquid-phase Microextraction
MRLs	Maximum residual limits
PBD	Plackett-Burman design
PDMS	Polydimethylsiloxane
POC	Point-of-care
PON	Point-of-need
PSA	Primary secondary amine

QuEChERS	Quick, easy, cheap, effective, rugged and safe
RGB	Red, Green, Blue
ROI	Region of interest
RSD	Relative standard deviation
RSM	Response surface methodology
SDME	Single-drop microextraction
SPE	Solid-phase extraction
SPME	Solid-phase microextraction
UHPLC–TMS	Ultra high performance liquid chromatography coupled with tandem mass spectrometry
µ-PAD	Microfluidic paper based analytical device
WHO	World Health Organization

1. INTRODUCTION

1.1. Background of the Study

A pesticide is a chemical substance used to control pests and diseases by repelling, preventing, destroying, or reducing damage caused by pests to boost modern agricultural production (Pang et al., 2016; Sharifzadeh et al., 2018). Pests can be pathogens of plants, insects, birds, mammals, weeds, mollusks, nematodes, and microbes that compete with humans for food, destroy property, spread or transmit disease. Pesticides are classified by their chemical class into organochlorines, organophosphate (OP), carbamates (CM) and pyrethroids (Nerın et al., 2002; Pandey et al., 2010). Among these classes, OP and CM account for approximately 70% of total pesticide application (Chen et al., 2009; Pundir and Malik, 2019; Shelton et al., 2014). Almost 90% of all pesticides are used in the agricultural sector, with the rest used in non-agricultural sectors including industry, commerce, government, home and garden (Atwood and Paisley-Jones, 2017). Unfortunately, the amount of applied pesticides that reach the target pests is 0.1%. The remaining 99% have serious impacts on public health and beneficial biota via soil, water and air contamination (Guillette and Iguchi, 2012; Pimentel, 1995; Schwarzenbach et al., 2006).

The use of pesticides in Ethiopia to control crop pests can be traced back to the mid-1940s when arsenic was used to control desert locusts. The use of agricultural inputs, including pesticides, was introduced in the 1960s through an agricultural advisory system for smallholders. Since then, the use of pesticides has been gradually increasing the import of various types of pesticides by about 3346.32 tons (Assefa, 2011) and with the development of the current floriculture sector, the average import of pesticides exceeds 2400 tons per year (Teklu, 2016).

The toxic mechanisms of OP and CM are based on the inhibition of acetylcholinesterase (AChE) in insects, fish, birds, and mammals, allowing the accumulation of the neurotransmitter at the nerve endings, which causes cholinergic overstimulation (Pundir and Chauhan, 2012). This, in turn, causes neurotoxic symptoms, including headache, excessive salivation, convulsions, respiratory depression, and even death. Therefore, the monitoring of pesticides in food and environmental samples is a serious issue. Codex Alimentarius, WHO and the European Union established maximum residue levels (MRLs) to regulate pesticide levels in the water, vegetables, and fruits to ensure consumer safety and regulation of foreign trade (EC, 2005; Hamilton et al., 2003).

There are many well established conventional analytical methods that have been reported with high sensitivity and selectivity for the detection of pesticides, including gas chromatography (GC) (del Castillo et al., 2019), gas chromatography-mass spectrometry (GC-MS) (Andraščíková and Hrouzková, 2016; Cunha and Fernandes, 2011; Ghani et al., 2018; Rai et al., 2016), high-performance-liquid chromatography (HPLC) (Bedassa et al., 2017; Seebunrueng et al., 2014), liquid chromatography-tandem mass spectrometry (Ma et al., 2020), gas chromatography-tandem mass spectrometry (Li et al., 2017), capillary electrophoresis (Cacho et al., 2018), immu nochips (Gong et al., 2013), enzyme-linked immunosorbent assays (Qian et al., 2009), and ultra-high performance liquid chromatography coupled with tandem mass spectrometry (Chen et al., 2013). However, these instruments are expensive, require time-consuming sample preparation, and highly trained personnel, and difficult to use on-site (Gambacorta et al., 2005; Izquierdo et al., 1996; Menezes et al., 1998). Thus, there is still great demand for the development of very simple, low-cost, portable, environmental, and user-friendly detection approaches, particularly in

developing countries and remote areas where a lack of sufficient laboratory infrastructure and professional experts.

Microfluidic paper-based analytical devices (µ-PADs) have great potential to fill this gap as such devices are simple, low-cost, portable, rapid and are highly demanded in developing countries (Martinez et al., 2009).

Thus, µ-PADs have been showing considerable promise in both point-of-need (PON) and point-of-care (POC) diagnostics due to several inherent advantages including; a small footprint, small reagent volumes, small waste volumes, increased portability and accessibility for detection relative to conventional laboratory testing methods (Adkins, 2016). Although, the original purpose of developing µ-PAD was to use it as a point of care (POC) for biomedical purposes, currently their application have been extended to food safety assessments and environmental monitoring (Rattanarat et al., 2013).

Several studies have reported on the use of colorimetric µ-PAD for the detection of OP and CM pesticides via AChE inhibition (Apilux et al., 2015; Badawy and El-Aswad, 2014; Fernández-Ramos et al., 2020; Jin et al., 2020; Kavruk et al., 2013; Kim et al., 2018; Sankar et al., 2020). However, for the majority of the studied pesticides, high limit of detection (LOD) that goes beyond the permissible limit have been reported. This implies that the sensitivity of the reported µ-PADs are not adequate enough to predict the threshold concentration that might cause environmental threat. Thus, in this study, a miniaturized DLLME method has been used as an enrichment technique to improve the analytical sensitivity of µ-PAD for trace analysis of pesticides in water samples.

On the other hand pesticide residue determination in vegetables remains challenging because of the trace amount of target analytes and complex interference in matrices (Farajzadeh et al., 2011; Li et al., 2017; Rizzetti et al., 2016). For these reasons, efficient extraction, clean up, and preconcentration steps are required prior to analysis. Anastassiades et al. (2003) developed QuEChERS (quick, easy, cheap, effective, rugged, and safe) extraction, which has proven to be an attractive sample preparation technique for pesticide multiresidue in fruits and vegetables.

However, its main limitation is the low enrichment factor (Cunha and Fernandes, 2011). On the other hand, dispersive liquid-liquid microextraction (DLLME) is known to have high enrichment factor (Beshana et al., 2022a; Viñas et al., 2014), however, due to the complexity of the food sample matrix, it is difficult to use DLLME alone as a preconcentration/extraction technique for analyzing pesticides residues in agricultural products (Asensio-Ramos et al., 2011b). Several researchers have combined QuEChERS and DLLME to complement the limitations of each extra ction method (Andraščíková and Hrouzková, 2016; Chen et al., 2013; Cunha and Fernandes, 2011; Ghani et al., 2018; Li et al., 2017; Ma et al., 2020; Rai et al., 2016; Young, 2005) and conducted pesticide analysis using the conventional analytical techniques. In the present study, QuEChERS-DLLME have been coupled with μ-PAD to widen the application scope of μ-PAD to solid matrices such as vegetables.

The traditional approach for the optimization of experimental parameters is to change one-variable-at-a-time while keeping other variables constant. But this method is very time consuming and unable of achieving the true optimum condition since it disregards the interaction among variables (Lundstedt et al., 1998). To solve this problem, experimental design response surface methodology (RSM) have been applied extensively to optimize extraction procedures (Ahmadvand et al., 2015; Candioti et al., 2014; Ceylan et al., 2008). However, there are very

limited use of multivariate approach in the microfluidic paper based analytical devices. Thus, in this work, experimental conditions of µ-PADs were optimized using both univariate and multivariate optimization techniques for comparison. Subsequently, the multivariate approach has been extensively employed in DLLME-µ-PADs, hyphenated QuEChERS-DLLME-µ-PADs for quantitative extraction, preconcentration and analysis of OP and CM pesticides in water and lettuce vegetable samples.

1.2. Objectives of the Study

1.2.1. General Objective

The main objective of this research is to develop a sensitive µ-PADs coupled with miniaturized sample preparation techniques for the determination of OP and CM pesticides from water and lettuce samples.

1.2.2. Specific Objectives

- To develop µ-PAD for the determination of OP and CM pesticides using univariate optimization techniques.
- To develop µ-PAD for the determination of OP and CM pesticides using multivariate optimization techniques based on Box-Behnken Design.
- To couple DLLME with µ-PAD as preconcentration techniques for the determination of OP and CM pesticides in water samples.
- To combine QuEChERS-DLLME with µ-PAD to enhance the analytical performance of µ-PAD in determining OP and CM pesticides in lettuce vegetables.

2. LITERATURE REVIEW

2.1. Historical Development of µ-PADs

The first microfluidic device was developed in 1975 and some of them evolved from thin-layer and gas chromatography separation techniques (Terry, 1975; Terry et al., 1979). Ukrainian scientists N.A. lzmailov and his student M.S. Shraiber published the article in the journal Farmatsiya (Pharmacy) (Izmailov and Shraiber, 1938). They were searching for appropriate methods for the rapid analysis of plant extracts. They coated microscope slides with a suspension of various adsorbents (calcium, aluminum, and magnesium oxide), then applied one drop of each sample solution and solvent. The components of the sample which were separated appeared as concentric rings fluoresced in various colors under a UV lamp (Shostenkot et al., 2000).

The beginning of microfluidics can be traced back to the invention of analytical methods (i.e. gas phase chromatography, high-pressure liquid chromatography, and capillary electrophoresis), which have revolutionized chemical analysis. The first real lab-on-a-chip for gas chromatography was created in 1979 at Stanford University with the incorporation of a LASER as optical detection technique which enhanced miniaturization by reducing the volume of sample required and improving accuracy (Terry et al., 1979). This was followed by an exploration of versatile microanalytical techniques for analysis.

After the end of the cold war in the 1990s, biological and chemical weapons posed a major military and terrorist threat. To overcome these threats, the Defense Advanced Research Projects Agency (DARPA) of the US Department of Defense designed to support a series of programs intended at developing field-deployable microfluidic systems that help to detect biological and chemical threats. This influenced the rapid growth of microfluidic technology. The arrival of high

throughput genomic techniques in the 1980s and other areas of microanalysis related to molecular biology required enhanced sensitivity and resolution of analytical methods which can be met by employing microfluidic technologies. This is the first time a miniaturized operation has been pushed to the level of a single cell. In the 1990s, microelectronics promoted the growth of microfluidics and sought its applications in the fields of chemistry, biology, and biomedical fields. In the earlier era, silicon and glass based fluidic microsystem were replaced by plastics as they required heavy infrastructure and electronics. The major point of this focus was on integrating the various chemical, biological and biomedical protocols onto a single chip. Such schemes enable the complete implementation protocol beginning with sample collection up to analysis and are called micro total analysis systems (Manz et al., 1990).

In the early 2000s, micro-channels fabrication techniques using polymers such as PDMS were highly preferred since they reduced the production time and cost-effectively. These were generally known as soft-lithography techniques (Lisowski and Zarzycki, 2013). In 2004, Whiteside's group introduced POCKET, a portable microfluidic-based system that addressed the requirements of simple diagnostic devices in developing countries (Sia et al., 2004). It was used for carrying out immunoassays with the same efficiency as bench-top ELISA, but in a lesser time in a cost-effective manner (Sia and Whitesides, 2003). Conventional microfluidic devices seemed to be too complicated and expensive to be used on a large scale in developing countries which marked a shift towards paper-based microfluidics, which are widely referred to as paper-based analytical devices (PADs). In developing countries, conventional microfluidic devices seemed to be too complicated and expensive to be used on a large scale which marked a shift towards paper-based microfluidics, which are widely referred to as paper based analytical devices (PADs). Whiteside's Group of Harvard University described the concept of micro PADs (μ-PAD) in 2007 (Martinez et

al., 2007). µ-PAD technologies have found a wide range of applications in recent years, including health diagnostics, biochemical analysis, forensics, and food and environmental quality control (Li et al., 2012).

2.2. Paper-Based Microfluidic Devices

Since Whitesides and his coworkers introduced the first microfluidic paper-based analytical device (µ-PAD) in 2007, the field has grown exponentially and had a clear impact on academics and industry (Martinez et al., 2007). The rapid growth of µ-PAD is because of some of its capabilities, such as its potential to make use of small quantities of samples and reagents and to carry out separation and detection with high resolution and sensitivity at low cost and rapidly (Martinez et al., 2007). In general, this technology can analyze complex, small volumes of biochemical samples from 10^{-9} to 10^{-18} L using fluid channels in a single analytical run with dimensions ranging from tens to hundreds of micrometers (Whitesides, 2006). As indicated in earlier reports, microfluidic fabrication involved the use of glass (Ruano et al., 2000), silicon (Harris et al., 2003), and polymers such as Polydimethylsiloxane (PDMS) (McDonald and Whitesides, 2002) as substrates.

Paper has recently become a very promising substrate material for µ-PAD fabrication for several reasons. Since an abundant, inexpensive, lightweight, biodegradable, easily printed, short assay time, simple readout method (naked eye), coated and impregnated, its cellulose composition is particularly compatible with proteins and biomolecules, it is accessible almost everywhere, provides power free fluid transport via capillary action, has a high surface-to-volume ratio for chemical interaction and detection, and has the capacity for storing reagents in active form within the fiber network and white; which is a good medium for colorimetric tests (Dou et al., 2015; Li et al., 2012; Martinez et al., 2009; Yetisen et al., 2013). As compared to traditional microfluidic

materials (i.e., glass, silicon, polymers) µ-PADs may lack high resolution and mechanical robustness (Nge et al., 2013). It has been functioning as a substrate to construct microfluidic devices for a variety of diagnostic tests (Martinez et al., 2007). µ-PAD is constructed by patterning hydrophilic channels separated by a hydrophobic barrier. The pattern is created by depositing a hydrophobic material on the paper substrate that serves as a barrier to guide the liquid wicking in the wanted direction. Hence, these devices are designed to achieve four simple capabilities in one analytical device (Zhang et al., 2014). These capabilities are as follows: (1) the distribution of a sample into multiple regions, allowing for multiple analyses or replicating one analysis multiple times, (2) wicking of the sample solution without the need for a pump or other external force due to capillarity, (3) the ability to analyze with small volumes, and (4) the generation of minimal hazardous waste. Lateral flow format and well-shaped format are two common types of patterns that were used for chemical analysis as shown in Figure 1.

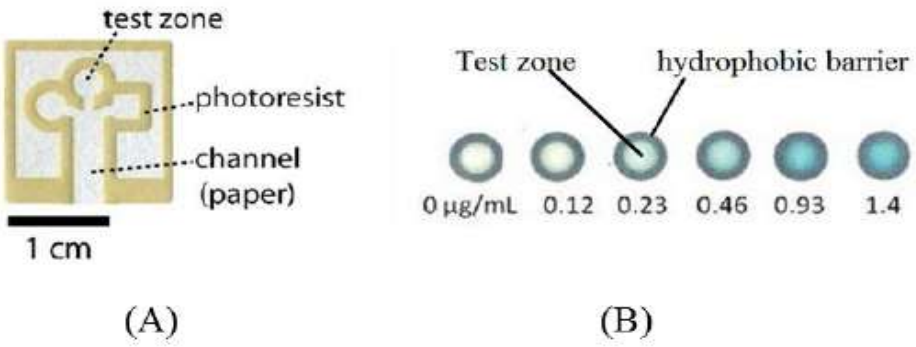

Figure 1. Patterns of µ-PADs: Lateral flow format (a) and well-shaped format (b) (Adapted from Jokerst et al.(2012)).

2.3. Fabrication Techniques of µ-PADs

Device fabrication is one of the core novelties of µ-PADs. The novelty of µ-PADs is a result of their low-cost relative to conventional analytical methods. Manufacturing methods are often aimed at reducing costs per device, increasing production, or adding assay capabilities (Jenkins et al., 2015). It is fabricated from a variety of hydrophobic substances that have been used to define hydrophilic micro-channels on paper from relatively expensive agents such as photoresist SU-8 (~ \$0.1 for patterning filter paper of 100 cm^2) (Martinez et al., 2008), the less expensive agents such as wax (~ \$0.01 for patterning filter paper of 100 cm^2) (Carrilho et al., 2009a) to the extremely cheap agents such as alkyl ketene dimer (AKD, ~ \$0.00001 for patterning filter paper of 100 cm^2) (Li et al., 2010b). The main purpose of prototyping paper microfluidic devices is to form hydrophobic/hydrophilic interfaces on a cellulose substrate to manipulate/control fluid flow. A total of nine technologies for manufacturing paper-based microfluidic devices have been reported in the literature (Elsharkawy et al., 2014; Rosenfeld and Bercovici, 2014; Sones et al., 2014; Viola et al., 2013): These include (1) wax printing, (2) inkjet printing, (3) photolithography, (4) flexographic printing, (5) plasma treatment, (6) laser treatment, (7) wet etching, (8) screen-printing, and (9) wax screen-printing.

2.3.1. Wax Printing

One of the promising technologies for the fabrication of µ-PADs is wax printing. It offers numerous advantages such as lower production costs (both wax and paper are cheap and easy to obtain), disposability, environmentally friendly, ease of fabrication (5-10 min), and few steps for mass production. The cost of wax printed µ-PAD is \$0.001 per device of 1 cm^2 since the cost of solid ink is around \$0.0001/cm^2 and the cost of a standard filter paper is around \$7/m^2 (Carrilho et

al., 2009a). Moreover, the setup of a laboratory for wax printing is not expensive since around $1000 is required for the two pieces of equipment that are needed, i.e., a wax printer (e.g., FUJIXEROX Phaser 8560, Japan is around $800) and a heater (around $200) (Martinez et al., 2010). A desktop scanner might be used for the readout are around $100 instead of expensive monitoring equipment (Cheng et al., 2010). Wax printing enables fabricating large numbers (> 100) of paper-based analytical devices in a single batch. This technology is very useful for prototyping paper-based microfluidic devices to implement low-cost bioassays in remote settings. As shown in Figure 2, the three different steps of the fabrication process consisted of (i) designing the shape of the pattern, (ii) printing the wax pattern on the paper using a wax printer, and (iii) heating the patterned paper on a hot plate (Carrilho et al., 2009a). The porous structure of the filter paper enables the wax to penetrate into the paper to form a well-defined microchannel on the paper. However, the main disadvantages of this technique are the use of expensive wax printers and heating equipment, as well as lower device resolution (Songjaroen et al., 2011) and the melting of the wax during long term storage under ambient air conditions, the possibility of cross-contamination of the samples with the wax, and the modification of device dimensions (channels) over time (Yetisen et al., 2013).

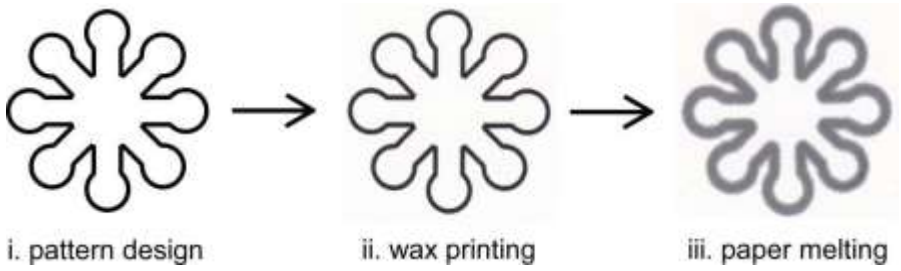

Figure 2. Fabrication of patterning paper by using wax printing (Adapted from Carrilho et al. (2009a)).

2.3.2. Inkjet Printing

Inkjet printing is a viable alternative to wax printing that is gaining popularity in the fabrication of µ-PADs. Toluene is used as the printed reagent in this process to remove hydrophobic polystyrene that was pre-patterned on the paper using inkjet etching to create hydrophilic designs (Abe et al., 2008). Li et al. (2010a) recently used inkjet printing to create barriers. To define hydrophilic regions, an alkyl ketene dimer (AKD) reagent was printed onto paper and polymerized by heat. Similarly, UV curable inks have been used in inkjet processes as an alternative to more volatile and environmentally harmful organic solvents (Maejima et al., 2013). Finally, Wang et al. (2014) presented an environmentally friendly approach that combined inkjet etching with the printing of sol-gel barriers in the paper. This type of barrier could withstand a variety of organic solvents and surfactants that could not be used in wax or AKD printing barriers. Similar to wax printing, inkjet printing can be used to create 3D devices by incorporating hydrophobic reagents into the paper matrix itself (Maejima et al., 2013).

Only inkjet printing enables flow channel fabrication and reagent printing in test zones with relatively high throughput and reproducibility (Abe et al., 2008; Maejima et al., 2013). However, the disadvantage of this technique is that it usually requires multiple print layers to create the device, which can lead to print resolution problems. Many of the solvents used to solubilize sensing reagents are volatile, which can lead to clogging or errors in printed reagent amounts.

2.3.3. Photolithography

Martinez introduced the first chemical fabrication of µ-PADs using photolithography by pattering chromatography paper with SU-8 2010 photoresist. This type of patterning is based on entire hydrophobization, followed by selective dehydrophobization of the paper (Martinez et al., 2007; Martinez et al., 2010). With this technique, high resolution and very small dimensions of chemical

resistant solid barriers can be formed. However, there are two potential limitations to this fabrication process. One is that the cured photoresist is easily damaged by bending and folding. Second, photolithography requires expensive equipment enclosed by clean rooms and a complex manufacturing process. The same group used an epoxy negative photoresist to reduce the cost and increase the flexibility (Martinez et al., 2008), and SC (cyclized poly(isoprene) derivative) photoresist (Carrilho et al., 2009b), and introduced UV lamp and hotplate to eliminate the use of lithography machine (Martinez et al., 2008). Moreover, a laser directing method was used to avoid the use of photomasks (He et al., 2015a). He et al. (2013) avoided the adoption of high-cost photoresists by fabricating photolithographic coupling of hydrophobic silane to paper fibers followed by deep UV-lithography. He et al. (2015b) generated a dynamic photomask LCD and digital micro mirror device to decrease the time and cost of photomask fabrication. A desktop stereo lithography 3D printer and an ultraviolet resin were used for µ-PAD fabrication, the so called, dynamic mask photo curing (DMPC).

2.3.4. Flexographic Printing

This is a simple method based on the flexographic printing technique that can be used to fabricate µ-PADs. The entire process contains only one step. That is, the hydrophobic barrier area (polystyrene) is printed on the filter paper to form liquid-carrying boundaries and layers on the filter paper, allowing the formation of a hydrophobic barrier structure that partially or completely penetrates the substrate (Olkkonen et al., 2010). This method may not be suitable to be used for prototype fabrication in the lab, however, it can be used for mass production of µ-PADs and has a promising future (Xia et al., 2016). Although it is the fastest method, it requires a specialized flexographic printer and can only print one reagent at a time (Cate et al., 2014).

2.3.5. Plasma Treatment

Plasma treatment has been commonly utilized μ-PADs fabrication techniques on paper substrates. The filter paper was previously hydrophobized paper by dipping it into the alkyl ketene dimer (AKD)-heptane solution, then followed by heat treatment in fume hood to facilitate evaporation of heptane. Then, the filter paper was heated in an oven to cure the AKD, and render the paper hydrophobic (Li et al., 2008). Hydrophilic patterns applied hollow metal mask guided plasma to make the exposed area of interest to be hydrophilic, which would form a hydrophilic flow path in hydrophobic filter paper (Li et al., 2008). In this way, the regions of the paper exposed to the plasma become hydrophilic defining the microfluidic pathway. This plasma treatment process has no effect on the flexibility or surface topography of paper. However, this process requires customized masks, vacuum plasma reactors, and hot plates that restrict the wide applicability of this technique (Yetisen et al., 2013).

2.3.6. Laser Treatment

Lasers have been widely used for the fabrication of polymer or glass-based microfluidics; the violent temperature rises on the laser-focused spot cause the material to melt down and evaporate rapidly, and continued laser scans on the surface of material could be used to fabricate microchannel on polymer, glass, and silicon materials. The CO_2 laser and UV laser are the most commonly used laser devices. CO_2 lasers are commonly used to directly ablate microchannels with Gaussian-like profiles on thermoplastics (Liu et al., 2018), and the UV laser is usually used for the fabrication of glass-based microfluidics (Cheng et al., 2005).

2.3.7. Wet Etching

There are two steps of the µ-PADs fabrication process by selective wet etching of hydrophobic filter paper (Cai et al., 2014). First, patterning of the filter paper hydrophobically by using trimethoxyoctadecylsilane solution as a pattering agent. Next, a paper mask penetrated with NaOH solution (containing 30% glycerol) is aligned onto the hydrophobic filter paper, allowing the etching of the silanized filter paper by the etching reagent. The masked region then becomes extremely hydrophilic, while the unmasked region remains extremely hydrophobic. Therefore, hydrophilic channels, reservoirs, and detection zones are created and separated by hydrophobic barriers.

2.3.8. Screen Printing

This is a versatile µ-PADs fabrication technique where the liquid material is transferred onto the substrate via screen using an automatic tool or manually, which regulates the amount of printed material and pressure applied on the substrate (Dungchai et al., 2011; Metters et al., 2013). Then, the paper substrate may be subjected to heat, allowed to dry, or other treatments. As compared to wax printed by a commercial printer, the screen printing method is much thicker layers of printed material can be applied. There are also less strict requirements for the size, planarity, shape, and thickness of the selected paper substrate. The main advantages of screen-printing techniques are fast fabrication times, low costs, flexibility, and capability of mass production (Yafia et al., 2015). Another variation of this technique utilizes spraying of material through a pre-defined micro stencil instead of squeezing through a screen as in conventional screen-printing, i.e. a mask containing the pattern to be transferred (Tao et al., 2011).

2.3.9. Wax Screen-printing

Wax screen printing was also used to fabricate µ-PADs in two simple steps as follows: (1) printing patterns of solid wax on the surface of the paper using a simple screen-printing method and (2) melting of the printed wax into the paper to form hydrophobic barriers using a hot plate. This is schematically shown in Figure 3. Wax printing conventionally needs a wax printer for fabrication of µ-PADs (at $2500 US) but screen printings are cheap (at $5 US per 100 cm^2) and can easily obtained from local market, and is also environmentally friendly. In addition, this method is accomplished without the use of a clean room, UV lamp, organic solvents, or complex instrumentation. The major advantage of this method as compared to the previous is that it requires only a common hot plate (or similar surface) and a common printing screen, making it ideal for the fabrication of the µ-PADs in developing countries (Dungchai et al., 2011). As screen printing is very common in fabricating bits of printing materials, this method is suitable for small number µ-PADs fabrication.

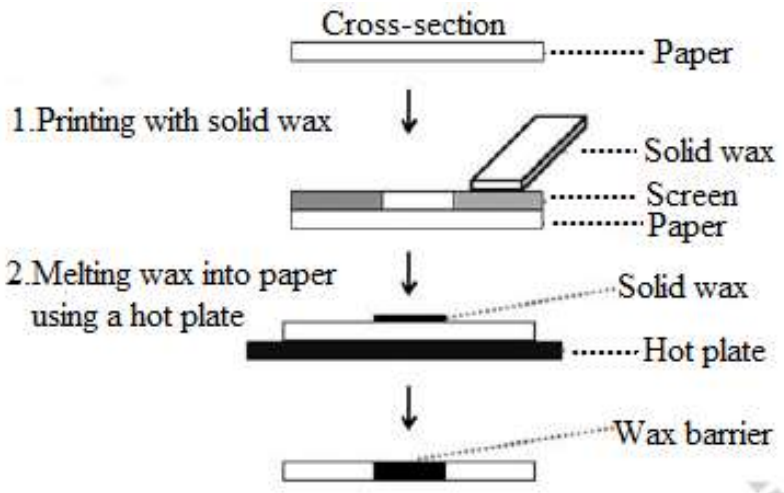

Figure 3. Schematic diagram of fabrication step for wax screen-printing method (Adapted from Dungchai et al.(2011)).

2.4. Determination Methods in µ-PADs

There are several detection methods for µ-PADs. Since the analyte is driving via capillary action, the detection of optical, electrical, or chemical properties can be harnessed by transduction. During transduction, the conversion of a bio/chemical reaction into a visible signal is required for sensing applications. A large variety of sensing mechanisms have been proven to be powerful detection methods for environmental analysis in combination with µ-PADs. Among that colorimetric, fluorescence, chemiluminescence, and electrochemical techniques are the most common ones (Yetisen et al., 2013).

Colorimetric detection is the most widely used detection method of environmental pollutants by using µ-PADs technologies. This method is most common because the paper substrate provides a bright, high-contrast, colorless background for reading color changes (Cate et al., 2014; Nery and Kubota, 2013). The results of this method can be qualitative, semi-quantitative, or quantitative, depending on the goals of the test. Qualitative assays are usually performed without an external instrument to provide yes/no results that are easy to determine visually (Li et al., 2015b). Semi-quantitative analysis may use a color map to estimate the relative quantity of the analyte based on a previously created calibration curve (Lin et al., 2016). Quantitative analysis of µ-PAD requires more rigorous and carefully controlled measurements to obtain accurate and precise analyte levels (Alkasir et al., 2015; Ismail et al., 2016). This detection method is based on the reaction of the target substance with chemical reagents. During the analysis, direct visualization or computer software techniques are used to obtain the results. Computer software is the preferred method because direct visualization is affected by different lighting environments, changes in color perception, and different colors of dry and wet paper (Liana et al., 2012). No special equipment is

required for colorimetric detection (Evans et al., 2014). Therefore, digital photographs and digital scans are typically used to analyze color changes and can be used in areas of limited resources. ImageJ software is used to analyze the intensity of color changes. Colors can be analyzed as RGB (Red, Green, Blue), CMYK (Cyan, Magenta, Yellow, Key), HSV (Hue, Saturation, Value), or grayscale(Birch and Stickle, 2003).

Although colorimetric detection is widely used, this method has some drawbacks. The unevenness of illumination when using a digital camera is one of the problems with this technique. An enclosure or mounting frames are often used to solve this problem. However, the possibility of error due to color variation still exists. Better results can be obtained by repeating the same reaction multiple times (Jayawardane et al., 2014). Since the color distribution of the test paper is inhomogeneity, it is difficult to determine the final color with the naked eye (Bruzewicz et al., 2008). In addition, colorimetric sensors are typically affected by background noise on paper and samples. Therefore, the selectivity and sensitivity are low, and the detection limit is not very low. Colorimetric sensing has been used successfully to detect glucose, proteins, and other biomolecul es (Barr et al., 2011; Wang et al., 2010; Wei et al., 2015), enzymes and their inhibitors (Hossain et al., 2009), metal particulates (Mentele et al., 2012), and bacteria (Shafiee et al., 2015), separation of red blood as a pre-treatment process of blood samples (Jarujamrus et al., 2012; Songok et al., 2014), and for immunoassays (Wei et al., 2015).

Electrochemical detection is the most widely studied method in μ-PAD due to its high selectivity, sensitivity, low cost, portability, minimal equipment, and low power consumption (Dungchai et al., 2009). In contrast to the colorimetric sensors, they showed higher sensitivity and selectivity, and faster sensor response, allowing the detection and quantification of analytes even in the nanomolar range (Jiang et al., 2016; Li et al., 2012). In addition, unlike colorimetry,

electrochemical has the advantage of being unaffected by light conditions and contaminants in the sample, resulting in a more stable signal (Yamada et al., 2015). In addition, the porosity and roughness of the paper substrate increase the surface area of the deposited material and improves the response of the electrochemical sensor (Sarfraz et al., 2011). However, the drawback of this structure is the physical attachment of the electrodes to the paper, which can be difficult to control (Hu et al., 2012). This method uses biomolecules such as cholesterol, lactic acid, uric acid, glucose (Li et al., 2016; Nie et al., 2010a), drugs and neurotransmitters (Rattanarat et al., 2012), nucleosides, and DNA (Cunningham et al., 2014), metals (Nie et al., 2010b), and ions (Cui et al., 2014), gaseous samples (Sarfraz et al., 2011), pH change (Lei et al., 2012), and immunoassays (Zang et al., 2012).

Nonetheless, increased sensitivity for electrochemical detection and faster response can be achieved by further miniaturization. For field use, powerful and portal electrochemical devices are key to the successful commercialization of electrochemical-based µ-PADs. However, the main drawbacks of this method are the increased cost of detection tools per test and the complexity of point care devices (Yetisen et al., 2013). Inexpensive and simple devices have been demonstrated and electrochemical detection has been achieved using mobile phones in resource-constrained settings (Nemiroski et al., 2014).

Fluorescence detection methods are based on the measurement of light emission during a chemical reaction. Fluorescence measurements are much more sensitive than other photometric measurements. This is because the signal of the analyte depends on both the concentration of the analyte and the intensity of the light (Chen et al., 2016; Xin-Ran et al., 2015). Fluorescence detection with µ-PAD is most often reported by measuring the fluorescence quenched by the analyte rather than directly measuring the emission. Fluorescence quenching or direct emission is

detected using a commercially available fluorimeter, a plate reader capable of detecting fluorescence, or a mobile camera with the appropriate software application (Petryayeva and Algar, 2013). However, commercially available white papers are typically treated with different brightening agents. This can interfere the fluorescence signal by causing high background noise (Pelton, 2009). Generally, µ-PADs with fluorescence sensors were used for studying bacteria (Rosa et al., 2014), bacteria growth (Funes-Huacca et al., 2012), proteins (Carrilho et al., 2009b; Liu and Crooks, 2011), DNA (Ali et al., 2009), cancer cells (Liang et al., 2016), drugs (Caglayan et al., 2016), and for immunoassays (Liang et al., 2012).

Chemiluminescence is a light-generation phenomenon caused by a chemical reaction, in which chemical energy is converted into light energy as electrons move from an excited state to a lower energy level. It is considered an efficient and sensitive analytical technique for µ-PAD (Nuchtavorn and Macka, 2016). However, device manufacturing in this way is complicated because the measurements were made in the dark (Nery and Kubota, 2013). Therefore, the cost of a portable chemiluminescence reader is relatively expensive. When compared to fluorescence, CL has no external light source, which reduces background noise (Nuchtavorn and Macka, 2016). In µ-PADs, this sensing method was adopted for biomolecules detection (for hormones, glucose, and uric acid) (Yu et al., 2011), measuring hybridization of DNA (Wang et al., 2013), DNA detection (Liu and Zhang, 2015), cancer detection (Wang et al., 2015), immunoassays (Wang et al., 2012), metal detection (Alahmad et al., 2016), and pesticide detection from food products (Liu et al., 2014).

2.5. Basic Principles of Colorimetric Detection

Analysis of pesticides is based on the inhibition of AChE activity by pesticides. AChE is irreversibly inhibited by pesticides and reversibly inhibited by heavy metals (Danzer and Schwedt, 1996; Kukla et al., 1999; Marquis and Lerrick, 1982). Comparison of AChE activity before and a fter environmental exposure of a sample can provide an estimate of the level of contamination. A s shown in Figure 4, the most commonly used colorimetric assay method for pesticide detection uses acetylthiocholine as a substrate of AChE, and the production of thiocholine is measured by Ellman (1959). DTNB (5, 5-dithiobis-(2-nitrobenzoic acid) reacts with thiocholine to produce TNB, 2-nitro-5-thiobenzoic acid, a yellow product with maximum absorption at 412 nm. The enzyme inhibition mechanism is based on the formation of a complex via a reversible/irreversible reaction of pesticides with AChE active sites (Chauhan et al., 2011). An enzyme inhibitor lowers the substrate binding capacity due to direct interaction between the enzyme and the inhibitor. The inhibitor typically binds to a remote site and induces a conformational change in the active site, reducing catalytic turnover and changing substrate binding capacity (Andrić et al., 2010; Darreh-Shori and Soininen, 2010). As a result, the TNB detection signal is inversely proportional to the concentrations of pesticides in the samples.

However, the presence of heavy metals in the sample may have a negative effect on this method. Because thiols have a high affinity for heavy metals (Friedman, 1973; Krężel et al., 2001; Majid et al., 2002), the thiocholine produced by the enzymatic reaction could react with heavy metals present in the sample solution. When using this spectrophotometric determination of AChE activity, such metal binding is expected to interfere with the reaction described in Figure 4, resulting in an overestimation of pesticide level. To avoid this problem, a separation step appears

to be necessary in which the pesticides are first extracted into the organic phase. This would eliminate the presence of heavy metals and other water-soluble enzymatic inhibitors such as fluoride (Tran-Minh et al., 1990) and hypochlorite (Soldatkin et al., 1997) in the sample solution due to their low solubility in organic solvents.

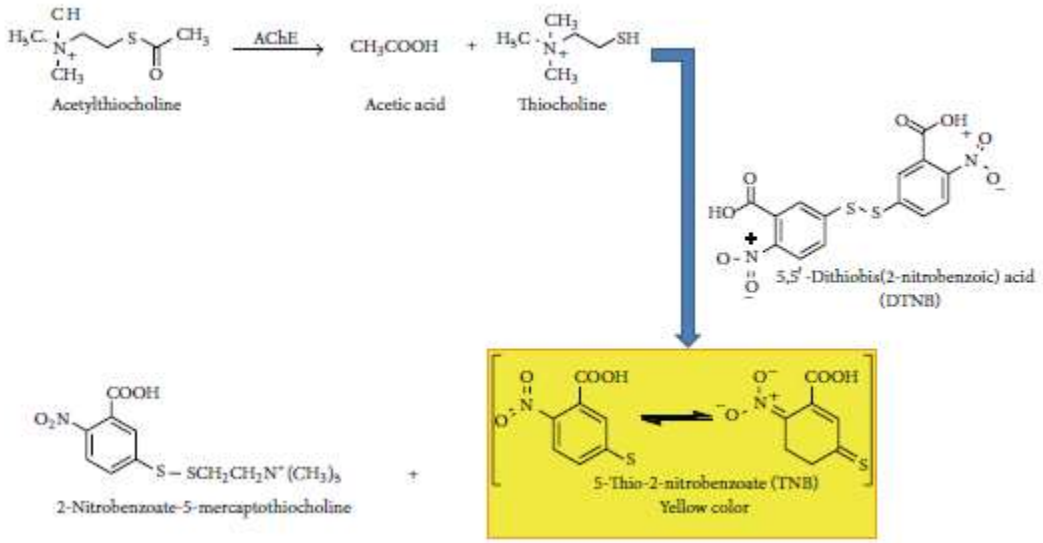

Figure 4. Common principle used in colorimetric assay method for pesticide detection: AChE hydrolyzes the acetylthiocholine and forms thiocholine base, which then reacts with DTNB to generate TNB, which is yellow in color (Adapted from Badawy and El-Aswad (2014)).

Most OP insecticides are actually relatively weak inhibitors of AChE because they contain a P-S moiety. The compounds are metabolized by cytochrome P450 to produce oxygen analogs, called oxons, which are very potent AChE inhibitors. The inhibition of AChE following exposure to OP insecticides is thought to be mainly caused by the oxygen analogs and not the parent compounds. CM anticholinesterase is thought to inhibit AChE in a manner similar to OP. However, instead of electrophilic phosphorus as in the case of OP, CM contains electrophilic carbonyl carbons that are susceptible to nucleophilic attack by the active site serine oxygen (Figure 5). The resulting

carbamylated enzyme intermediate inhibits the enzyme activity until the water molecule attacks the carbonyl carbon to reactivate the enzyme and produce a carbamic acid derivative (Figure 5). This rate of reactivation is not as fast as that of acetylation intermediates, but much faster than that of phospylated enzyme.

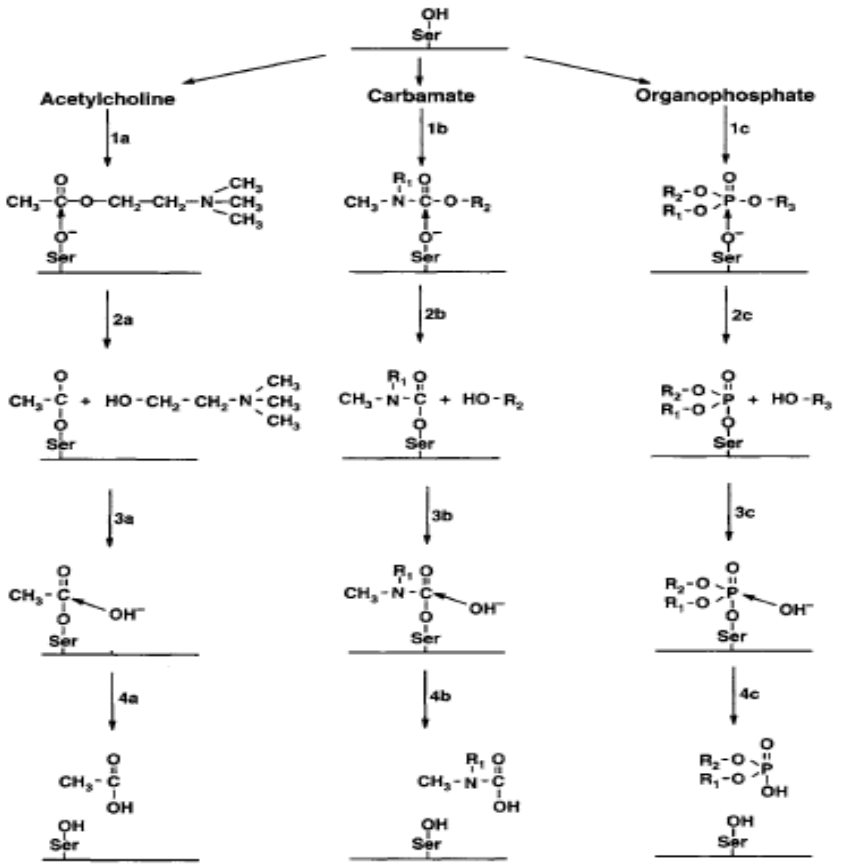

Figure 5. Interaction of ACh, CM and OP with active site serine of cholinesterase. Step 1 represents the formation of a stable Michaelis complex and the initiation of the nucleophilic attack on the active site serine of AChE. Step 2 is the acetylation of this serine and the release of the leaving group. Step 3 represents the nucleophilic attack of a hydroxyl ion. Step 4 represents the subsequent regeneration of the active enzyme.

2.6. Pesticide Classification

Pesticides are a class of chemicals used to control weeds, bacteria, insects, and fungi. Pesticides are a broad category that includes insecticides, herbicides, fungicides, rodenticides, wood preservatives, garden chemicals, and household disinfectants (Eldridge, 2008). Pesticides differ from one another in terms of their identity, physical and chemical properties. Pesticides are classified according to their chemical composition, functional groups, mode of action, toxicity, and the type of target pest (Kim et al., 2017). Similarly, Drum (1980) classifies pesticides into three major categories based on the mode of entry, target pest/function, and chemical composition. The most common classification of pesticides is based on their chemical composition. This classification provides information about the efficacy, physical and chemical properties of the respective pesticides. According to this classification there are three main groups namely organochlorines, organophosphates, and carbamate pesticides (Nerın et al., 2002; Pandey et al., 2010).

2.6.1 Organochlorine Pesticides

Organochlorine pesticides are a class of persistent organic compounds that contains five or more chlorine atoms in their structure. Previously, it was most commonly used to combat malaria and typhoid fever, but its use is banned in most developed countries (Aktar et al., 2009). However, due to its need for a variety of pests, organochlorine pesticides are most commonly used for pest control in developing countries. These pesticide groups were the first man-made organic pesticides used in agriculture and public health. Most of these pesticides are used to control a variety of insects and have a long-term residual effect on the environment. It also acts as a nervous system disruptor, causing convulsions and paralysis in the insect, as well as death (Jayaraj et al., 2016). Some

representative examples of organochlorine pesticides are: DDT (1), dieldrin (2), methoxychlor (3), chlorinated (4), heptachlor (5), aldrin (6), endrin (7), toxaphene (8), mirex (9) and lindane (10) and their chemical structures are presented hereunder (Figure 6).

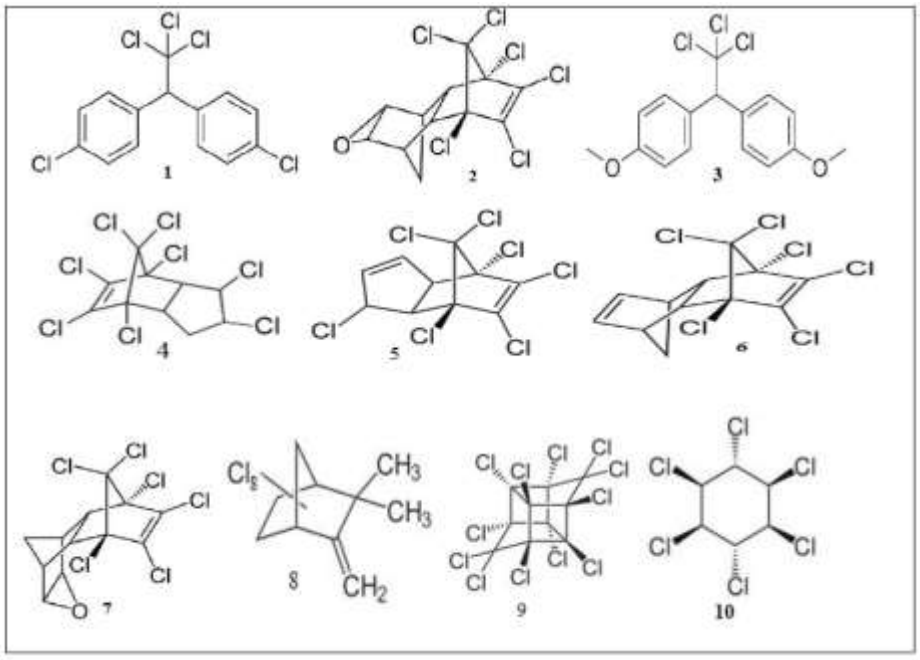

Figure 6. Examples of organochlorine insecticide structures (Adapted from Hodgson (2004)).

2.6.2. Organophosphate Pesticides

Organophosphate pesticides are thiophosphoric acid esters or phosphoric acid esters. They are one of the most commonly used insecticides throughout the world. Organophosphorus pesticides are more toxic to vertebrates and invertebrates by inhibiting acetylcholinesterase, which results permanently in an accumulation of the acetylcholine neurotransmitter. As a result, it disrupts the muscle response, causing respiratory and myocardial dysfunction, paralysis, and death. Unlike organochlorine pesticides, organophosphate insecticides are relatively non-persistent in the environment (a few hours to several months) and easily decompose by chemical and biological reaction exposure to light, air, and soil, however, a small amount is detected in food and drinking

water (Crane et al., 1999). As a result, this group of pesticides minimizes water and soil contamination (Lucio, 2006). Chlorpyrifos and malathion are some examples of OP insecticides as represented in Figure 2.

2.6.3. Carbamate Pesticides

Carbamate insecticides are organic compounds derived from carbamic acid (NH_2COOH). These classes of insecticides are not generally persistent and easily break down in the environment within a week or a month (Goel and Aggarwal, 2007). Carbamate is one of the most popular pesticides used in gardens, lawns, and household crops to kill cockroaches, ants, fleas, crickets, aphids, scales, whiteflies, race bugs, and whiteflies. Some CM control mosquitoes and some have been found in groundwater at levels high enough to cause concern (Ortiz-hernández and Sánchez-salinas 2010). Carbamate has a similar mechanism of action to OPs in that it reversibly inactivates the acetylcholinesterase enzyme, resulting in the termination of nerve signals and the death of pests due to poisoning (Krieger, 2001). Under this group, some of the insecticides that are most widely used include carbaryl, carbofuran, furathiocarb, and methomyl (Figure 7).

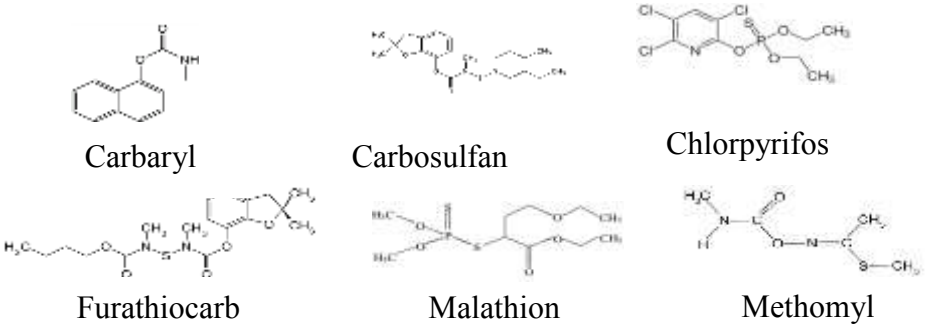

Figure 7. Examples of OP and CM insecticide structures.

2.7. Effect of Pesticides

Despite the beneficial use of pesticides in public health and agriculture, their use also has a negative impact on the environment and public health. Pesticides are one of the environmental pollutants due to their high bioactivity and toxicity. Most pesticides do not differentiate between pests and other incidental lifeforms. Improper use of these chemicals can be harmful to the environment, humans, animals, and other organisms. Pesticides are estimated to poison 500,000 to 1 million and 5,000-20,000 people die every year (Organization and Aquaculture, 1999; Yadav et al., 2015). Agricultural workers contributed to at least half of the poisoned people and 75% of pesticide deaths. The rest are poisoned by eating contaminated food.

2.7.1. Human Health Effects

Pesticides can enter the human body through oral exposure by consuming contaminated food and water, dermal exposure by direct contact with pesticides, and inhalation of pesticide-contaminated air, dust, and vapor (Singh et al., 2016). Pesticides are sprayed during agricultural activities, particularly during the production of fruits and vegetables; they enter soils and groundwater, where they can end up in drinking water and pollute the air. The toxicity of chemicals, as well as the length and magnitude of exposure, can all have a negative impact on human health (Lorenz, 2009). Chemical toxicity depends on the route of exposure (oral, dermal, and inhalation), the nature of the toxicant, the dose, and the organism. Toxicity can be either acute or chronic. Acute effects are harmful effects that occur as a result of a single exposure by any root of entry, which can be determined by examining test animals' inhalation, dermal, and oral toxicity. The application of pesticides on agricultural fields, whether intentional or unintentional, causes acute illness in

humans. It generally appears shortly after pesticide exposure (Dawson et al., 2010; Lee et al., 2011).

Chronic effects are any adverse effects that result from repeated small doses over a period of time. Some of the suspected chronic effects of pesticide exposure include birth defects, fetal toxicity, production of malignant tumors, genetic changes, blood disorders, nerve disorders, endocrine disruption, and reproductive effects. Chronic pesticide toxicity is more difficult to determine through laboratory testing than acute toxicity. Chronic illness in humans is caused by repeated and continued exposure to pesticides over a long period of time (which can range from several years to decades) (Germany, 2012). Symptoms are not immediately observed but will appear later. Some of the most common chronic diseases resulting from long-term exposure to pesticides are neurodegenerative diseases such as cancer (pediatric and adult brain cancer, renal cell cancer, lymphocytic leukemia, and prostate cancer), Parkinson's disease, Alzheimer's disease, cardiovascular diseases, including artery diseases, diabetes (type 2 diabetes), reproductive disorders, birth defects, hormonal imbalances, including infertility and breast pain and respiratory diseases (asthma, chronic obstructive pulmonary disease).

2.7.2. Environmental Effects

Extensive use and subsequent disposal of pesticides by institutions, farmers, and the public resulted in numerous potential sources of pesticides in the environment. Pesticides can easily disperse in the air, absorbed in the soil, or dissolved in water when sprayed in small agricultural areas, eventually reaching a much larger area. Its fate may vary once released into the environment. Direct application of pesticides to the environment can lead to pesticides washing off the soil and reaching nearby waters by runoff or percolating through the soil to reach lower groundwater (Sarmah et al., 2004). The effects of pesticides on the environment range from minor disruptions

to the normal functioning of ecosystems to the loss of biodiversity. The use of pesticides can have long-term effects. For example, long-lasting organochlorine pesticides in the environment contaminate groundwater, surface water, food, air, and soil.

i. **Impacts on the non-target organism**: Most insecticides used to control pests have the potential to harm non-target organisms such as earthworms, natural predators, and pollinators (Ware, 1980). This type of pesticide application leads to a reduction in earthworm populations. For example, some organophosphorus and carbamate pesticides are toxic to earthworms and reduce earthworm populations (Yadav and Devi, 2017). As a result, natural enemies such as predators and parasitoids are the most vulnerable to pesticides and are seriously affected. Reducing the number of destruction by these predators can worsen the problem of pests (Vickerman, 1988). Pollinators such as fruit flies, some beetles, bees, and birds are bioindicators of ecosystem processes affected by environmental pressures from insecticide application (Kevan, 1999). The use of pesticides causes direct loss of pollinators and indirect crop loss due to a declining population of pollinators (Fishel and Ferrell, 2010).

ii. **Loss of biodiversity**: Biological health is often measured in terms of biodiversity. The number of organisms living in balance with the environment was used to determine environmental health. Different types of organisms are dependent on different environments, from microorganisms to insects such as ants, wasps, and beetles, large animals such as birds and elephants, wild dogs, lions, tigers, foxes, wolves, and predators such as wild dogs, lions, tigers, foxes, wolves, and bears. That system is capable of maintaining balance without the dominancy of one species. The pests themselves can be beneficial to the biological system by controlling and consuming other pests. Therefore, endangering a single species from the use of pesticides can lead to significant changes that can lead to extinction in the environment. Pesticides, on

the other hand, may result in the extinction of a species critical to the overall functioning of the community, or they may promote the dominance of undesirable species, disrupting the dynamics of the food web in the community by breaking the existing nutritional linkages between species.

iii. **Impacts on soil micro-flora**: Nontarget pesticides used in agricultural activities accumulate in the soil. Furthermore, the indiscriminate and repeated use of insecticides exacerbates soil accumulation. Pesticides have an impact on soil microflora and properties due to a variety of transport, degradation, and adsorption/desorption processes (Hussain et al., 2009). The interaction between the degradable pesticide and the soil and the indigenous microorganism changes the diversity of microorganisms, biochemical reaction, and enzymatic activity. Finally, this disrupts soil fertility and the soil ecosystem (Hussain et al., 2009; Muñoz-Leoz et al., 2011). Pesticides can also kill or inhibit certain microorganisms by removing them from the competition (Hussain et al., 2009). Nitrogen fixation, ammonification, and nitrification are all essential biochemical reactions in the soil that can be harmed by activating or deactivating soil microorganisms or enzymes (Hussain et al., 2009; Muñoz-Leoz et al., 2011).

iv. **Impacts on water and air ecosystem**: Pesticides enrich water bodies in a variety of ways, including industrial effluent, accidental spillage, runoff and transport from spray equipment washing after spray operation, pesticide-treated soils, drift into lakes, river water, and streams ponds, and aerial spray to control water-inhibiting pests (Singh and Mandal, 2014). Similarly, the insecticide presence in the air is caused by a variety of factors, including volatilization, spray drift, and aerial pesticide application. The rate of volatilization of pesticides is affected by the time of treatment, the surface on which the pesticides settle, humidity, ambient

temperature, wind speed, and the vapor pressure of the ingredient, which poses a significant risk of atmospheric pollution in large cities (Trajkovska et al., 2009).

2.8. Classical Sample Preparation Techniques for the Analysis of Pesticide Residues

2.8.1. Liquid-liquid Extraction

Liquid-liquid extraction (LLE) is a classical sample pretreatment method of environmental, biological, and food samples for routine pesticide analysis (Carter-Franklin et al., 2007; Kataoka, 2003). LLE is the most common extraction method, but it is time-consuming, tedious, offers low enrichment of analytes, the formation of emulsions, requires large amounts of toxic organic solvents, and is not sensitive enough for trace analysis (Albero et al., 2005; Ravelo-Pérez et al., 2008; Topuz et al., 2005; Vogt and Heinig, 1999).

LLE is widely used to extract non-polar pesticides such as organophosphorus and organochlorine pesticides from water samples using organic solvents such as cyclohexane and hexane. Its applications also tend towards medium polar organic compounds, carbamate, triazine, and urea pesticides successfully extracted with dichloromethane or chloroform (Tadeo, 2019). LLE has been used for other matrices, including analysis of multiresidue of pesticides from fruits and vegetables with acetone followed by partitioning with dichloromethane (Gelsomino et al., 1997), wine and grapes (Miliadis et al., 1999), honey with acetonitrile: ethyl acetate (de Pinho and Neves, 2010), crayfish and rice samples with methylene chloride (Zhou et al., 1996), rice, seeds, and grain with acetonitrile (Akiyama et al., 2002).

2.8.2. Solid-phase Extraction (SPE)

Solid-phase extraction (SPE) was first introduced in the mid-the 1970s and became commercially available in 1978 (Hennion, 1999). It is the most widely used pretreatment alternative to the classical liquid-liquid extraction (LLE) of the environment (Kampioti et al., 2005; Li et al., 2009), food (Sanchez et al., 2006), and biological samples (De Alwis et al., 2006). SPE is recognized as a useful alternative to LLE because it overcomes many of the shortcomings of the latter approach (Zygler et al., 2010). It offers simplicity, the potential for polar pesticide extraction, faster analysis times, lower costs, and reduced amounts of organic solvents and disposal. In addition, the entire process can be automated (Raoul et al., 1997; Zygler et al., 2010).

The separation process comprises the partition of organic compounds dissolved in water between a solid sorbent and an aqueous phase, due to which analytes are selectively trapped on this sorbent (Lord and Pawliszyn, 2000). The trapping process is controlled by the following mechanisms:: (i) adsorption of the analytes dissolved in water on the surface of the sorbent (solid phase), primarily by Van der Waals forces, hydrogen bonds, hydrophobic effects, p-electron interactions, and cation- and anion-exchange processes; (ii) possibility of dissolving the analyte in some organic solid sorbents; (iii) partition of the analyte between the sample in the form of a thin film coated or chemically bound to a solid support and the liquid sorbent (liquid stationary phase) (Wardencki et al., 2007). This method is based on the omission of the extract containing the target analyte through a column filled with the appropriate adsorbent or bypassing the appropriate solvent through the SPE column to which a suitable amount of the sample was previously added. The selective solvent can be used to first elute the co-extract from the SPE column and then the target analyte.

Alternatively, if undesirable co-extracts from the sample matrix remain on the SPE column, the analyte can be eluted directly.

2.9. Modern Sample Preparation Techniques for Pesticides Analysis

2.9.1. Solid-phase Microextraction

Solid-phase microextraction (SPME) is a relatively new technique introduced in the early 1990s by Lord and Pawliszyn (2000). SPME is simple to automate, rapid, solvent-free extraction method, and employed reagents can be reused (Baltussen et al., 2002; Vas and Vekey, 2004). This method allows analysis of samples in the three-physical state (liquid, gas, and solid), which is used for extraction of both volatile and nonvolatile compounds from different matrices and determines trace or ultra-trace levels of organic and inorganic analytes from a sample of complex matrices (Li et al., 2015a; Płotka-Wasylka et al., 2015). It is a simple two-stage technique that includes the sorption of analytes into the sorbent phase and desorption (solvent or thermal) of analytes from the sorbent phase and their introduction into separation or detection devices for analysis (Namiesnik et al., 2015; Płotka-Wasylka et al., 2015). In microextraction, the equilibrium of analytes between the sample and fused silica (metal fiber) coated with the appropriate sorption material mounted to the syringe needle. The type and nature of the coating affect the efficiency of the extraction and final sensitivity of the analysis (Amiri, 2016; Płotka-Wasylka et al., 2015).

Based on the position of the fibers with respect to the sample, microextraction can be applied in two modes (Płotka-Wasylka et al., 2015). Direct SPME (DI-SPME), where the fiber coating is exposed to gas or liquid samples, and the analytes are transferred directly from the matrix to the stationary phase (Figure 8a). Head space SPME (HS-SPME) analysis is primarily used for sampling gases or volatile compounds. Here, the fiber coating is exposed to the gaseous headspace

above the sample and the analytes are transferred from the sample to the gas phase. The gas phase is in direct contact with the sample to avoid fiber contamination and improve selective SPME while prolonging its lifetime (Figure 8b) (Ma et al., 2012; Malik et al., 2006).

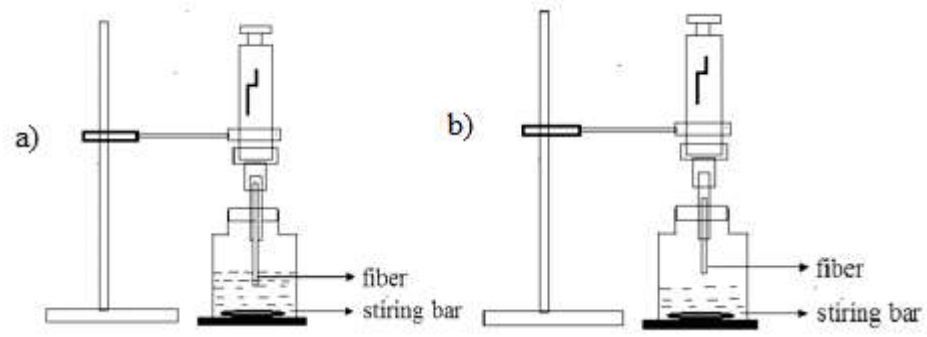

Figure 8. Schematic diagram of DI-SPME (a) and HS-SPME (b) (Adapted from Zhang et al., (2012)).

2.9.2. Liquid-phase Microextraction (LPME)

The main difference between single-drop microextraction (SDME) and LPME is the form of the analyte-acceptor phase. The solvent is in the form of a suspended drop and placed in a hollow fiber in SDME and LPME, respectively (Lambropoulou and Albanis, 2007a). A single configuration o f LPME combines analyte extraction, preconcentration, and sample injection as compared to clas sical LLE (Farajzadeh et al., 2014b). The three main categories of LPME are SDME, hollow fibe r liquid-phase microextraction (HF-LPME), and dispersive liquid-liquid microextraction (DLLM E). Analytes are transferred from the donor phase (usually aqueous) to the acceptor phase through an organic phase immobilized in pores in the hollow fiber. In the two-phase mode, the solvent in the pores of the fiber is the same as the solvent present in the fiber (Figure 9). In three-phase mode, the solvent introduced into the pores of the fiber is different from the solvent inside the fiber (Figure 9). Three-phase mode is applied to extract polar analytes whereas the two-phase mode is

used to extract non-polar and semi-polar analytes. The amount of solvent in the fiber is about 10-25 µL (Rasmussen and Pedersen-Bjergaard, 2004).

The selection of solvent is a critical parameter for LPME application as in LLE. Thus, the solvent should have a good affinity to the target analyte, low water solubility, good stability during the whole extraction procedure, and excellent chromatographic behavior. The nature of disposable hollow fiber eliminates the possibility of cross-contamination, thus providing enhanced reproducibility. As it has a small pore size which prevents large molecules and particles present in the donor solution from entering the acceptor phase providing effective matrix/analyte separation (Delavari, 2015). The advantage of LPME over SDME is the presence of fibers that support organic solvents. This slows down the process of solvent dissolution or evaporation (in HS-SDME mode). However, a disadvantage of LPME is a lack of precision, which may be caused by the completely manual operation, from fiber preparation and conditioning to the handling of extract.

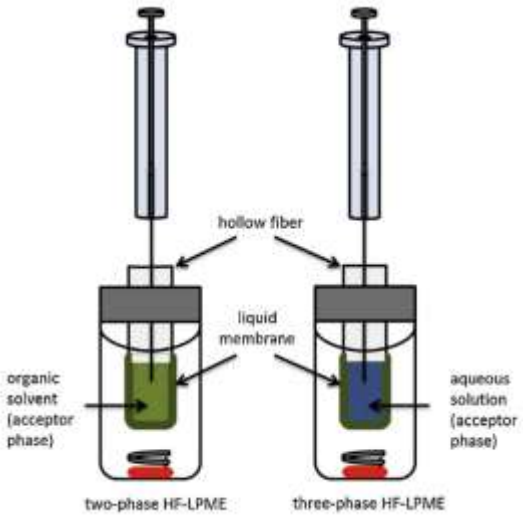

Figure 9. Liquid-phase microextraction: Two-phase and three-phase HF-LPME configurations (Adapted from Filippou et al. (2017)).

2.9.3. Single-drop Microextraction

The single-drop microextraction (SDME) technique uses a suspension of a micro drop (1-10 μL) of water-immiscible organic solvent in an aqueous solution (Farajzadeh et al., 2014a). SDME modes are schematically given in Figure 10 which is a new, simple, fast, and environmentally friendly method (Li et al., 2007). The methodology of SDME is based on two-phase and three-phase distribution systems. Direct immersion SDME (DI-SDME) is the simplest two-phase system, where a solvent micro drop hanging from the tip of a microsyringe needle is directly immersed into the aqueous phase. Headspace SDME (HS-SDME) is the simplest three-phase system, where the micro drop is suspended in the vapors, which consist of the volatile compounds, formed over the aqueous sample. After extraction is completed, the droplet is pulled back into the microsyringe and injected into an analytical instrument. Mass transfer and higher extraction efficiency can be achieved by rapid stirring (Asensio-Ramos et al., 2011a; Farajzadeh et al., 2014b; Han and Row, 2012). Drop stability can be affected by intense conditions such as high stirring speeds, extended extraction period, and high temperatures, as well as suspended particles in dirty samples. There is also a matrix interference with DI-SDME, whereas completely absent in HS-SDME application (Farajzadeh et al., 2014b). Since the organic solvent is a critical factor in SDME, high purity, water immiscible solvents, such as dichloromethane, trichloromethane, carbon tetrachloride, hexane, cyclohexane, and xylene, usually constitute the micro drop. 1-octanol, toluene, dodecanol, and undecanol are also used because of their compatibility with GC systems (Farajzadeh et al., 2014a; Spietelun et al., 2014).

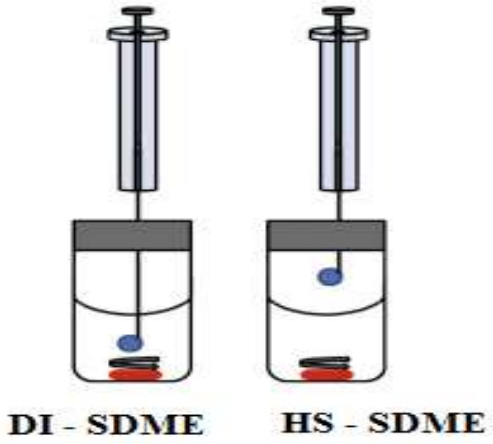

Figure 10. Schematic Diagram of SDME modes: DI- and HS-SDME (Adapted from Filippou et al. (2017)).

2.9.4. Dispersive Liquid-liquid Microextraction Method

Rezaee et al. (2006) successfully introduced the first DLLME procedure as inexpensive, fast, simple, and environmentally friendly extraction technique based on the ternary solvent system. When the disperser and extractant are mixed and rapidly introduced into the aqueous solution, a cloudy solution appears, indicating the equilibrium between the fine droplets of the extraction solvent and the aqueous sample. The emulsified droplets have a high interface between the extraction and the aqueous sample achieved in a few seconds, and the extraction is almost instantaneous (Ban et al., 2000; Demeestere et al., 2007). In addition, compared to traditional solvent extraction methods, DLLME is easier to operate, faster, cheaper, easier to handle, environmentally friendly, consumes less organic solvent, has a higher EF and is compatible with both GC and Liquid chromatography (Farré et al., 2010; Tankiewicz et al., 2011).

DLLME limitations are primarily related to extraction solvent requirements. The success of the extraction depends on the choice of extraction and dispersion solvent and its volumes (Hyötyläinen

and Riekkola, 2008; Rezaee et al., 2006). The extraction solvents should have low water solubility, has the ability to extract the target analytes, and needs to be compatible with the analytical instrument used. Furthermore, when injected into the sample with the disperser solvent, it should form a cloudy solution. Because of these characteristics, the use of extraction solvents is limited, particularly when a solvent with a higher density than water (like chlorobenzene, chloroform, carbon tetrachloride, or tetrachloroethylene) is required than water should be used (Kocúrová et al., 2012). Traditionally, chlorinated solvents are used, but they are toxic solvents, albeit in small amounts. Also, most chlorinated solvents are non-polar, limiting the extraction of more polar compounds. Halogenated hydrocarbons commonly used as extraction solvents are dense and incompatible with reverse phase LC elution modes that require additional steps to evaporate them prior to LC analysis (Rezaee et al., 2010).

Due to these disadvantages, several modifications have been proposed aimed at making the techniques more environmentally friendly and robust. The changes include new devices and less toxic solvents, expanding the operating range of DLLME. Alternatives such as automatization, use of less toxic and safe extraction solvents (ionic liquids, surfactants, etc.), use of solvents with a lower density than water (methanol, ethanol, acetonitrile, acetone), extraction without the dispers er solvent, the elimination of the centrifugation step, the use of ultrasound and use of vortex have been a focus of interest in the analytical chemistry (Kocúrová et al., 2012; Spietelun et al., 2014). Several factors affect the extraction efficiency of DLLME, including the type and volume of extraction and dispersion solvents, extraction time, sample amount, pH, and salt addition (Herrera-Herrera et al., 2010). The most important parameters are related to the selection of disperser solvent for the extraction of the analytes. A suitable disperser solvent should be miscible with both the extraction and aqueous phases for the formation of the cloudy solution that enhances the

interaction between the two phases, as these interactions give rise to high extraction efficiency (Yilmaz and Soylak, 2016).

2.9.5. QuEChERS (Quick, Easy, Cheap, Effective, Rugged and Safe) method

Anastassiades and his coworkers developed the QuEChERS (quick, easy, cheap, effective, rugged, and safe) procedure in 2003 as a new technique for extracting pesticides from vegetables and fruits (Anastassiades et al., 2003). Since then, it became a highly versatile technique that has been applied to a diverse range of substances and matrices (Romero-González et al., 2011; Wiest et al., 2011). This basic procedure is based on a liquid partitioning with acetonitrile followed by a dispersive SPE clean-up with primary secondary amine (PSA) (Anastassiades et al., 2003; Lehotay et al., 2005b). The basic procedure consists of two steps. The homogenized sample is extracted and partitioned using a water-miscible organic solvent in the presence of salts and/or buffers, respectively, to induce liquid separation and stabilize acid or base sensitive analytes. After shaking and centrifuging, the supernatant can be further extracted and purified using the dispersed solid phase extraction (DSPE) technique. Again, the mixture can be centrifuged and the supernatant directly analyzed or concentrated as needed.

The extraction solvent used in this technique is acetonitrile, ethyl acetate, or acetone, but other solvents can be used (Lesueur et al., 2008; Maštovská and Lehotay, 2004). Acetonitrile is the recommended solvent because it separates from water more easily than acetone, allows for better removal of residual water with magnesium sulfate, and has fewer lipophilic compounds such as fat, pigments, and waxes co-extracted from the matrix (Lehotay, 2007). However, this solvent has drawbacks such as a large expansion of the solvent during GC evaporation, interference with the GC detector, and considerable toxicity. Another option is acetone, a water-miscible organic solvent that allows extraction in a single extraction step (Cunha and Fernandes, 2011; Maštovská and

Lehotay, 2004). Ethyl acetate has the advantage of being partially miscible with water, but at the same time, it extracts lipids and waxes, resulting in lower recovery of basic compounds (Maštovská and Lehotay, 2004). Extraction of several pesticides from various food matrices has been successfully evaluated using acetonitrile, such as barley, fruits, and baby foods (Anastassiades et al., 2003; Lambropoulou and Albanis, 2007b; Lehotay et al., 2005b).

Depending on the solvent used, the addition of salts induces phase separation and leads to higher recovery rates of polar compounds because of the "salting out" effect (Brondi et al., 2011; Li et al., 2011). Also, the addition of drying agents such as magnesium sulfate or sodium sulfate improves recovery rates, as they reduce the water phase and promote partitioning of the compounds into the organic phase (Brondi et al., 2011; Kvíčalová et al., 2012). Magnesium sulfate is preferable to other salts as it has a higher capacity for water removal and hydration is an exothermic reaction. Thus, heating to 40-45°C helps extraction/partition, especially for nonpolar compounds.

Regarding the promoting of section separation and the salting-out effect, an extensive variety of various salts, which include magnesium sulfate, sodium sulfate, ammonium acetate, sodium chloride, sodium acetate, sodium citrate tribasic dihydrate, sodium citrate dibasic sesquihydrate, and combinations of those had been tested to induce acetonitrile/water phase separation during the analytes extraction step (Lu et al., 2018; Ruiz-García et al., 2016; Zhou et al., 2018) (González-Curbelo et al., 2014). Overall, the 2:1 or 4:1 ratio of $MgSO_4$ and NaCl combination ($MgSO_4$:NaCl, w/w) is the most widely used in QuEChERS extraction (Dušek et al., 2016; Fontana and Bottini, 2016; Hamed et al., 2017; Rejczak and Tuzimski, 2017; Shabeer et al., 2018), since $MgSO_4$ allows best salting-out of acetonitrile and co-extracting some undesirable polar compounds from sample

matrix-like sugars, whereas NaCl controls the polarity of the extraction solvents and thus increases the selectivity of extraction (Rejczak and Tuzimski, 2015).

The QuEChERS method has the advantages of high recovery, consume low solvent volume, and glassware, less labor and bench space, ruggedness, and lower reagent costs (Hercegová et al., 2006; Lehotay et al., 2005a; Lehotay et al., 2005b). During the cleanup process, organic acids and other potential contaminants are removed. The main drawback of QuEChERS is that at 1 g of sample per milliliter of final extract, the concentration of the extract is lower than that of the concentrated extract obtained by most conventional methods. As a result, the final extract must be concentrated to a greater extent in order to provide the required sensitivity and achieve the desired limits of quantification. Despite this limitation, quantitative results from a large number of pesticides show that combining QuEChERS with hyphenated methods of detection allows scientists to achieve efficient and effective pesticide residue monitoring in food.

3. MATERIALS AND METHODS

3.1. Chemicals and Reagents

All pesticide standards (carbaryl, carbosulfan, chlorpyrifos, furathiocarb, malathion, and methomyl) were of analytical grade with purity above 98% and purchased from Sigma Aldrich (St. Louis, USA). AChE (EC 3.1.1.7, Type VI–S, 500 UN from Electrophorus electricus), primary-secondary amine (PSA), DTNB (purity > 98%) as chromogenic substance, acetylthiocholine iodide (ATChI) (purity > 98%) as artificial substrate, bovine serum albumin (BSA) (purity > 98%) for enzyme stabilizer, tris(hydroxymethyl)aminomethane (Tris) (purity > 98%), and activated charcoal for the cleanup were purchased from Sigma-Aldrich (St. Louis, USA). HPLC grade acetonitrile, methanol, acetone, and ethanol were purchased from BIOCHEM Chemopharma (ZA Cosne Sur Loire, France) and used as a solvent. Sodium hydroxide pellets, sodium chloride, anhydrous magnesium sulfate, and hydrochloric acid were obtained from HiMedia Laboratory (LBS Marg, Mumbai, India). Deionized water was used throughout the study to prepare a buffer solution, which was used to prepare the working solution of enzymes and substrate.

A Tris buffer stock solution (10 mM) of pH 8.0 was prepared in deionized water and stored at 2–8°C. The solution pH was adjusted by using 2.0 M HCl and NaOH solutions. The stock solutions of ATChI (50 mM) and BSA (1 mg mL^{-1}) were prepared in Tris buffer and stored at 2–8°C until used. The stock solution of AChE (100 U mL^{-1}) was prepared in Tris buffer and kept in a freezer at -20°C until used. The stock solution of DTNB (50 mM) was prepared in ethanol and kept at 2–8°C. Pesticides stock solution (250 mg mL^{-1}) was prepared in methanol and stored at 2–8°C and protected from ambient light. Working solutions of ATChI, AChE, DTNB, and pesticides were

prepared daily by diluting the stock solution to the desired concentration using Tris buffer, BSA solution, ethanol, and Tris buffer solution containing 4% of methanol, respectively.

3.2. Apparatus

A wax printer (ColorQube 8580N, Xerox, CT, USA) was used to print the design of the μ-PADs on a sheet of filter paper (200 × 200 mm, Chromatography Paper 1CHR, Whatman™, GE Healthcare Lifesciences, UK). A drying machine (DHG-9055, Zhengzhou, Henan, China) was used to heat the printed sheets of the paper to penetrate wax to the backside of the sheets. A desktop scanner (Canon PIXMA G2400 Series, Shihen, Vietnam) was employed to capture images of the μ-PADs that were dried before scanning. An electronic balance (Adam Equipment Company, UK) was used for weighing during various experiments. To measure pH values Adwa pH meter, model 1020 (Romania) were used. A centrifuge, Model 800 (China, Beijing), and EXL 3 water purification system (VIVAGEN. Co. Ltd., South Korea) were used in the process of sample preparation and analysis.

3.3. Design and Fabrication of μ-PADs

The pattern of the device was designed in the form of a paper zone using Microsoft Office PowerPoint 2016 as shown in Figure 11. A well-shaped pattern was created with a diameter of 10 mm serving as a detection zone on the paper. The blue color was identified as a hydrophobic zone, which can be easily distinguished from the final yellow color expected in the hydrophilic zone. The designed layers were printed on a sheet of filter paper (Chromatography Paper 1CHR, WhatmanTM, GE Healthcare Lifesciences, UK) using a wax printer at Okayama University, Japan. The patterned paper was heated at 150 °C for 2 min in an oven in order to melt the wax and create a hydrophobic barrier throughout the thickness of the Whatman filter paper (Carrilho et al.,

2009a). The printed blank µ-PADs were transported to Ethiopia, where reagents for the detection of pesticides were optimized. Finally, the backside of the device was sealed with scotch tape and was ready for reagent and target analyte loading for colorimetric determination.

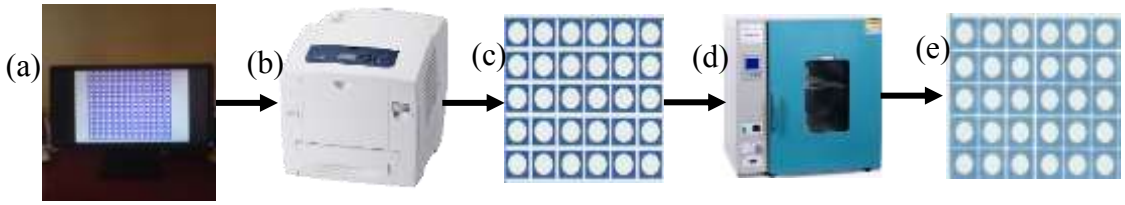

Figure 11. Fabrication processes of µ-PADs: µ-PADs design (a), wax printer (b), printed µ-PADs (c), drying machine (d) and heated µ-PADs.

3.4. Assay Procedure of Pesticides Analysis

As shown in Equation 1 the concentration of the pesticides was calculated as a ratio of the difference in initial AChE activity (control) and final AChE activity after incubation with pesticides to the original enzyme activity. The percentage of enzyme inhibition was determined and a calibration curve was constructed by plotting the pesticide concentration against inhibition percentage (Nouanthavong et al. (2016). The assay procedure for the control (where no pesticide was added) was carried out by the addition of DTNB solution to the test zone and dried for 5 min at room temperature (Figure 12a). Then, AChE solution was loaded on the paper and dried for 15 min at room temperature. Finally, ATChI solution was added to the paper zone. The yellow color intensity was developed instantly after adding ATChI substrate to the detection zone and dried for 5 min at room temperature, image was scanned and analyzed. The same procedure was followed except for incubation of each pesticide by mixing 5 µL of 9 U mL^{-1} AChE and 5 µL of each pesticide solution in a test tube followed by incubation for 10, 15, 15, 5, 10, and 20 min for

carbaryl, carbosulfan, chlorpyrifos, furathiocarb, malathion, and methomyl pesticides, respectively. The presence of pesticides reduces the activity of AChE and results in reduced yellow color intensity (Figure 12b). However, high concentrations of pesticides inhibit the total activity of AChE, as manifested in the absence of yellow color (Figure 12c).

$$\text{Inhibition percentage (I\%)} = ((Io - Ii)/Io)*100 \qquad (1)$$

Where Io and Ii represent the initial AChE activity and final AChE activity after incubation with pesticides, respectively.

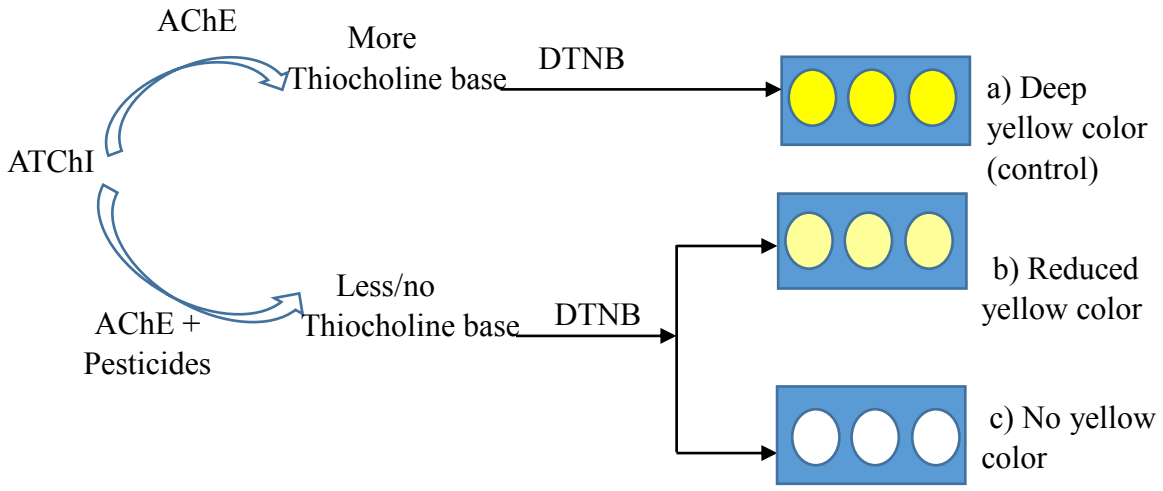

Figure 12. Assay procedure of µ-PADs for the analysis of pesticides.

3.5. Quantitative Image Processing

The developed color intensity was inversely correlated with the target analyte concentration for quantification due to the inhibitory effect of pesticides. The color signal generated by the reaction of AChE, DTNB, and ATChI can be determined by naked eyes for qualitative analysis. For further quantitative analysis, the color image on the µ-PAD in the form of Joint Photographic Experts Group (JPEG) was captured by using a desktop Scanner. ImageJ 1.46s software (National Institutes of Health, USA) was used to analyze the region of interest (ROI) of the images. A

procedure reported by Nouanthavong et al. (2016) was followed for color intensity analysis of ImageJ software. Eight-bit mean grayscale value was set and adjusted based on the gray intensity to yield higher intensity values. Finally, the blue-colored wax background was effectively removed by applying a color threshold window and inverted. The color intensity at a test zone was measured as a mean gray color intensity in the RGB (Red, Green, and Blue) channels.

3.6. Method Validation for the Univariate Optimization of μ-PAD

The univariate optimization technique was carefully studied in order to achieve a final complex formation reaction, thus, the highest sensitivity and maximum mean color intensity. Nine experimental variables were carefully and independently investigated to obtain optimal experimental conditions. This included the effects of the concentrations (AChE, ATChI, and DTNB), volumes (AChE, ATChI, and DTNB), incubation time, image capturing time, and storage temperature. In this optimization technique, only one parameter is changed while others are kept constant at a specific value to monitor the former's influence on the experimental response (Bezerra et al., 2008).

Once the experimental parameters were optimized, the analytical merits of the method were assessed under the optimized conditions. Linearity was studied in the concentration range of 1 to 16 mg L^{-1} and triplicate analyses were carried out at each concentration level. The limit of detection (LOD) was calculated as three times the standard residuals of the response divided by the slope of calibration curves (Shrivastava and Gupta 2011). For repeatability (intra-day precision), the concentration levels in the linear range were analyzed in triplicate on the same day under the same experimental conditions. Similarly, the intermediate precision (inter-day precision) was evaluated in triplicate analysis of pesticides concentration on three different days under the

same experimental condition. The accuracy of the developed method was determined after DLLME extraction of spiked tap water with 1 mg L^{-1} of each pesticide standard solution. The DLLME procedure was carried out according to Chen et al. (2010).

3.7. Multivariate Optimization of µ-PADs

Analytical method optimization by the design of experiment (DOE) has been frequently used because of its advantage of reducing the number of experimental sets, which results in lower consumption of chemicals and considerably less laboratory work (Ferreira et al., 2007). Response surface methodology is a statistical and mathematical technique for designing experiments, determining the optimal operating conditions, and fitting the models (Bezerra et al., 2008; Box and Draper, 1987; Lundstedt et al., 1998). It is also used to identify relationships among the effects of experimental variables. MODDE software version 13 (Umetrics, Umeå, Sweden) was used in the DOE using Box − Behnken design (BBD). BBD is the second-order design and one of the most efficient methods using the three-factor, three-level design to validate and investigate process parameters affecting assay (Dehghani et al., 2017). The independent variables such as concentrat ions (AChE (A), ATChI (B), and DTNB (C)) and volumes (AChE (D), ATChI (E), and DTNB (F)) were selected for optimization. Each variable was studied at three level codes as -1 (low), 0 (central point), and +1 (high) (Bagheri et al., 2017). The levels and ranges of the factors used in this study are presented in Tables 1 and 2. The total number of experimental runs in each case (both for concentration and volume) was 15 which included three central points and 12 factorial points based on the following equation 2.

$$N = 2k\,(k-1) + Co = 2*3(3-1) +3 = 15 \qquad (2)$$

Where k is the number of factors, and Co is the number of central points.

A statistical analysis of variance (ANOVA) based on BBD was used to determine the suitability, fitness, and significance of the model coefficients. Various statistical parameters provided by the MODDE software, namely, ANOVA, lack of fit test, and multiple determination coefficient (R^2) tests, were used to determine the model significance. *F*-test was also applied to determine the significance of the effects.

Table 1. Range and levels of parameters in BBD for concentration optimization

Parameters	Symbol	Levels		
		-1	0	1
Concentration of AChE (U mL^{-1})	A	1	6.5	12
Concentration of ATChI (mM)	B	1	3	5
Concentration of DTNB (mM)	C	1	3	5

Table 2. Range and levels of parameters in BBD for volume optimization

Parameters	Symbol	Levels		
		-1	0	1
Volume of AChE (µL)	D	0.5	1.5	2.5
Volume of ATChI (µL)	E	0.5	1.5	2.5
Volume of DTNB (µL)	F	0.5	1.5	2.5

3.8. Multivariate Optimization of DLLME

3.8.1. DLLME Procedure

A tap water sample was collected from Addis Ababa University, Arat Kilo campus. Then DLLME was carried out under optimized parameters. A 5 mL water sample was taken in a 5 mL volumetric flask and 4.8% (w/v) NaCl was added and then spiked with different standard concentrations of target analytes (one concentration level of a single analyte is spiked at a time).

As it is shown in the schematic procedure of the DLLME, a mixture of acetone (0.48 mL) and *n*-hexane (47 µL) was injected into the sample solution using a 1.5 mL syringe (gastight, Hamilton, USA) (Figure 13a). A cloudy solution (water/acetone/*n*-hexane) was formed in the solution, and at this stage, the pesticides in the water sample were extracted into fine droplets of *n*-hexane (Figure 13b). After 6 min, more acetone (0.48 mL) was slowly injected into the aqueous bulk as a demulsifier to break the emulsion (Figure 13c). The emulsion was then separated into two phases in 5-10 s (Figure 13d). A microsyringe was then used to collect the organic phase (Figure 13e). The organic phase was dried at room temperature for 6 h and the residue was reconstituted with 50 µL methanol. The reconstituted sample was incubated with AChE, and 1.7 µL of the incubated mixture was added to the detection zone for µ-PAD analysis.

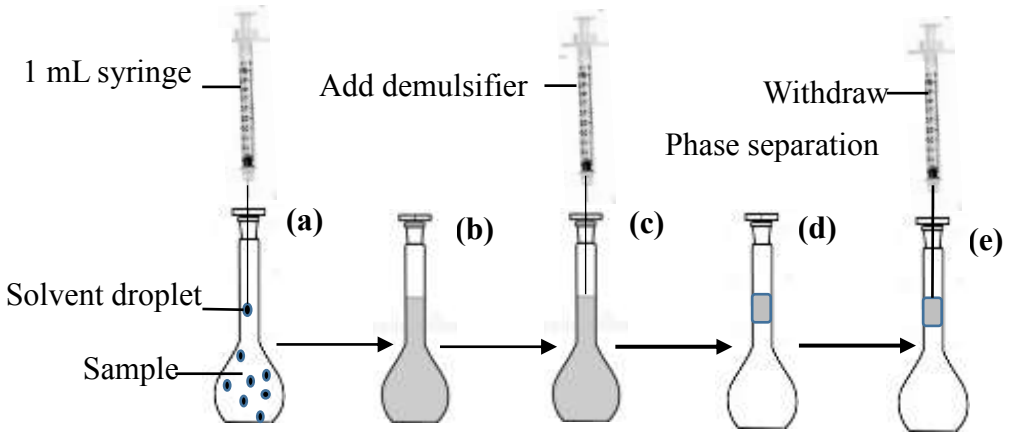

Figure 13. Schematic procedure of DLLME: Injection of extraction solvent and disperser solvent into the aqueous sample (a), formation of emulsion for extraction (b), addition of terminating solvent to break up the emulsion (c), phase separation (d), and collection of low-density extraction solvent in the upper layer (e).

3.8.2. Experimental Design

The extraction procedure was optimized using the BBD. MODDE software was used to optimize and model the values of independent parameters such as volume of extraction solvent *n*-hexane (A), the volume of dispersive solvent acetone (B), extraction time (C), and NaCl amount (D). During the optimization process, carbaryl pesticide was used as a representative pesticide in this study. In each of the four studied variables, high and low setpoints were selected to design the experiment and were coded at three levels (-1, 0, and +1) corresponding to low, middle, and high levels. Therefore, a total of 27 experimental runs were designed based on the equation $N = 2k (k-1) + Co$. Where N, k, and Co represent the total number of experimental runs, the number of factors, and the replicate number of central points, respectively (Table 3). ANOVA was used to evaluate the goodness-of-fit determination of the mathematical model to the experimental data

using the coefficient of determination (R^2) and the adjusted coefficient of determination (R^2 *adj*). In addition, Fisher *F*-test was used to examine the consistency of the model and the model term was evaluated as a *p*-value with a 95% confidence level.

Table 3. Design matrix in the BBD for DLLME extraction parameters optimization

Parameters	Code	Levels		
		-1	0	1
Volume of *n*-hexane (µL)	A	30	50	70
Volume of acetone (mL)	B	0.20	0.45	0.70
Extraction time (min)	C	2	6	10
NaCl amount (%w/v)	D	0	5	10

3.8.3. Method Validation

In order to evaluate the performance of the DLLME, the blank tap water samples spiked with all analytes at different concentrations of pesticides were enriched with DLLME and were finally analyzed by the µ-PADs system under optimized experimental conditions. Prior to the spiking procedure, water samples were analyzed and found to be free of pesticide contamination. The EF was defined as the ratio of the concentration of analyte in the organic phase (C_{org}) to the concentration of the initial analyte in the aqueous sample (C_{aq}) and calculated based on equation (3) (Berijani et al., 2006; Rezaee et al., 2006). Linearity was investigated with seven different concentrations levels in the range of 0.625-40 µg L^{-1} for carbaryl, furathiocarb, malathion, and methomyl, and 1.25-40 µg L^{-1} for carbosulfan and chlorpyrifos. Triplicate analyses were performed at each concentration level. The ratio between the amounts of the analytes after spiking (C_f) and analyte standard added (C_a) was calculated as the percent recoveries as indicated in equa

tion (4) (Peris-Vicente et al., 2013). Recoveries at the spiked concentration of 1 and 5 µg L^{-1} were calculated in triplicates for each spiked level.

$$EF = C_{org}/C_{aq} \quad (3)$$

$$\%R = (C_f / C_a) * 100 \quad (4)$$

3.9. Multivariate Optimization of QuEChERS-DLLME

3.9.1. Sample Preparation by QuEChERS–DLLME

The lettuce vegetable sample was collected from a cultivated garden at Yeka Abado residential condominium site (Addis Ababa, Ethiopia). Lettuce samples (150 g) were chopped in a warring blender. The extraction procedure (QuEChERS-DLLME) of pesticides from lettuce vegetables was depicted in Figure 14. (i) 5 g of chopped homogenized fresh sample was added to a 50 mL Teflon centrifuge tube; (ii) pesticides standard of different concentrations were added to previously prepared chopped sample in a Teflon centrifuge tube and kept for 30 min; (iii) 10 mL acetonitrile was added and shaken vigorously for 1 min, (iv) 2 g of $MgSO_4$ and 1 g of NaCl were added and shaken immediately for 1 min; (v) the solution was centrifuged for 3 min at 4000 rpm; (vi) a 7 mL aliquot of the upper layer was transferred into a 15 mL Teflon centrifuge tube containing 150 mg activated charcoal, 80 mg PSA, and 2 g $MgSO_4$; (vii) the extract was centrifuged for 3 min at 4000 rpm and filtered through 0.45 µm filter paper;(viii) 1 mL of the extract was transferred into a volumetric flask containing 4 mL of distilled water (disperser medium); (ix) 47 µL of *n*-hexane as extraction solvent was added and the cloudy solution was formed; (x) 0.5 mL of extract from QuEChERS was added slowly into the aqueous bulk to break up the emulsion and the emulsion was cleared into two phases in 5 to 10 s; (xi) the upper layer was collected using a microsyringe;(xii) the collected organic phase was dried for 6 h at room temperature; (xiii) the residue was reconstituted in 15 µL methanol; (xiv) the reconstituted residue was incubated with

AChE; (xv) the mixture solution was added to the detection zone of the paper-based devices for final analysis.

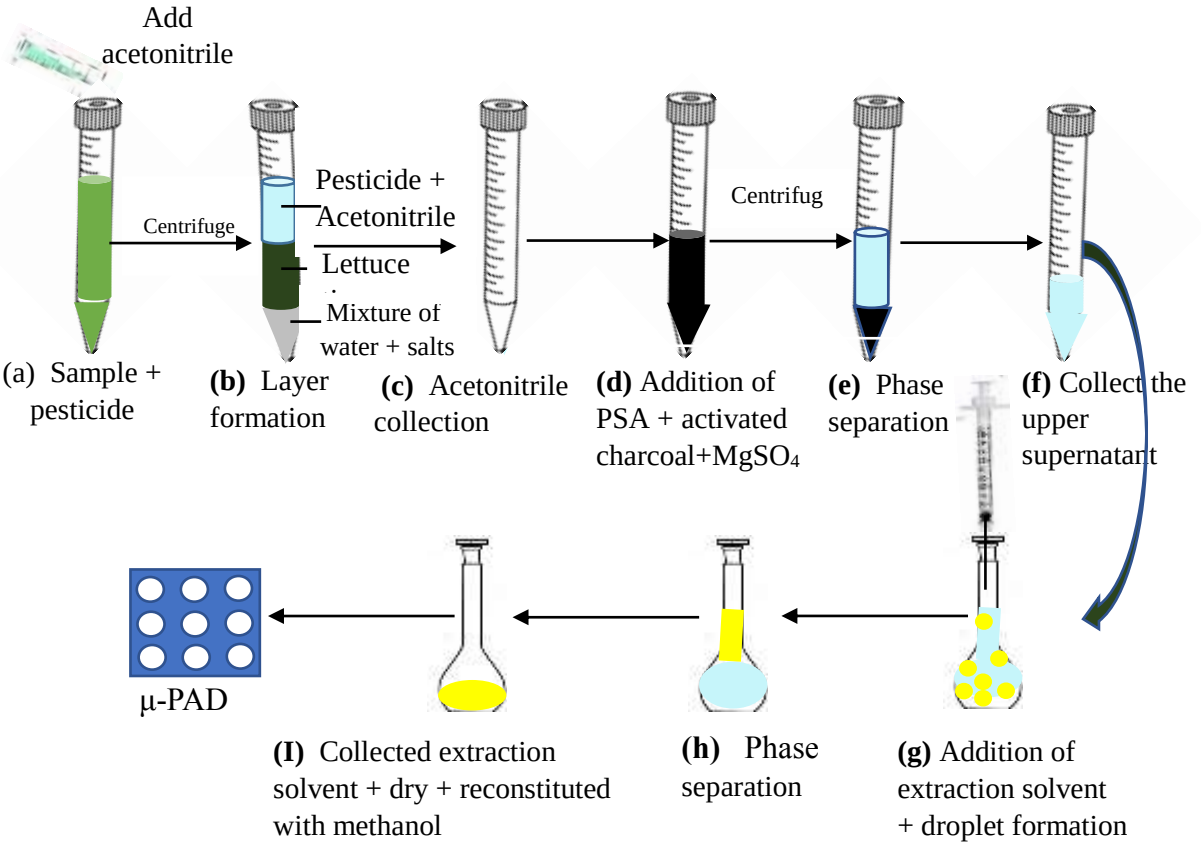

Figure 14. The schematic diagram of the QuEChERS-DLLME procedure; QuEChERS (a-f) and DLLME procedure (g-i).

3.9.2. Experimental Design

Plackett-Burman experimental design (PBD) was used for screening the main variables affecting the extraction efficiency of pesticides. A PBD can examine up to N-1 factor ($f \leq N-1$) in N experiments (N is a multiple of 4) (Dejaegher et al., 2007; Khodadoust and Ghaedi, 2013). A multivariate approach based on 2^{7-4} PBD was used for preliminary screening of the following seven factors: Volume of acetonitrile (A), volume of disperser medium (B), amounts of NaCl (C),

amount of $MgSO_4$ (D), amount PSA (E), amount of activated charcoal (F), and extraction time (G). Each variable was examined at two levels: = −1 for low level and +1 for high level. Table 4 depicts the experimental factors and their corresponding levels used in the PBD. The response was calculated as an inhibition percentage (%) obtained for the analytes.

Table 4. Experimental factors, their levels, and runs studied by PBD for extraction and clean up parameters

Factors	Symbol	Levels	
		Low (-1)	High (+1)
Volume of acetonitrile (mL)	A	5	10
Volume of disperser medium (mL)	B	2	4
Amount of NaCl (g)	C	0.5	2
Amount of $MgSO_4$ (g)	D	1	4
Amount of PSA (mg)	E	80	200
Amount of activated charcoal (mg)	F	150	300
Extraction time (min)	G	5	10

Following the preliminary screening of the most significant parameters, the optimum working conditions were attained using central composite design (CCD) (Box et al., 2005; Bruns et al., 2006). Three quantitative variables (volume of acetonitrile, amount of activated charcoal, and extraction time) were further optimized by CCD. To construct the design, high and low setpoints were selected for each studied variable. The experimental factors and their levels in the optimization process are shown in Table 5. The total number of design points needed (N) is determined by the following equation 5:

$$N = 2^f + 2f + No \qquad (5)$$

Where f and No is the number of variables and center points (f = 3, No = 3), respectively (Morgan, 1995). In this particular work, 17 experiments had to be run for the CCD. The statistical parameters, namely ANOVA, multiple determination coefficient tests, and LOF test, were used to determine the model significance.

Table 5. Design matrix, experimental factors and their levels studied by CCD for QuEChERS–DLLME extraction and clean up parameters

Parameters	Code	Levels		
		Low (-1)	Central (0)	High (+1)
Volume of acetonitrile (mL)	A	5	7.5	10
Amount of activated charcoal (mg)	F	150	225	300
Extraction time (min)	G	5	7.5	10

3.9.3. Method Validation

The performance of the developed analytical method was evaluated based on validation parameters like linearity, LOD, accuracy, and precision. The Lettuce vegetable was selected as a matrix for all the optimization and validation experiments. Linearity was studied using matrix-matched calibrations by spiking the appropriate volumes of standard working solution to 5 g of blank Lettuce vegetable at seven concentration levels (0.01, 0.02, 0.04, 0.08, 0.16, 0.32, and 0.64 mg kg^{-1}). The calibration standards were run in triplicate, and average values were reported. Method accuracy was studied in lettuce vegetable samples spiked at two concentration levels (0.05 and 0.5 mg kg^{-1}) in triplicate analysis. The method precision was studied by determining the percent relative standard deviation (%RSD) at two concentration levels (0.05 and 0.5 mg kg^{-1}). Intra- and inter-day experiments were achieved in a day and for three different days, respectively.

4. RESULTS AND DISCUSSION

4.1. μ-PAD for the Detection of OP and CM Pesticides Using Univariate Optimization

4.1.1. Background of the study

In optimizing analytical methods there are two approaches namely univariate and multivariate. The multivariate optimization schemes are advantageous for involving a design in which the levels of all the variables are changed simultaneously. In contrast, in the case of the univariate commonly named as one-variable-at-a-time (OVAT), only one parameter is changed while others are kept constant at a certain value in order to monitor the former's influence on the experimental response (Bezerra et al., 2008).

However, irrespective of this limitation (demanding more time and costly), the univariate optimization is still being used more frequently than multivariate in the development of μ-PADs. In this section a univariate optimization of the μ-PAD has been used for the analysis of six pesticides of which two CM pesticides (Carbosulfan and Furathiocarb) were not studied before. Furthermore, this study will serve as a baseline for comparison with the multivariate approach employed in the subsequent sections of this dissertation.

4.1.2. Optimization of parameters affecting μPADs

i. Effect of Enzyme Concentration

The effect of AChE concentration was tested by varying the amounts of AChE between 1 and 15 U mL^{-1}. As the concentration of enzyme increases from 1 to 15 U mL^{-1}, the color intensity was increased up to 9 U mL^{-1}. Concentration above 9 U mL^{-1} resulted saturation of the active binding site of the enzyme and maximum yellow color intensity was observed (Figure 15). Therefore, 9

U mL^{-1} concentration was selected as an optimum AChE concentration by observing the color intensity produced by the enzymatic hydrolysis of ATChI and was used throughout the study. More enzyme was required in the previous study by Kavruk et al. (2013) (12 U mL^{-1}) compared with the present study.

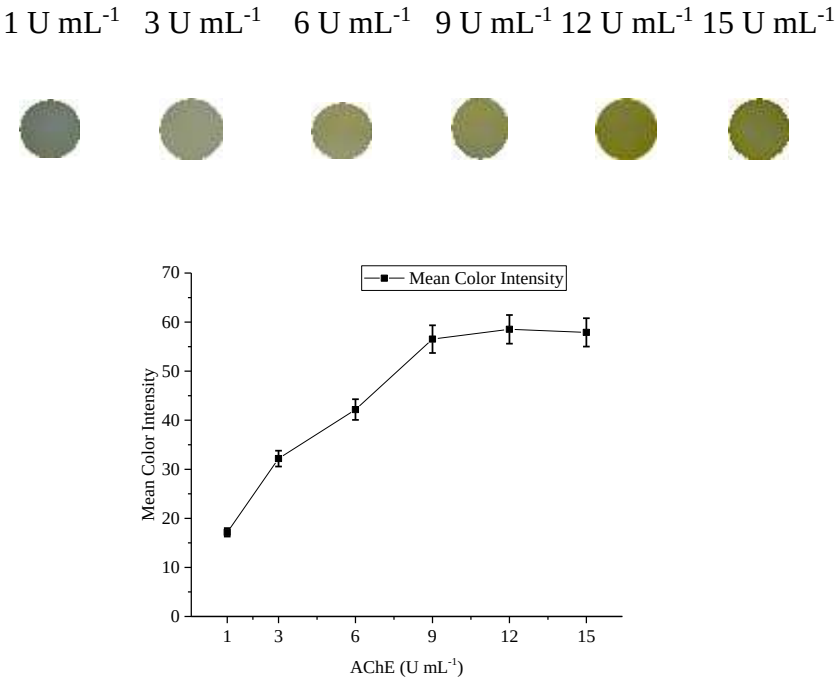

Figure 15. Color response of AChE concentrations with visual presentation of µ-PAD. Experimental conditions: ATChI; 5 mM and DTNB; 5 mM, image capturing time; 7 min, 2.5 µL of each of AChE, ATChI and DTNB; n = 3.

ii. Effect of Substrate Concentration

ATChI substrate for AChE is another key parameter that affects enzyme assay. Figure 16 shows the variation in signal and visual images depending on the substrate concentration. The reaction rates of AChE at various substrate concentrations were investigated in the range of 1 to 5 mM. The signal increases as the ATChI concentration rises, reaching a stable signal at 4 mM. For substrate

concentrations above this value, the enzyme reaches saturation (Snejdarkova et al., 2003). Thus, the inhibition level (%) increases with increasing the substrate concentration (Kok et al., 2002). The concentration selected as optimal was 4 mM because the signal is steady at that value, which was similar to the value obtained by Kavruk et al. (2013) (4 mM).

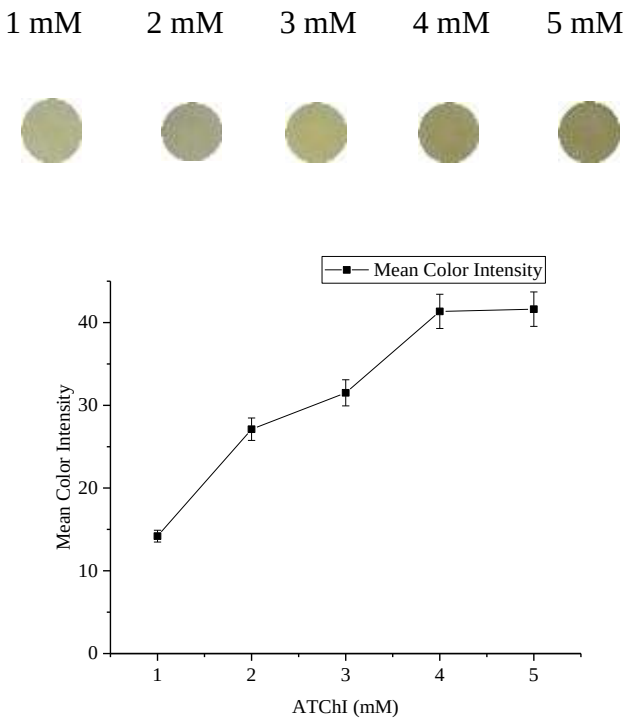

Figure 16. Color response for ATChI concentrations with visual presentation of µ-PAD. Experimental conditions: AChE; 9 U mL^{-1}, DTNB; 5 mM, image capturing time; 7 min, 2.5 µL of each of AChE, ATChI and DTNB; n = 3.

iii. Effect of Ellman's Reagent Concentration

To select the optimal DTNB for the determination of enzyme activity, different concentration of DTNB (1-5 mM) was investigated. As shown in Figure 17, color intensity increases with concentration ranges until it reaches 3 mM. After 3 mM, the color intensity becomes constant. As

a result, 3 mM concentration was the optimum point and was used for further analysis. A similar concentration of DTNB was reported by Kavruk et al. (2013) using a portable bioactive paper-based sensor.

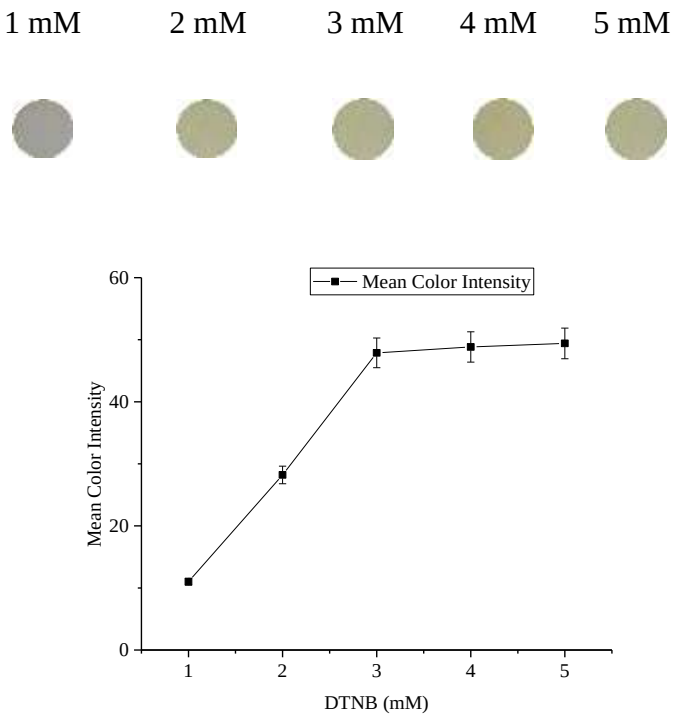

Figure 17. Color response of DTNB concentrations with visual presentation of µ-PAD. Experimental conditions: AChE; 9 U mL^{-1}, ATChI; 4 mM, image capturing time; 7 min, 2.5 µL of each of AChE, ATChI and DTNB, n = 3.

iv. Effect of Reagent Volume

A distinctive feature of the microfluidic paper-based device is low reagent deposition for micro-scale detection. To optimize the amount of volume to be deposited, the volume of ATChI, DTNB, and AChE varied from 1 to 2.5 µL by monitoring the intensity of the yellow complex (TNB anion). As can be seen in Figure 18, the mean color intensity increases as the volume of ATChI and DTNB increases up to 2 µL while the color intensity showed an increment up to 1.5 µL for AChE.

Therefore, 2 µL of both ATChI and DTNB and 1.5 µL of AChE were sufficient volumes for the assay. All other studied volumes were either not enough for the reaction or caused an overflow from the detection zone. On the other hand, it takes a longer readout time if the volume is larger than the optimum values.

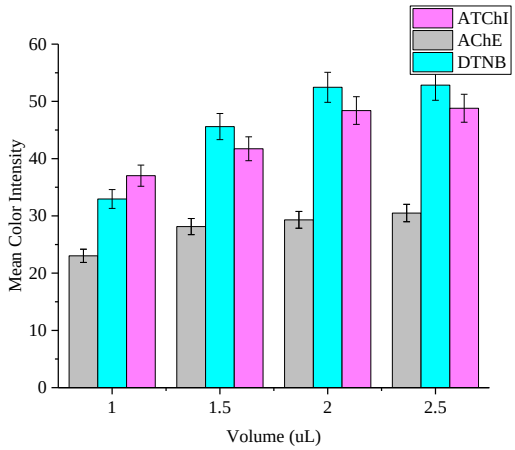

Figure 18. Effects of the volume of AChE, ATChI, and DTNB on color responses. Experimental conditions: AChE; 9 U mL^{-1}, image capturing time; 7 min, ATChI; 4 mM and DTNB; 3 mM, n=3.

v. Effect of Incubation Time

The effect of incubation time on the efficiency of AChE was studied by incubating 5 ppm of each pesticide with AChE at various incubation times (0, 5, 10, 20, and 25 min). Figure 19 shows that the degree of inhibition increased with the increase of the incubation time up to 10, 15, 15, 5, 10, and 20 min for carbaryl, carbosulfan, chlorpyrifos, furathiocarb, malathion, and methomyl pesticides, respectively. The incubation time reached a plateau after 10, 15, 15, 5, 10, and 20 min, indicating the binding interaction with active target groups in the enzyme could reach saturation (Du et al., 2007). The decrease in enzyme activity was less pronounced beyond these points, and therefore, the incubation times were selected as 10, 15, 15, 5, 10, and 20 min for respective

pesticides. The degree of inhibition increased with the incubation period (Dăneţ et al., 2003; Jaffrezic-Renault, 2001; Reybier et al., 2002). This value compares favorably with most of the data reported in the literature. For example, Apilux et al. (2015) used an incubation time of 10 min for the detection of organophosphate (dichlorvos and pirimicarb) and carbamate (carbaryl and carbofuran) pesticides while Hossain et al. (2009), Badawy and El-Aswad (2014) and Kavruk et al. (2013) found 5 min as an optimal incubation time for pesticide detection. Nouanthavong et al. (2016) also found 15 min as the optimum condition for enzyme activity.

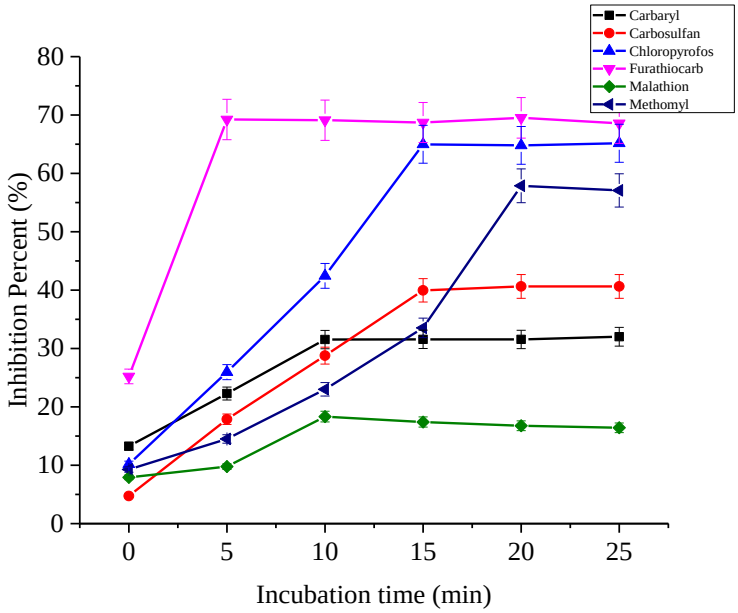

Figure 19. Effects of different incubation times on AChE activities. Experimental conditions: AChE; 9 U mL^{-1}, ATChI; 4 mM and DTNB; 3 mM, image capturing time; 7 min, 2 µL of each DTNB and ATChI; 1.5µL of AChE, 5 ppm of each pesticide; n=3.

vi. Effect of Image Capturing Time

The measurement of image capturing time on µ-PAD after all reagents were loaded is an important parameter. To find the optimum color image capturing time, various scanning times (5, 10, 20, 40,

80, and 160 min) were tested after complex formation. As shown in Figure 20, the intensity of the yellow color image on µ-PAD was observed to decrease with an increase of time from 5 to 160 min. The dense visible yellow color image was obtained after 5 min scanning. However, after 10, 20, 40, 80, and 160 min, color intensity decreased by 12, 14, 27, 37, and 50%, respectively. Hence, 5 min was taken as an optimum time for image capturing after the addition of ATChI throughout the study.

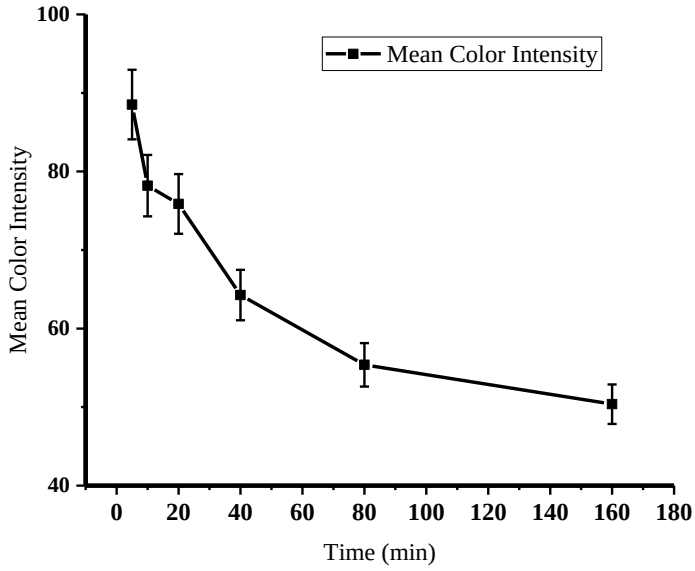

Figure 20. Effects of image capturing time on µ-PAD. Experimental conditions: AChE; 9 U mL^{-1}, ATChI; 4 mM and DTNB; 3 mM, 2 µL of each DTNB and ATChI; 1.5 µL of AChE, Incubation time; 10 min, n=3.

vii. Effect of Storage Temperature

The storage stability of the µ-PAD assay was examined for 7, 15, 30, 45, 60, and 90 days. The prepared µ-PADs were stored at three different temperatures: room temperature (RT), 4 ^{o}C, and -20 ^{o}C. Figure 21 depicts a plot of mean color intensity as a function of storage temperature at

various times. The responses of the µ-PADs stored at RT progressively decreased by 15% and 67% in the subsequent 7 and 90 days, respectively. Conversely, paper devices stored at 4 ^{o}C and -20 ^{o}C refrigerators were relatively stable for 7 and 45 days, respectively. Approximately 85% of enzyme activity were retained during device storage at RT, 4 ^{o}C, and -20 ^{o}C for 7, 15, and 60 day s, whereas only 33, 46, and 65% of the enzyme activity was retained during µ-PADs storage for 90 days, respectively. The µ-PADs devices stored in the dark at -20 ^{o}C showed responses consistent with that of freshly prepared devices for as long as 30 days.

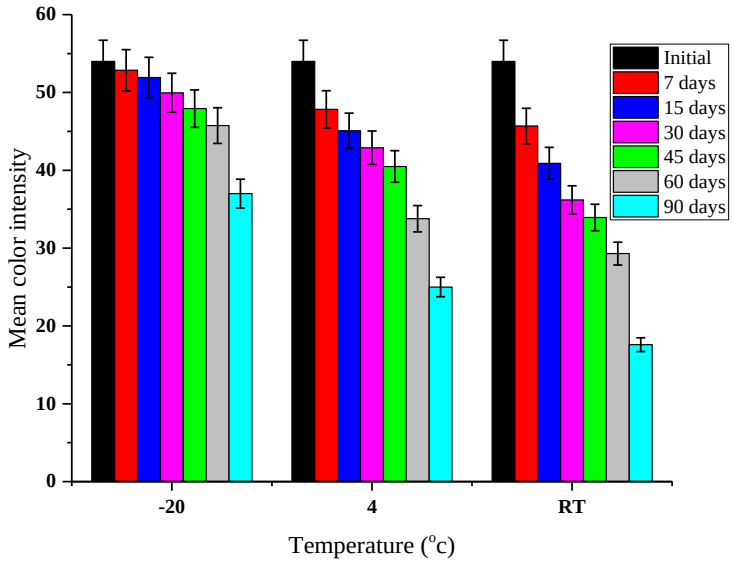

Figure 21. Effect of storage temperature. Experimental conditions: AChE; 9 U mL^{-1}, ATChI; 4 mM and DTNB; 3 mM, 2 µL of each DTNB and ATChI; 1.5 µL of AChE, Incubation time; 10 min, image capturing time; 5 min, n=3.

viii. Interference Study

Heavy metals are known to interfere with the AChE inhibition assay for pesticides (Aidil et al., 2013; Arduini et al., 2005; Sabullah et al., 2015). Therefore, four heavy metals were tested (Cu^{2+},

Zn^{2+}, Fe^{+2}, and Pb^{2+}) to evaluate the extent of interference in the developed method. The ratio of carbaryl to other metal interferences were studied in 1:1, 1:5, 1:10, 1:50, 1:100, 1:500 and 1:1000. The result (Figure 22) showed that at 1:1 and 1:5 ratios, less than 20% of inhibition percentage was observed for all the studied heavy metals. However, the inhibition percentage of all metals were higher than 46% at a metal concentration of 50 ppm and greater. The degree of interference the metals are in the order of Pb (II) > Fe (II) > Zn (II) > Cu (II).

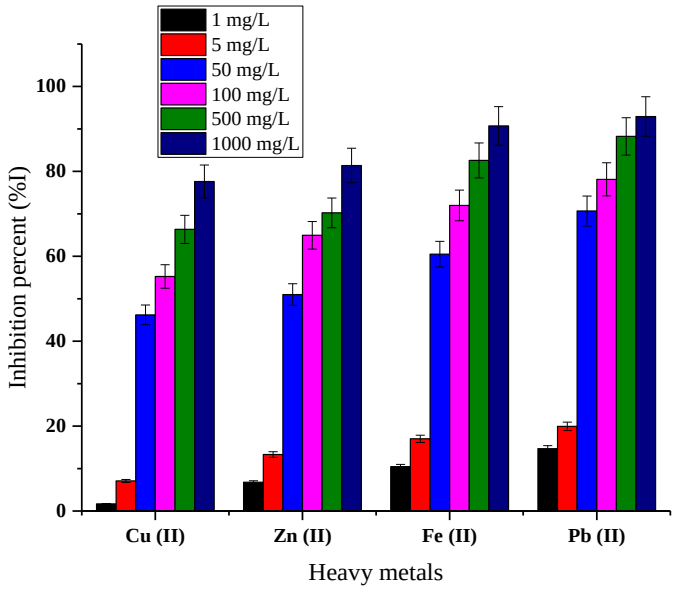

Figure 22. Effect of interfering ion and pesticides for carbamate detection. Experimental conditions: AChE; 9 U mL^{-1}, ATChI; 4 mM and DTNB; 3 mM, 2 µL of each DTNB and ATChI; 1.5 µL of AChE, Incubation time; 10 min, n = 3, 1 mg L^{-1} of carbaryl solution and interfering ratio at 1, 5, 50, 100, 500 and 1000.

The selectivity/specificity of the enzyme-based assay was evaluated in terms of cross reactivity of carbaryl with respect to chlorpyrifos, malathion, and methomyl. Cross-reactivity (CR) was defined as the percentage ratio of the midpoint of the inhibition curve (IC_{50}) value of the target analyte to

the IC_{50} value of the cross reactive related compounds as indicated on Equation 6 (March et al., 2009):

$$CR = \frac{(IC50\ (target\ compound)}{(IC50\ (related\ analytes)} * 100 \qquad (6)$$

Table 6 indicates the cross-reactivity of the AChE based pesticide detection. The interference found became small. The highest interference was obtained with methomyl, which has a cross-reactivity of 5.5%. In contrast, interference from other tested similar compounds chlorpyrifos and malathion pesticides was considered lower (<5%) and small. These results indicate that high selectivity was achieved using AChE-based μ-PAD optimized for the detection of carbamate pesticides.

Table 6. Cross-reactivity (CR) of the AChE based pesticide detection.

Pesticides	IC_{50} (mg L^{-1})	CR (%)
Carbaryl	2	100
Chlorpyrifos	41	4.878
Malathion	45.5	4.3956
Methomyl	36.1	5.5402

4.1.3. Merits of Analytical Method

The performance of the developed analytical method was evaluated in terms of linearity, precision, LOD and recovery under optimized parameters. The results are summarized in Table 7. The assay result indicates a linearity range of 1-16 mg L^{-1} with correlation coefficient (R^2) in the range of 0.9945-0.9992. This implies the developed method exhibited a wide range of good linear relationship between inhibition percentage (%) and the corresponding concentration which enables quantitative determination of the target analytes. LOD were found to be in the range of 0.24-0.33

mg L^{-1}. Lower LOD (more sensitive method) was observed for carbaryl in this study compared to the value reported by Apilux et al. (2015) and Lee et al. (2018), which were 0.5 mg L^{-1} and 10 mg L^{-1}, respectively. However, Jin et al. (2020) reported LOD value of 0.25 mg L^{-1} for carbaryl, which is more sensitive compared to our result (0.33 mg L^{-1}). As shown in Table 7, satisfactory precisions (RSD less than 10%) were obtained in all cases (Sante, 2017). The observed percentage recoveries were in the range of 87-94% which validates the accuracy of the developed method.

Robustness is the ability of an analytical procedure to remain unaffected by small but deliberate variations in the method parameters (Jimidar et al., 1998). The robustness of this method was performed by evaluating small variations of the concentration of volume of AChE, ATChI, and DTNB, and color development time at ±3%. The variation of the parameters resulted in a small decrease of the mean color intensity up to 1.85% (**Annex 1**). However, the mean color intensity obtained by varying concentrations, volumes, and color development time were not significantly affected by these small changes. Therefore, this method is robust for small changes in concentration and volume, and color development time.

In conclusion, the optimized parameters were 9 U/mL of AChE, 4 mM of ATChI, 3 mM of DTNB, 2 µL volume of ATChI and DTNB, 1.5 µL volume of AChE, 10 min incubation time and 5 min of image capturing time. Under the optimized conditions, the proposed method has shown an acceptable performance in terms of linearity, precision, selectivity, robustness, sensitivity and accuracy. This result confirms that µ-PAD can be applied for the detection of the target analytes.

Table 7. Analytical features for development of µ-PAD for pesticide detection

Pesticides	Linear range (mg L^{-1})	R^2	LOD (mg L^{-1})	Rep* (%RSD)	Repr** (%RSD)	Recovery at 1 mg L^{-1} (%)
Carbaryl	1-16	0.9992	0.33	4.90	9.23	86.84
Carbosulfan	1-16	0.9987	0.24	5.37	9.62	91.0
Chlorpyrifos	1-16	0.9998	0.28	3.75	8.55	85.21
Furathiocarb	1-16	0.9981	0.32	4.14	7.15	94.30
Malathion	1-16	0.9945	0.30	2.87	6.51	92.67
Methomyl	1-16	0.9971	0.32	2.67	7.12	79.83

Rep***-** Repeatability; Repr****-** Reproducibility

4.2. Multivariate Optimization of Operational Parameters in µ-PADs

4.2.1. Background of the study

Many researchers have reported the optimization of µ-PADs using univariate optimization techniques in the determination of pesticides (Apilux et al., 2015; Badawy and El-Aswad, 2014; Beshana et al., 2022b; Fernández-Ramos et al., 2020; Jing et al., 2021; Kavruk et al., 2013; Kim et al., 2018; Sankar et al., 2020). However, the disadvantage of the univariate optimization technique is that it does not consider the interaction among the parameters studied. Besides that, it is also time consuming and costly due to the increased number of experiments to be conducted and the increased consumption of reagents and chemicals (Lundstedt et al., 1998). Hence, in order to overcome these limitations, a multivariate optimization has been discovered and used in the modern analytical chemistry field. There are many multivariate optimization methods and one of the most relevant methods is response surface methodology (RSM). RSM is a mathematical and statistical methods collection used in optimizing processes based on the polynomial equation's fit to the experimental responses with the interest of making statistical previsions whilst describing a set of the data's behavior (Bezerra et al., 2008; Hao and Sulaiman, 2019). This approach has been extensively used in optimizing wastewater treatment (Ince and Ince, 2019; Salahi et al., 2013; Wang et al., 2007), renewable energy production (Galindo Padilha et al., 2022; Sedighi et al., 2018) and miniaturized sample preparation techniques (Bolzan et al., 2015a; Bolzan et al., 2015b; Zhou et al., 2013) but very limited use in the case of µ-PADs. In this section RSM approach has been used to optimize experimental parameters (concentration and volume of AChE, ATChI, and DTNB) that affect the enzyme inhibition assay of OP and CM pesticides in µ-PADs.

4.2.2. BBD Analysis

4.2.2.1. Concentration Optimization

Different concentrations of AChE, ATChI, and DTNB were tested by BBD. Annex 2 Table shows the summary of 15 experimental runs and the response obtained. Equation (7) illustrates the relationship between the three variables and the mean color intensity (Y) of experimental data using multiple linear regression analysis:

$$Y = 58.18 – 1.456A – 5.801B – 1.961C + 0.0924A*A + 0.240B*B – 0.0798C*C$$

$$0.2482A*B – 0.0518A*C + 0.6250B*C \quad (7)$$

Where Y denotes the sum of mean color intensity as a function of A, B, and C.

In the ANOVA results displayed in Table 8, the significance of each factor and interactions were evaluated at a 95% confidence level. The coefficient of determination *R*-squared and adjusted *R*-squared of the model were 0.988 and 0.966, respectively, showing that the model was well-fitted with the responses and indicating a good relationship between predicted and experimental values of the response. The nonsignificant *p*-value (0.255 > 0.5) of the lack of fit implies that the quadratic model is suitable for predicting the response and adequately fits the experimental data. The Fisher variance ratio (*F*-statistics) was used to measure how well the variables describe the variation in data about the mean. The larger *F*-value indicates that the estimated factors are real and adequately explains the variation in the data. Hence, the selected quadratic model is highly significant as indicated by Fisher's *F*-test ($F = 45.46$) and very low *p*-value ($p = 0.00$). In general, smaller *p*-values and larger Fisher's *F*-values indicate more significant coefficient terms (Arunachalam and Annadurai, 2011).

Table 8. ANOVA results for acquired model for concentration optimization

Source of variation	Degree of freedom	Sum of the square	Mean square	*F*-Value	*P*-Value
Model	9	165.768	18.4187	45.50	0.000
A	1	27.158	27.1585	67.08	0.000
B	1	67.08	24.2904	60.00	0.001
C	1	25.992	25.9920	64.20	0.000
A*A	1	28.862	28.8616	71.29	0.000
B*B	1	3.409	3.4087	8.42	0.034
C*C	1	0.376	0.3761	0.93	0.379
A*B	1	29.812	29.8116	73.64	0.000
A*C	1	1.300	1.2996	3.21	0.133
B*C	1	25.000	25.000	61.75	0.001
Error	5	2.024	0.4048		
Lack-of-Fit	3	1.664	0.5546	3.08	0.255
Pure Error	2	0.360	0.1802		
Total	14	167.792			

*Significant ($p < 0.05$), Adjusted $R^2 = 0.966$, $Q^2 = 0.836$ and $R^2 = 0.988$.

The summary of the model fit plot given in Figure 23a shows that the percent of the variation of the response predicted by the model (Q^2) is 84%. This indicates that only 16% of the variation of the response was not predicted by the model. The model validity result (0.65 > 0.25) indicated that there is no lack of fit of the model. The model reproducibility (98%) depicts that the variation of the response under the same conditions, often at the central points, was obtained compared to the

total variation of the response. The linear (main), quadratic, and interaction effects of the concentration of AChE, ATChI, and DTNB are presented in Figure 23b.The result has revealed that the concentration of AChE in the linear model has a positive significant effect on the mean color intensity whereas the concentration of ATChI and DTNB has a negative significant effect on the response. The quadratic effects of both AChE and ATChI concentrations showed a positive significant effect on the intensity. The results also indicate that the interaction effects of AChE and ATChI as well as ATChI and DTNB have a positive significant effect on the response. However, the rest of the terms (quadratic effect of DTNB and interaction effects between AChE and DTNB) did not show a significant effect on the response.

The model accuracy can be seen from the linear relationship between the predicted and observed mean color intensity depicted in Figure 23c. The result indicated that most of the plots were scattered monotonously around the line, therefore, there is a good correlation between predicted and observed responses and indicates the fitness of the suggested quadratic model. To better understand the relationship between the independent variables (A, B, and C) and the response (mean color intensity), two-dimensional contour plots were analyzed. In Figure 23d, the mean color intensity decreases with increasing concentration of ATChI and DTNB from 1 to 5 mM. With the increase in the concentration of ATChI above 1 mM, the enzyme reaches saturation (Snejdarkova et al., 2003). Moreover, the contour plot of the concentration of AChE vs. DTNB (Figure 23e) revealed that the intensity increases with decreasing concentration of DTNB and increasing concentration of AChE. With regard to the concentration of AChE, the mean color intensity decreases as the concentration of AChE increases to 9 U mL^{-1} and then starts to increase as the concentration of AChE increases from 9 to 12 U mL^{-1}. Hence, the lowest concentration of AChE was selected to minimize reagent use (Figure 23f). The model estimated an overall response

value (mean color intensity) of 49.96 under optimal conditions (Table 9). According to the optimization plots (Table 10), the optimum concentrations of AChE, ATChI, and DTNB were 1 U mL^{-1}, 1 mM, and 1 mM, respectively. The factor contributions of concentrations of AChE, ATChI, and DTNB on the response were 33.08%, 49.42%, and 17.50%, respectively; the concentration of ATChI had the highest contribution.

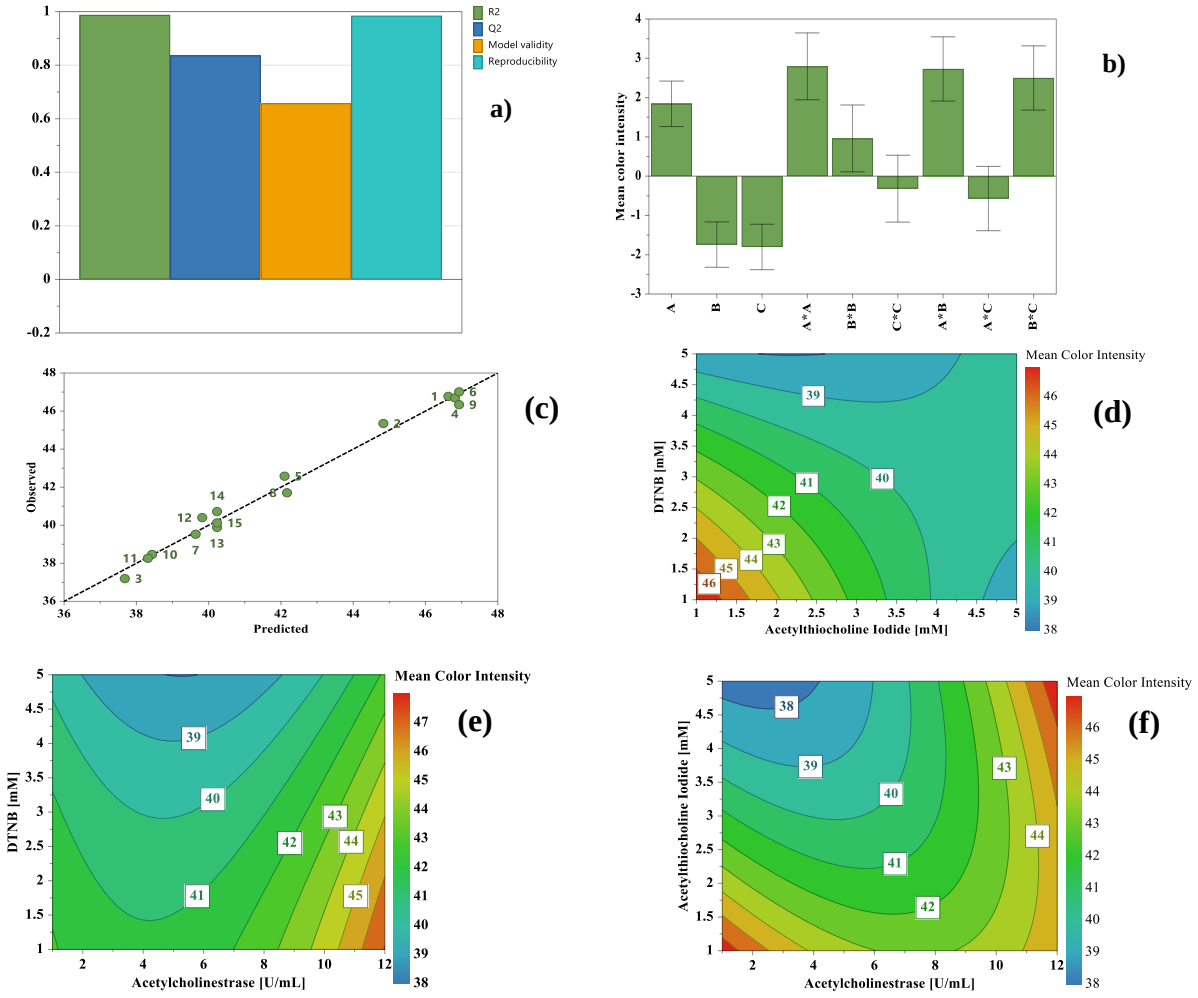

Figure 23. Plot of the summary of model fit (a), coefficient plot for the independent variable (b), linearity plot of the correlation between observed and predicted values (c), response contour plot of concentration of: ATChI vs. DTNB (d), AChE vs. DTNB (e) and AChE vs. ATChI (f).

Table 9. Predicted response of concentrations optimization

Response	Criterion	Value	Graph
Mean color intensity	Maximize	49.9594	

Table 10. Optimal conditions and factor contribution of concentrations optimization

Factor	Value	Graph	Factor contribution
A	1.00067	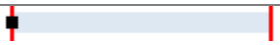	33.0858
B	1.00017	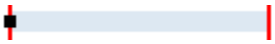	49.4162
C	1.02803	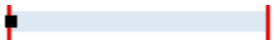	17.498

4.3.1.2. Volume optimization

The empirical relationship between the experimental results and input variables is expressed by a second-order polynomial equation with the interaction terms. The regression Equation (8) generated for coded factors is presented below.

$$\text{Mean color intensity} = 5.59 + 21.04D + 9.13E + 17.58F - 4.552D*D + 0.676E*E - 5.334F*F - 2.257D*E + 0.177D*F - 1.145E*F. \quad (8)$$

The predicted values of mean color intensity along with the experimental values are given in Annex 3 Table. The linearity plot (Figure 24a) indicates a satisfactory correlation ($R^2 = 0.995$ and $R^2\text{adj} = 0.986$) between the predicted and the actual (observed) response values of mean color intensity. The ANOVA summary result shown in Table 11 demonstrates that the model was significant with *F*-value of 113.56 and *p*-value of 0.000. The lack of fit value ($P = 0.552 > 0.05$) is not significant relative to the pure error. In addition, a summary of the model fit plot is shown in Figure 24b.

The result demonstrates that the percent of the variation of the response predicted by the model (Q^2) was 95%. The value of Q^2 indicates that only 5% of the variation of the response was not predicted by the model. The model validity result (0.85 > 0.25) indicated that there is no lack of fit of the model. The model reproducibility (99%) depicts the variation of the response under the same conditions, often at the central points.

Table 11. ANOVA results for the acquired model for volume optimization

Source of variation	Degree of freedom	Sum of the square	Mean square	*F*-value	*P*-value
Model	9	639.886	71.098	113.56	0.000
D	1	145.181	145.181	231.89	0.000
E	1	292.941	292.941	467.91	0.000
F	1	0.118	0.118	0.19	0.683
D*D	1	76.496	76.496	122.18	0.000
E*E	1	1.686	1.686	2.69	0.162
F*F	1	105.058	105.058	167.81	0.000
D*E	1	20.385	20.385	32.56	0.002
D*F	1	0.126	0.126	0.20	0.672
E*F	1	5.244	5.244	8.38	0.034
Error	5	3.130	0.626		
Lack-of-Fit	3	1.831	0.610	0.94	0.552
Pure Error	2	1.299	0.649		
Total	14	643.016			

*Significant ($p < 0.05$), Adjusted R^2 = 0.986, Q^2 =0.95 and R^2 =0.995.

The fitting of the data to various models, such as the linear, quadratic, and interactive, was performed to acquire the regression equations, and the results are presented as the coefficient plot in Figure 24c. The volume of AChE and ATChI in the linear model has a positive significant effect on the response. The quadratic effect of the model result demonstrates that the volume of AChE and DTNB has a negative significant effect on the response. The result shows that the interactive effect of the volume of AChE and ATChI, and ATChI and DTNB has a negative significant effect on the response. However, the linear effect of the volume of DTNB, quadratic effect of the volume of ATChI, and interactive effect between AChE and DTNB do not show a significant effect on the response.

Figure 24d shows the contour plot which demonstrates the effects of the volume of AChE vs. DTNB on the response. The result indicates that the mean color intensity increases with the increase in the volume of AChE and DTNB to 1.72 and 1.4 µL, respectively. However, the increase in the volume of AChE and DTNB beyond this value did not lead to any further increase in intensity and rather caused a slight decrease. This may be due to the concentration in the reactant volume already consumed during the reaction with the substrate concentration. Figure 24e demonstrates the contour plot between the volume of AChE and ATChI showed that the color intensity increases with increasing ATChI volume from 0.5 to 2.5 µL while increasing AChE volume from 0.5 to 1.72 µL. Furthermore, the contour plot of the volume of ATChI vs. DTNB indicated that the mean color intensity increases with increasing DTNB volume from 0.5 to 1.4 µL (Figure 24f).

In the volume optimization study, the RSM model gave an overall response value of 56.21 under optimal conditions (Table 12). The contribution of each factor to the mean color intensity was 5.68%, 87.67%, and 6.66% for the volume of AChE, ATChI, and DTNB, respectively. The overall

optimization results of the volume of AChE, ATChI, and DTNB were 1.72, 2.5, and 1.4 µL, respectively (Table 13). All other studied volumes were either not enough for reaction or caused an overflow from the detection zone.

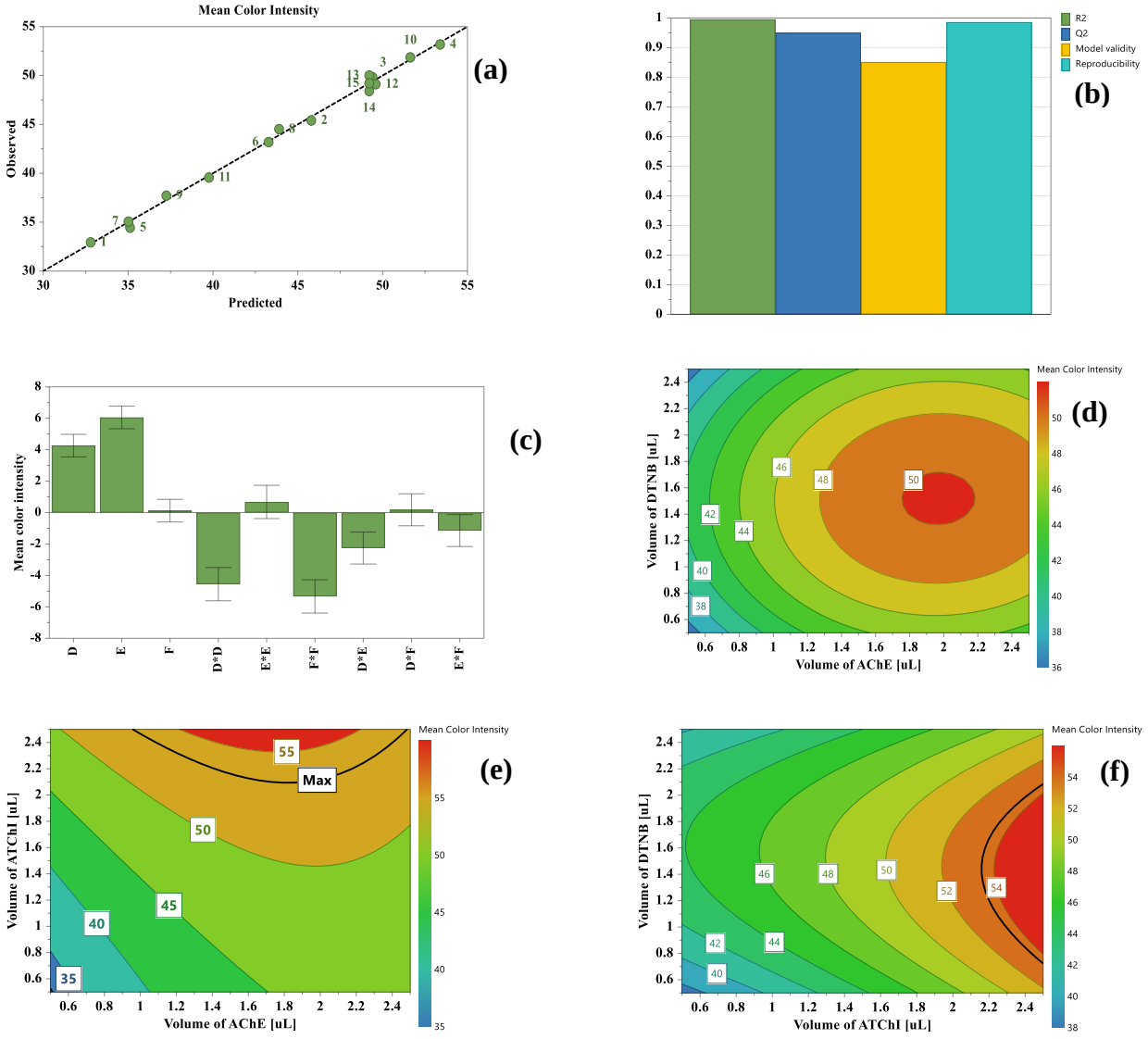

Figure 24. The linearity plot of the correlation between observed and predicted values (a), plot of the summary of model fit (b), coefficient plot for the independent variable (c), response contour plot of volume of: AChE vs. DTNB (d), AChE vs. ATChI (e) and ATChI vs. DTNB (f).

Table 12. Predicted response of volume optimization

Response	Criterion	Value	Graph
Mean color intensity	Maximize	56.2059	

Table 13. Optimal conditions and factor contribution of volume optimization

Factor	Value	Graph	Factor contribution
D	1.71556	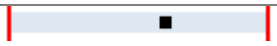	5.67942
E	2.49998		87.66500
F	1.40409	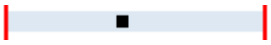	6.65562

4.2.3. Analytical Merits

Under optimized conditions, analytical merits such as linearity, LOD, precision, and accuracy were evaluated. The results showed that the proposed method is linear in the range of 0.5 to 16 mg L^{-1} for carbaryl, carbosulfan and furathiocarb, and 0.5 to 8 mg L^{-1} for chlorpyrifos, malathion and methomyl. The determination coefficient values (R^2) were 0.9992, 0.9990, 0.9999, 0.9995, 0.9993, and 0.9998 for carbaryl, carbosulfan, chlorpyrifos, furathiocarb, malathion, and methomyl, respectively, indicating good linearity for all target analytes. The results for LOD for respective pesticides were 0.15, 0.17, 0.13, 0.12, 0.14, and 0.15 mg L^{-1}.

The method precision was tested by analyzing 0.5 mg L^{-1} standard solutions on the same day and on different days. As shown in Table 14, appreciable relative standard deviations (RSD) for intra- and inter-day precision were obtained in the range of 3.8–8.0% and 7.2–11.0%, respectively.

4.2.4. Determination of Pesticides in Real Water Samples

Both the tap and river water samples were analyzed for target analytes prior to spiking. The result revealed that the mean color intensity of AChE activity (control) and AChE inhibition assay for the tap and river water did not show statistically significant difference in the mean color intensity (*t*-test ($p = 0.48$) at probability of 0.05). This implies that both the tap and river water samples are free of OP and CM pesticide contamination. Therefore, to evaluate the applicability of the proposed method, water samples were spiked with 0.5 mg L^{-1} carbaryl, carbosulfan, chlorpyrifos, furathiocarb, malathion, and methomyl. As shown in Table 14, very good recoveries in the range of 78–97% and 79–96% were observed for tap water and river water, respectively. All the recoveries were in good agreement with the acceptable recovery range (70–120%) established by the European Commission for pesticide residue analysis in food and feed samples (Ferreira et al., 2007).

Table 14. Average recovery (%) and precision (RSD, %) obtained for water sample

Pesticide	Added (mg L^{-1})	Tap water	River water	Rept[a] (RSD, %)	Repr[b] (RSD, %)
		Recovery ± SD (%)	Recovery ± SD (%)		
Carbaryl	0.5	87 ± 0.12	84 ± 0.40	7.98	9.23
Carbosulfan	0.5	91 ± 0.04	89 ± 0.38	6.17	9.62
Chloropyrifos	0.5	94 ± 0.10	96 ± 0.26	7.76	10.98
Furathiocarb	0.5	78 ± 0.05	79 ± 0.25	5.42	7.15
Malathion	0.5	97 ± 0.08	91 ± 0.36	7.20	9.59
Methomyl	0.5	81 ± 0.14	88 ± 0.17	3.75	8.55

4.2.5. Comparison of the New µ-PADs with Other Reported Methods in the Literature

The result obtained for µ-PADs was compared with similar analytical techniques reported for the determination of OP and CM pesticides (Apilux et al., 2015; Jin et al., 2020; Kavruk et al., 2013; Kim et al., 2018). As shown in Table 15, the comparisons were made in terms of parameters such as linearity range, LOD, and R^2 values. In comparison to similar methods, the proposed method has comparable linearity ranges and offers better R^2, as well as the lowest LOD values, except for methomyl, compared with the reported methods. Thus, the proposed technique can be considered as one of the preferred alternatives, having a promising future for easy detection of target pesticides.

Table 15. Comparison of the present assay with other reported µ-PAD methods

Methods	Analyte	Linear range (mg L^{-1})	Correlation coefficient	LOD (mg L^{-1})	Reference
µ-PAD	OP and CM	0.5-16	0.9990-0.9999	0.12-0.17	Present study
µ-PAD	Chlorpyrifos	1-100	0.9600	8.60	(Kim et al., 2018)
µ-PAD	Malathion	-	-	2.50	(Kavruk et al., 2013)
µ-PAD	Carbaryl	0.1-25	-	0.50	(Apilux et al., 2015)
µ-PAD	Carbaryl	0.1-10	0.9951	0.77	(Jin et al., 2020)
µ-PAD	Chlorpyrifos	0.1-10	0.9984	0.25	(Jin et al., 2020)

4.2.6. Comparison of Univariate and Multivariate Optimization for the Detection of Pesticides

Multivariate optimization is more advantageous than univariate optimization in terms of efficiency. The multivariate optimization required 30 runs (less resource and time) to obtain optimum parameters while the univariate requires 52 runs. In addition, as shown in Table 16, multivariate optimum parameter requires significantly less concentration of AChE, ATChI, and DTNB and less volume of DTNB than that of univariate optimization. Furthermore, multivariate optimization improved the LOD values of univariate optimization by 55%, 29%, 54%, 64%, 53%, and 53% for carbaryl, carbosulfan, chlorpyrifos, furathiocarb, malathion, and methomyl, respectively. These differences imply that there are interactions among the independent variables, because when there is significant interaction between the factors, the optimal conditions indicated by the univariate studies will be different from the optimal values of the multivariate optimization (Ferreira et al., 2007). The larger the interaction effects, the greater the difference that will be found using univariate and multivariate optimization strategies (Ferreira et al., 2007). Therefore, the multivariate approach has been sufficiently demonstrated to be more efficient and effective than the univariate approach for the μ-PADs optimization in the determination of OP and CM pesticides.

Table 16. Comparison between univariate and multivariate optimization approaches

Optimized parameter	Univariate	Multivariate
Concentration		
AChE (U mL^{-1})	9	1
ATChI (mM)	4	1
DTNB (mM)	3	1
Volume (µL)		
AChE	1.5	1.72
ATChI	2	2.5
DTNB	2	1.4
Limit of detection (mg L^{-1})		
Carbaryl	0.33	0.15
Carbosulfan	0.24	0.17
Chlorpyrifos	0.28	0.13
Furathiocarb	0.32	0.12
Malathion	0.30	0.14
Methomyl	0.32	0.15

4.3. DLLME Combined with µ-PAD for the Determination of OP and CM Pesticides in Water Sample

4.3.1. Background of the Study

Several studies have reported the use of colorimetric µ-PAD for the detection of OP and CM pesticides via AChE inhibition. Badawy and El-Aswad (2014) for profenofos and methomyl pesticides; Sankar et al. (2020) and Kim et al. (2018) for chlorpyrifos; Kavruk et al. (2013) for malathion; Apilux et al. (2015) for dichlorvos, pirimicarb, carbaryl and carbofuran; Fernández-Ramos et al. (2020) and Jin et al. (2020) for carbaryl and chlorpyrifos have demonstrated the use of µ-PAD. For the majority of the studied analytes, high limit of detection (LOD) in the range of 0.065-8.6 mg L^{-1} had been reported. All the reported LODs are far above the permissible limit set by various regulatory bodies. For example, according to WHO guideline value (GV), the maximum acceptable value/concentration for malathion, chlorpyrifos, carbaryl and carbofuran are 50, 20, 5 and 5 µg L^{-1}, respectively. This indicates that the sensitivity of the reported µ-PADs are not adequate enough to predict the threshold concentration that might cause environmental threat. Therefore, to overcome this limitation, we used miniaturized DLLME techniques for enrichment to significantly improve the LOD of µ-PAD. To the best of our knowledge, there are no reports in the published literature for the determination of the OP and CM compounds in water samples using DLLME as the preconcentration technique coupled to µ-PAD. Furthermore, in this study multivariate optimization of DLLME for carbosulfan, chlorpyrifos, furathiocarb and methomyl have been reported for the first time.

4.3.2. Optimization of DLLME

4.3.2.1. Selection of Extraction and Disperser Solvent

Low-density solvent, *n*-hexane was used as an extraction solvent. Miscibility of disperser solvents in both aqueous and extraction solvents is a major requirement for selection. The disperser solvent is used to increase the dispersion of the fine droplets of the extraction solvent in the aqueous solution and enhances the contact area between extraction solvent and aqueous solution, thereby improving the extraction efficiency (Xia et al., 2012). It also functions as a demulsifier (terminating solvents) that break up the emulsion formed by destabilizing the interface film between the droplet and water (Jia et al., 2010). In this work, acetone, acetonitrile, and methanol were studied as dispersers and terminating solvents. As shown in Figure 25, acetone extract provided the highest inhibition percentage, followed by methanol and acetonitrile. Therefore, acetone was selected for further analyses in this study.

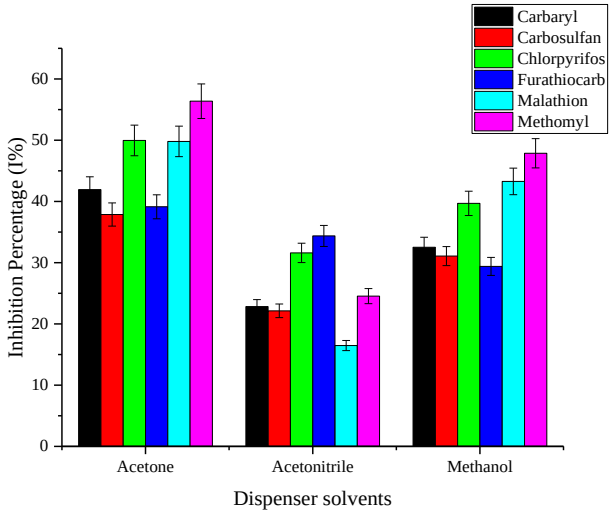

Figure 25. Effect of disperser solvent on the inhibition percentage. Conditions: 50 µL of n-hexane; acetone as dispersive solvent and demulsifier of 1 mL (0.5 + 0.5 mL) and extraction time 6 min (1 µg L^{-1} of each pesticide).

4.3.2.2. Selection of Salt Type

Adding salt to the sample solution reduces the solubility of the analyte in the aqueous sample and facilitates the transfer of the target analyte from the aqueous phase to the organic solvent phase (Cai et al., 2007; Wen et al., 2013). In this experiment, NaCl, Na_2CO_3, and $MgSO_4$ were studied to evaluate the effect of salt on the inhibition percentage (Figure 26). Sodium chloride has induced more effective phase separation, for all the analytes studied hence it was used as salting-out agent throughout this work.

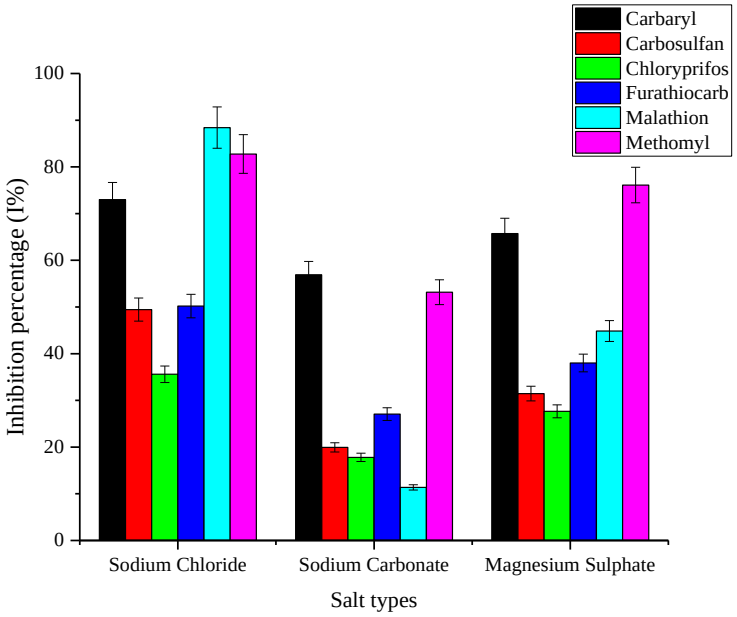

Figure 26. Effect of different salt addition to the inhibition percentage. Conditions: 50 µL of *n*-hexane; 1.00 mL (0.5 + 0.5 mL) of acetone and extraction time 6 min (1µg L^{-1} of each pesticide).

4.3.2.3. Experimental Design

4.3.2.3.1. BBD Statistical Analysis

The summary of 27 experimental runs and the response obtained are shown in Table Annex 4. The polynomial in equation (9) depicts the empirical relationship between the inhibition percentage (I%) and the four independent variables.

$$I\% = -276.1 + 5.127A + 425.8\,B + 33.15\,C + 16.655D - 0.03020A^2 - 369.3\,B^2 - 1.2596\,C^2 - 0.6499D^2 - 0.247A*B - 0.2968\,A*C - 0.0796\,A*D - 3.53\,B*C - 8.23\,B*D - 0.4456\,C*D \quad (8)$$

The results of ANOVA for extraction of pesticides are shown in Table 17. A large value of F (85.82) indicates that most of the variables in the response can be explained by the regression equation, and probability values less than 0.05 are considered to be statistically significant. The nonsignificant value of LOF (P = 2.59 > 0.05) implies that the quadratic model is suitable for predicting the response and adequately fits with the experimental data.

The regression model showed a high correlation (0.98) between the observed and predicted responses (Figure 27a), suggesting that the proposed model equation yields satisfactory and accurate results. It implies that the predicted values were close to the observed values. The linear, quadratic, and interaction effects of the studied parameters on inhibition percentage are shown in Figure 27b. It revealed that the linear effect of the extraction time and volume of *n*-hexane have negative significance, whereas the volume of acetone has positive significant effect. However, the amount of NaCl did not show a significant linear effect. The quadratic and interaction effects of all the studied variables have negative significant effects on the inhibition percentage except the interaction between the volume of *n*-hexane and acetone.

The summary of the model fit plot is depicted in Figure 27c. The result showed that the percent of the variation of the response predicted by the model is Q^2 = 95%. This indicates only 5% of the

variation of the responses was not predicted by the model. The model validity result (0.71 > 0.25) indicated that there is no LOF of the model. Model reproducibility (99%) represents variability in response under the same conditions and is often obtained at center points.

Table 17. Results of ANOVA for DLLME extraction parameters

Source of variation	Degree of freedom	Sum of the square	Mean square	*F*-value	*P*-value
Model	14	7776.99	555.50	85.82	0.000
A	1	160.45	160.45	24.79	0.000
B	1	263.48	263.48	40.71	0.000
C	1	73.46	73.46	11.35	0.006
D	1	12.12	12.12	1.87	0.196
A*A	1	778.33	778.33	120.25	0.000
B*B	1	2841.40	2841.40	439.00	0.000
C*C	1	2166.35	2166.35	334.70	0.000
D*D	1	1407.97	1407.97	217.53	0.000
A*B	1	6.08	6.08	0.94	0.352
A*C	1	2254.35	2254.35	348.30	0.000
A*D	1	253.29	253.29	39.13	0.000
B*C	1	49.98	49.98	7.72	0.017
B*D	1	423.54	423.54	65.44	0.000
C*D	1	317.73	317.73	49.09	0.000
Error	12	77.67	6.47		
Lack-of-Fit	10	72.11	7.21	2.59	0.310
Pure Error	2	5.56	2.78		
Total	26	7854.66			

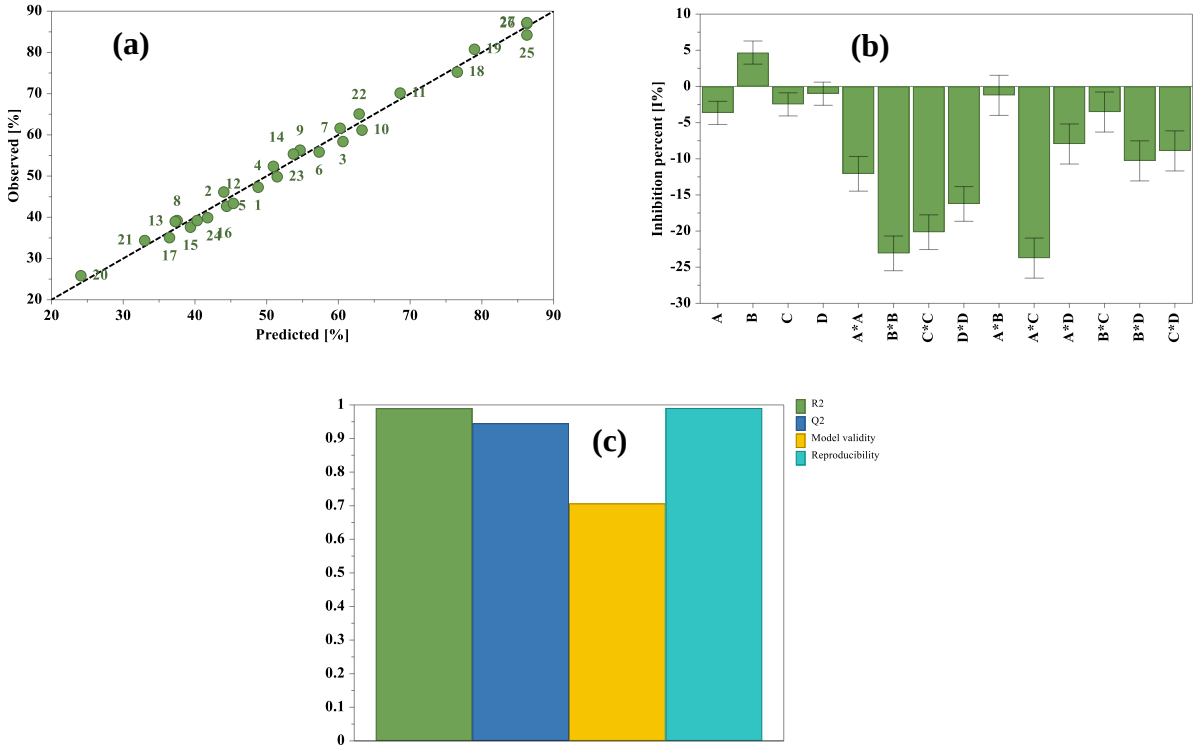

Figure 27. The linear plot of the correlation between observed and predicted values (a), coefficient plot for the effect of independent variable on the inhibition percentage (b), and plot of the summary of model fit (c).

4.3.2.3.2. Response analysis

The relationship between various independent parameters on the responses is represented with two-dimensional contour plots in RSM (Figure 28). These plots were obtained for a given pair of factors at fixed and optimal values of other variables. The contour plot in Figure 28 a and b shows the effects of the volume of *n*-hexane versus the volume of acetone and extraction time. At the lower and higher volume of *n*-hexane and acetone, and extraction time, the inhibition percentage of the pesticides is low, which indicated low extractability of the target pesticides. Inhibition percentage increases as the volume of *n*-hexane, the volume of acetone, and extraction time

increase in the range of 30-47µL, 0.2-0.48 mL, and 2-6 min, respectively and started to decrease beyond these ranges. At lower volume of *n*-hexane and acetone, extraction of the analytes is disturbed due to incomplete dispersion of the organic solvents in aqueous samples. Whereas at high volumes of the organic solvent, polarity of the aqueous sample decreases due to dissolution of disperser and extraction solvents in the aqueous phase that leads to a decrease in partition coefficients of analytes and extraction efficiencies (Farajzadeh et al., 2012). Figure 28 c shows the effect of the volume of acetone versus extraction time. Increasing the extraction time from 2 to 6 min will increase inhibition percentage as the volume of acetone and the salt amount increases from 2 to 0.48 mL and 0 to 4.8% (w/v), respectively and beyond the 6 min extraction time, the inhibition percentage decrease. This could be due to possible dissolution of disperser solvent in water (Tolcha et al., 2021). Figure 28 d depicts the effects of extraction time versus NaCl amount on inhibition percentage. The result indicated that the addition of NaCl has no significant effect on inhibition percentage (Figure 27b).

4.3.2.3.3. Selection of optimum conditions

Optimal conditions for the extraction procedure were derived to obtain the maximum inhibition percentage. RSM selects and predicts the best mode of operation for the range of variables used (Table 18). The model estimated a maximum inhibition percentage of 86.76% under the optimal condition of 47 µL n-hexane, 0.48 mL acetone, 6 min extraction time, and 4.8% (w/v) NaCl. A validation experiment was carried out under the optimal conditions and yielded 86.58% inhibition percentage, which is comparable to the model-predicted value of 86.76%. The model also predicts the contribution of each factor in the inhibition percentage to be 17.2, 32.1, 28.1, and 22.6%, for the volume of *n*-hexane, the volume of acetone, extraction time, and the amount of NaCl, respectively (Table 19).

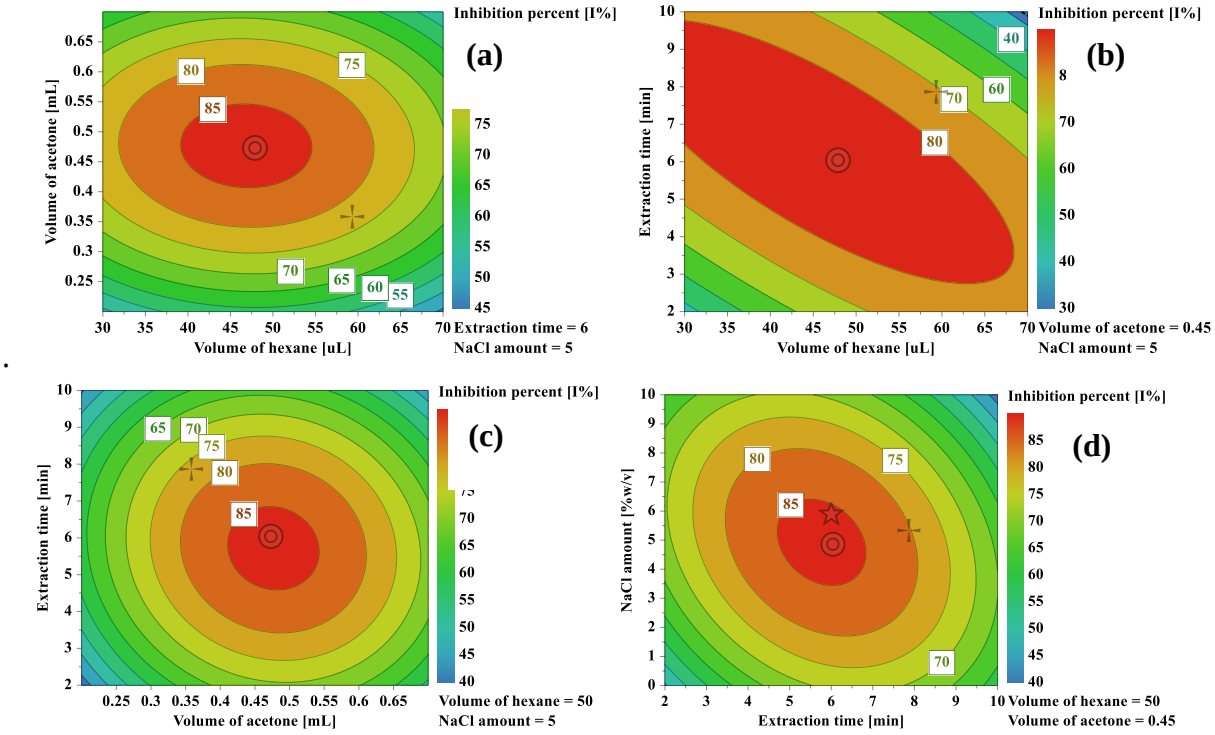

Figure 28. Response contour plots of independent variables: Volume of n-hexane vs. volume of acetone (a), volume of n-hexane vs. extraction time (b), volume of acetone vs. extraction time (c), and extraction time vs. NaCl amount (d).

Table 18. Predicted response for DLLME extraction parameters

Response	Objective	Value	Response range
Inhibition percentage	Maximize	86.8261	

Table 19. Optimal conditions and factor contribution of DLLME extraction parameters

Factor	Value	Factor range	Factor contribution
Volume of hexane	46.5657		17.1845
Volume of acetone	0.4778		32.1352
Extraction time	6.1212		28.0591
NaCl amount	4.8447		22.6213

4.3.3. Analytical Features

The analytical merits of the developed DLLME-µ-PADs method are depicted in Table 20. The DLLME method shows good linearity in the range of 0.625-40 µg L^{-1} with a correlation coefficient in the range of 0.9968-0.9987. EFs for the studied pesticides were in the range of 317-1471. The LODs of the studied pesticides were between 0.17 and 0.41 µg L^{-1}, which is below the maximum residue limits of EU for drinking water. The average recovery was found to be in the ranges of 79-97% with RSD between 2.21 and 10.46%.

4.3.4. Comparison of the Proposed DLLME-µ-PADs Method with Other µ-PADs Procedures

The performance of DLLME-µ-PADs method was compared to the previously reported µ-PAD method (Fernández-Ramos et al., 2020; Jin et al., 2020; Kim et al., 2018; Sankar et al., 2020) in terms of linear range, LOD, and correlation coefficient. As it can be seen in Table 21, the proposed analytical method has an equivalent or wider linear range and provides better correlation coefficient and lowest LOD value compared with the reported methods. This implies that the proposed method is an efficient and sensitive that can be used to extract/concentrate and measure pesticides in water samples.

In conclusion in this study, a miniaturized sample preparation (DLLME) and analysis method (μ-PAD) have been coupled to demonstrate a simple, rapid and sensitive analytical method for the determination of six pesticides in water sample. The DLLME method has been successfully optimized for the preconcentration step. The volume of *n*-hexane and acetone, and extraction time are found to be the critical operational parameters affecting the DLLME. Under the optimized experimental conditions, the developed method has offered high enrichment factors in the range of 317-1471 and lower LODs ranging from 0.17 to 0.41 μg L^{-1} for the analyses of trace level of target analytes.

Table 20. Method validation parameters

Pesticides	Linear range (µg L^{-1})	R^2	LOD µg L^{-1}	Repeatability (%RSD)		Reproducibility (%RSD)		Recovery (%)		EF
				1 µg L^{-1}	5 µg L^{-1}	1 µg L^{-1}	5 µg L^{-1}	1 µg L^{-1}	5 µg L^{-1}	
Carbaryl	0.625-40	0.9985	0.19	2.21	3.31	5.60	7.70	85.80	82.15	1421
Carbosulfan	1.25-40	0.9986	0.36	5.19	4.41	9.92	6.27	78.50	85.44	472
Chloropyrifos	1.25-40	0.9987	0.41	4.89	5.51	7.58	7.46	86.98	92.46	317
Furathiocarb	0.625-40	0.9968	0.17	4.01	5.09	9.94	10.46	90.76	93.17	1471
Malathion	0.625-40	0.9976	0.18	2.95	5.72	9.04	8.94	95.34	83.23	1000
Methomyl	0.625-20	0.9980	0.20	6.01	4.91	9.94	9.16	97.25	93.31	750

Table 21. Comparison of µ-PAD-DLLME with other µ-PAD techniques for the determination of the pesticides

Methods	Analyte	Linear range (µg L^{-1})	R^2	LOD (µg L^{-1})	Reference
µ-PAD-DLLME	OP and CM	0.625-40	0.9968-0.9987	0.17-0.41	This study
µ-PAD	Chlorpyrifos	100-1000	0.9980	65	(Sankar et al., 2020)
µ-PAD	Carbaryl	25-2500	0.9900	29	(Sankar et al., 2020)
µ-PAD	Chlorpyrifos	1000-100,000	0.9600	8600	(Kim et al., 2018)
µ-PAD	Carbaryl	0.24-20	0.9930	0.24	(Fernández-Ramos et al., 2020)
	Chlorpyrifos	2-45	0.9953	2	(Fernández-Ramos et al., 2020)
µ-PAD	Carbaryl	10-1000	0.9951	771	(Jin et al., 2020)
µ-PAD	Chlorpyrifos	100-10,000	0.9984	253	(Jin et al., 2020)

4.4. Combination of QuEChERS and DLLME for µ-PAD Device for the Determination of OP and CM Pesticide in Lettuce Vegetable

4.4.1. Background of the study

Determination of pesticide residues in vegetables remains difficult due to trace amounts of target analytes and complex interfering components in the vegetable matrix (Rizzetti et al., 2016). For these reasons, efficient extraction, clean up, and preconcentration steps are required prior to analysis. QuEChERS extraction has been accepted by many regulatory agencies for routine analysis of pesticides in food and agricultural good (Anastassiades et al., 2003; Aysal et al., 2007; Lehotay et al., 2005b). However, the main limitation is the low enrichment factor (Cunha and Fernandes, 2011). On the other hand, dispersive liquid-liquid microextraction (DLLME) is known to have high enrichment factor as it has been confirmed in the previous section of this study and other authors (Beshana et al., 2022a; Viñas et al., 2014). However, due to the complexity of the food sample matrix, it is difficult to use DLLME alone as a preconcentration/extraction technique for analyzing pesticides residues in agricultural products (Asensio-Ramos et al., 2011b).

Several researchers (Andraščíková and Hrouzková, 2016; Chen et al., 2013; Cunha and Fernandes, 2011; Ghani et al., 2018; Li et al., 2017; Ma et al., 2020; Rai et al., 2016; Young, 2005) have combined QuEChERS and DLLME to complement the limitations of each extraction method followed by quantification using bench top analytical instruments. In this section, the combined QuEChERS-DLLME has been optimized using RSM method, applied for the extraction of selected OP and CM pesticides and analyzed using (µ-PADs). It has been demonstrated that the sample pre-treatment by the QuEChERS-DLLME method, has significantly improved the analytical sensitivity of µ-PAD compared with those without sample pre-treatment.

4.4.2. Optimization of QuEChERS-DLLME

4.4.2.1. Screening of the Extraction Parameters

The PBD was used for screening the effects of factors regardless of the interaction among themselves (Hadjmohammadi et al., 2012; Maya and Ghani, 2019). Accordingly, seven factors were screened (volume of acetonitrile and disperser medium, amounts of NaCl, $MgSO_4$, PSA, an d activated charcoal, and extraction time) using methomyl as a representative pesticide. An ANOVA results at 95% confidence intervals are shown in a standardized main effect Pareto chart (Table 22). An ANOVA results at 95% confidence intervals are shown in a standardized main effect Pareto chart (Figure 29). The bar length is proportional to the significance of the variables on inhibition percent. The volume of acetonitrile, amount of activated charcoal, and extraction time have a significant effect on the inhibition percentage. Among these the amount of activated charcoal is the most critical factor. The experimental result shows that other factors (volume of disperser medium, amount of NaCl, $MgSO_4$, and PSA) have no significant effect on the inhibition percentage, and were fixed at a specific value in the process of optimizing the identified significant factors.

Table 22. Experimental runs and responses studied by PBD

Run	A	B	C	D	E	F	G	I%
1	5	2	0.5	4	200	300	5	23.14
2	10	2	0.5	1	80	300	10	23.7
3	5	4	0.5	1	200	150	10	77.33
4	10	4	0.5	4	80	150	5	44.13
5	5	2	2	4	80	150	10	72.91
6	10	2	2	1	200	150	5	47.92
7	5	4	2	1	80	300	5	26.5
8	10	4	2	4	200	300	10	25.01

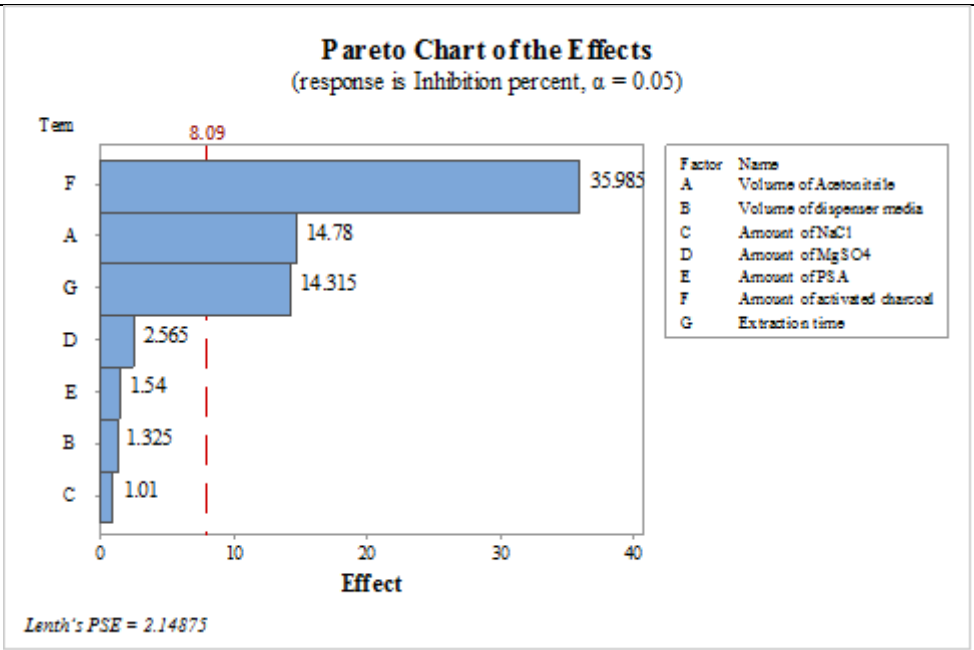

Figure 29. Standardized main effect Pareto chart for the PBD of screening experiment. The vertical line in the chart defines 95% confidence level.

4.4.2.2. Central Composite Design

Table Annex 5 represents a CCD experiments design matrix, runs, and their inhibition percentage. In the ANOVA results displayed in Table 23, the significance of each factor, interaction, and quadratic were evaluated at a 95% confidence level. The quality of fit of the model regression equation was expressed with the regression coefficient (R^2 = 0.993 and adjusted R^2 = 0.984). The result of R^2 and adjusted R^2 indicated that there is a good relationship between experimental data and predicted responses, showing the model was well-fitted with the responses. The statistical significance of all terms in a polynomial equation was estimated using an *F*-test at a 95% confidence interval. The model was found to be significant with p = 0.00 and an *F*-value of 111.59. The "Lack of Fit (LOF) *p*-value" of 0.242 implies the LOF is not significant relative to the pure error. The relationship between the inhibition percentage and the three selected factors is shown in Equation 10:

$$I\% = 160.6 - 11.67\,A - 0.6691\,F - 5.89\,G + 1.223\,A^*A + 0.001616\,F^*F + 0.103\,G^*G - 0.02396\,A^*F + 0.2540\,A^*G + 0.00760\,F^*G \quad (9)$$

Where I% is the sum of the inhibition percentage as a function of A, F, and G. The positive coefficients indicate that the inhibition effect is favored in the presence of high values of the respective variables within the range studied, while negative coefficients indicate that the reaction is favored in the presence of low values. In this case, a synergistic effect associated with A*A, F*F, G*G, A*G, and F*G while an antagonistic effect associated with A, F, G, and A*F can be concluded from the regression equation.

The adequacy of the regression model was checked by evaluating the observed and predicted experimental values. Figure 30a indicates that most of the data points are scattered around the 45° straight line, which implies that there is sufficient agreement between observed and predicted

responses. Figure 30b shows the summary of the model fit plot. The result demonstrated that the percent of the variation of the response predicted by the model was Q^2 = 94%, only 6% of the variation of the responses was not predicted by the model. The model validity result (0.64 > 0.25) indicates that there is no Lack of Fit of the model. The model reproducibility (99.4%) shows the variation of the response under the same conditions, often at the center points. The main, quadratic, and interaction effects of the volume of acetonitrile, amount of activated charcoal, and extraction time on inhibition percentage are shown in Figure 30c. The results revealed that the linear effect of A, the quadratic effects of A*A, and F*F, and the interaction effects of A*G and F*G have a positive significant effect on inhibition percentage, whereas the linear effects of F and G, and interaction effects of A*G have a negative significant effect. However, the quadratic effect of G*G does not show a significant effect on the inhibition percentage.

Table 23. Results o**f** ANOVA for QuEChERS-DLLME extraction and clean up parameters

Source of variation	Degree of freedom	Sum of the square	Mean square	*F*-value	*P*-value
Model	9	2025.55	225.062	111.59	0.000
A	1	636.17	636.166	315.42	0.000
F	1	235.71	235.710	116.87	0.000
G	1	33.64	33.636	16.68	0.005
A*A	1	156.52	156.525	77.61	0.000
F*F	1	221.30	221.302	109.72	0.000
G*G	1	1.11	1.109	0.55	0.482
A*F	1	161.46	161.460	80.05	0.000
A*G	1	20.16	20.161	10.00	0.016
F*G	1	16.25	16.245	8.05	0.025
Error	7	14.12	2.017		
Lack-of-Fit	5	12.64	2.528	3.42	0.242
Pure Error	2	1.48	0.739		
Total	16	2039.67			

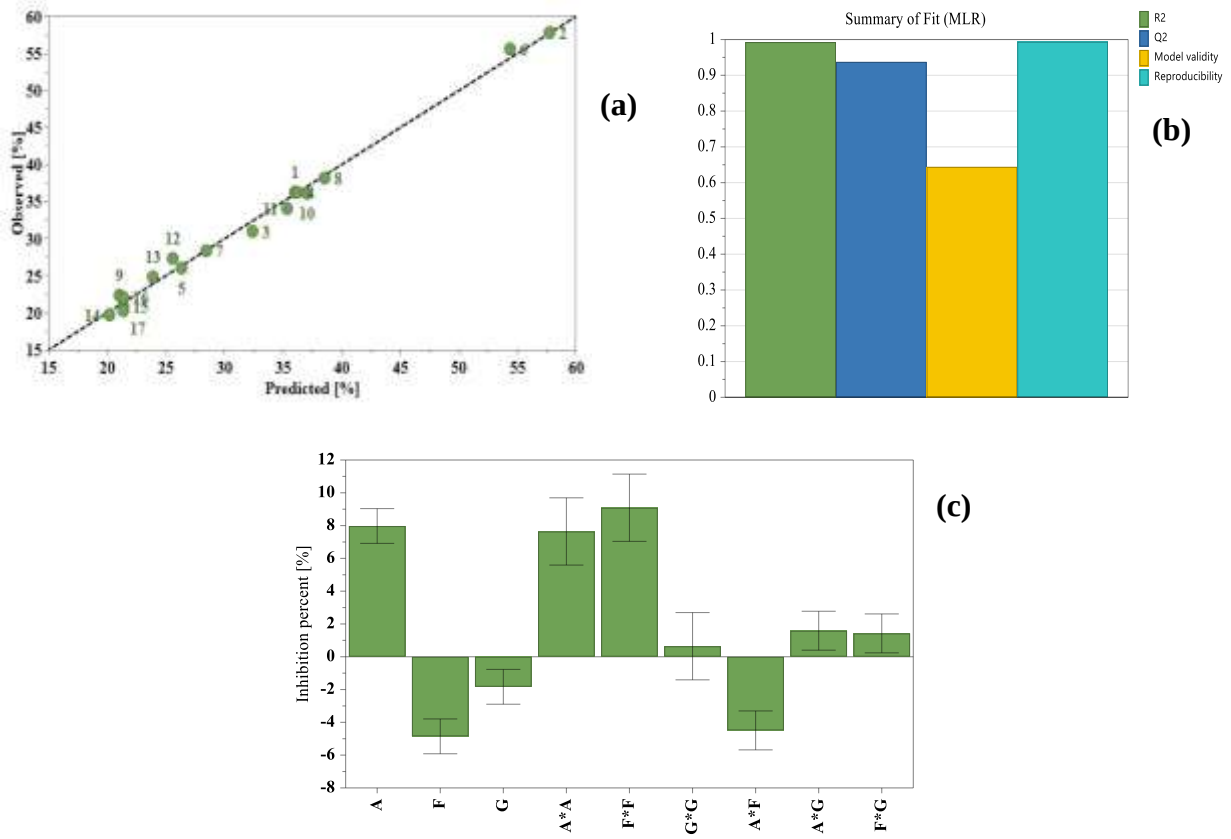

Figure 30. The linear plot of the correlation between observed and predicted values (a), plot of the summary of model fit (b), and coefficient plot for the effect of independent variable and their interactions on inhibition percentage (c).

Two-dimensional response contour plots were employed to characterize the effect of the independent variables on the inhibition percentage. The response contour plots show the influence of two variables on the response while the third variable was maintained at the center point, representing the specific inhibition percentage versus independent factors as indicated in Figure 31a-c. Figure 31a shows that the inhibition percentage increases with the increase of the volume of acetonitrile from 5 to 10 mL and the decrease in the amount of activated charcoal from 300 to 150 mg. At the low volume of acetonitrile, inhibition percentage decreases because extraction of

the analytes from the lettuce vegetable sample was not completed, and/or the cloudy state was not formed well in the DLLME step which led to low extraction efficiency (Farajzadeh et al., 2019). The plot, Figure 31b illustrates that inhibition percentage increases with the increase of the volume of acetonitrile and the decrease of the extraction time from 10 to 5 min. At the higher extraction time, inhibition percentage decrease, this may be due to possible dissolution of acetonitrile in the water (Tolcha et al., 2021). As can be seen in Figure 31c an increase in the amount of activated charcoal and extraction time leads to a decrease in the inhibition percentage. An increase in the amount of activated charcoal may lead to strong retention of pesticides resulting in low recoveries (BURSIĆ et al., 2016; Dos Santos et al., 2019; Singh et al., 2018).

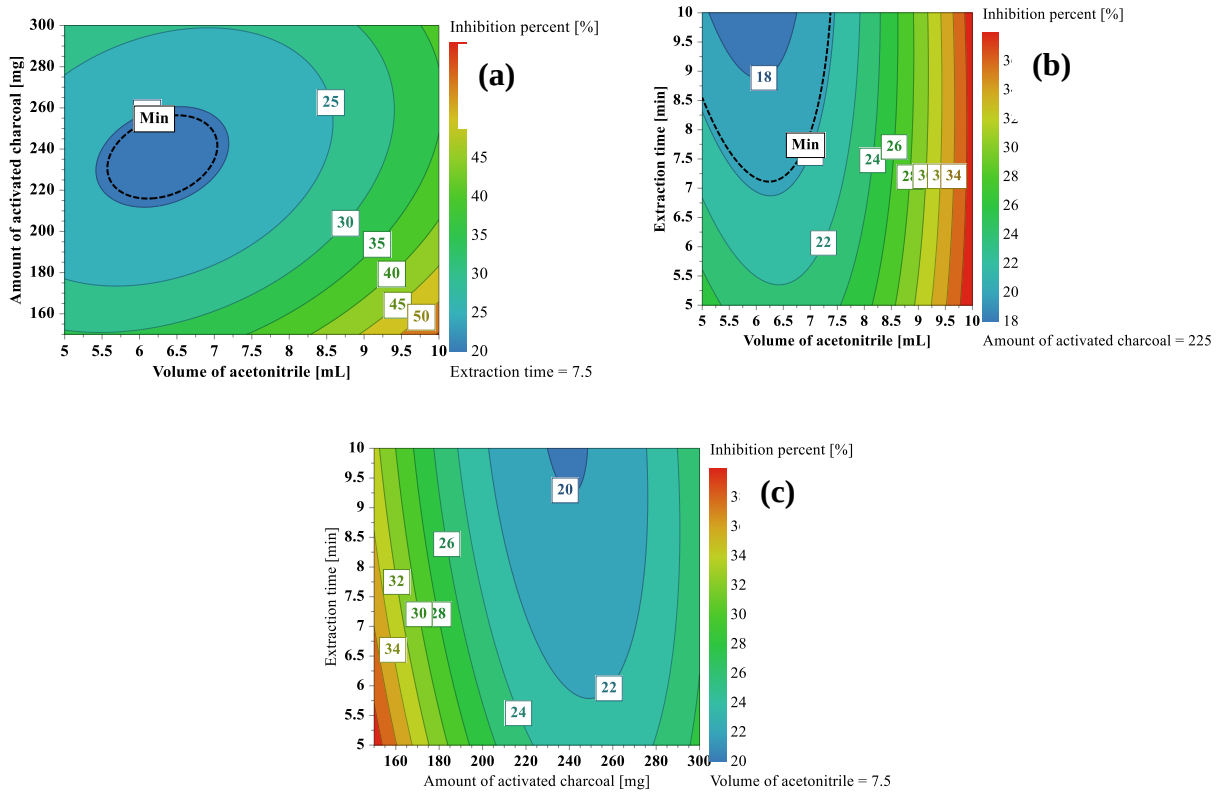

Figure 31. Response contour plots of independent variables: Volume of acetonitrile vs. amount of activated charcoal (a), volume of acetonitrile vs. extraction time (b), and amount of activated charcoal vs. extraction time (c).

4.4.2.3. Selection of Optimum Condition

In the optimization study, the RSM selects and predicts the best operating mode in the range of used variables. The model estimated a maximum inhibition percentage of 57.75% at the optimum conditions of 10 mL of the volume of acetonitrile, 150 mg of activated charcoal, and 5 min of extraction time (Table 24). Validation experiment under the optimum condition resulted in experimental inhibition percentage of 56.8 % which is almost the same to the model predicted value of 57.75%. As shown in Table 25, the factor contribution of the volume of acetonitrile, amount of activated charcoal, and extraction time on inhibition percentage are 52.6, 46.8, and 0.6%, respectively.

Table 24. Predicted response of QuEChERS-DLLME extraction and clean up parameters

Response	Objective	Value	Response range
Inhibition percentage	Maximize	57.7453	

Table 25. Optimal conditions and factor contribution of QuEChERS-DLLME extraction and clean up parameters

Factor	Value	Factor range	Factor contribution
Volume of acetonitrile	10		52.5604
Amount of activated charcoal	150		46.7504
Extraction time	5		0.689186

4.4.3. Analytical Method Validation

Table 26 depicts the results of method validation parameters. The linearity study in the concentration range of 0.01-0.64 mg kg^{-1} resulted in correlation coefficients of 0.9988-0.9997,

which shows good linearity for all studied pesticides. The enrichment factors for the studied pesticides ranged from 20 to 31. The method LOD was found to be in the range of 0.006-0.009 mg kg^{-1}, which was below MRL (0.01-0.02 mg kg^{-1}) as per EU 2016 for pesticides in the respective food commodities. The intra-and inter-day precision of the developed method at two concentration levels (0.05 and 0.5 mg kg^{-1}) were found to be in the range of 2.24-6.61% and 6.63-10.56%, respectively. The recovery obtained were in the range of 78.90 to 97.0%. Thus both recovery and %RSD results fulfilled the method acceptability criteria of the European Commission for pesticide residue analysis in food and feed samples (Sante, 2017) and could be applied to the analysis of real samples.

Table 27 compares the analytical parameters obtained using the present method with the reported values. The proposed method's LOD was significantly higher than the values reported byApilux et al. (2015) and Jin et al. (2020), and comparable to those employed sample preconcentration method (Farajzadeh et al., 2019). Moreover, our study's linear ranges were higher than those reported by Apilux et al. (2015) and lower than those reported by Jin et al. (2020) and Jing et al. (2021).

In conclusion, simple, and environmentally friendly sample preparation method was developed by coupling QuEChERS and DLLME for the µ-PAD analysis of pesticides in the Lettuce vegetables. The experimental conditions for QuEChERS-DLLME method were obtained using the PBD and CCD for screening and optimization of the most significant factors, respectively. The significant variables in the optimization study were found the amount of activated charcoal, the volume of acetonitrile and extraction time, of which the amount of activated charcoal is the most significant. The use of QuEChERS-DLLME considerably improved the preconcentration of the analytes and enriched them by a factor of 20 or more. The results of the QuEChERS-DLLME

method demonstrated satisfactory linearity, sensitivity, accuracy, and precision. Therefore, the developed method could effectively be utilized as an attractive alternative to the existing methods for the extraction of pesticides in Lettuce vegetables.

Table 26. Linear range, correlation coefficient, EF, LODs, recovery and precision of the QuEChERS-DLLME method

Pesticides	Linear range ($mg\ kg^{-1}$)	R^2	LOD ($mg\ kg^{-1}$)	Repeatability (%RSD)		Reproducibility (%RSD)		Recovery (%)		EF
				0.05 ($mg\ kg^{-1}$)	0.5 ($mg\ kg^{-1}$)	0.05 ($mg\ kg^{-1}$)	0.5 ($mg\ kg^{-1}$)	0.05 ($mg\ kg^{-1}$)	0.5 ($mg\ kg^{-1}$)	
Carbaryl	0.01-0.64	0.9992	0.009	3.21	2.29	9.71	8.62	88.97	94.94	30
Carbosulfan	0.01-0.64	0.9996	0.008	2.24	6.08	6.44	8.02	90.90	97.0	21
Chlorpyrifos	0.01-0.64	0.9997	0.006	5.91	6.61	9.91	8.15	87.74	90.11	22
Furathiocarb	0.01-0.64	0.9988	0.008	4.65	4.36	8.03	7.50	84.86	87.30	31
Malathion	0.01-0.64	0.9994	0.009	3.99	6.20	7.03	10.56	92.70	95.80	20
Methomyl	0.01-0.64	0.9996	0.007	4.53	5.60	6.63	8.93	79.0	94.6	21

Table 27. Comparison of QuEChERS-DLLME with other µ-PAD techniques

Methods	Analyte	Sample	Linear range (mg kg^{-1})	LOD (mg kg^{-1})	Reference
QuEChERS-DLLME	OP and CM	Lettuce	0.01-0.64	0.006-0.009	This study
QuEChERS	Carbaryl	Lettuce/Rice	0.1-5.0	0.5	(Apilux et al., 2015)
LPME	Carbaryl	Rice	0.3-80	0.007	(Jing et al., 2021)
LPME	Carbaryl	Wheat	0.3-80	0.006	(Jing et al., 2021)
LPME	Carbaryl	Bean	0.3-80	0.007	(Jing et al., 2021)
LPME	Carbaryl	Cabbage	0.3-80	0.008	(Jing et al., 2021)
-	Carbaryl	Lettuce	0.01-10	0.771	(Jin et al., 2020)
-	Chlorpyrifos	Lettuce	0.01-10	0.253	(Jin et al., 2020)

5. CONCLUSION AND RECOMMENDATIONS

5.1. Conclusion

Multivariate optimization of operational parameters in µ-PADs revealed satisfactory values of linearity, accuracy, and precision and over 29-64% improvement in the LOD obtained in the univariate optimization. The results confirm that RSM optimization is cost-effective, reduces the number of experimental runs, and requires a small amount of reagent. Thus, the RSM approach should be sought to enhance miniaturization in the analytical process. The use of DLLME and DLLME-QuEChERS method as a preconcentration steps significantly improved the sensitivity problem associated with µ-PADs.

The results of the study demonstrated that the µ-PAD has the potential to substitute or complement conventional analytical methods for environmental monitoring of OP and CM pesticides, particularly in resource-limited settings. Both the sample preparation and analysis methods developed in this study requires less expensive instrumentation and simple operational skills. Thus fulfilling the criteria of affordability, user-friendless, equipment-free operation, and deliverability to the end-users, as stipulated by the WHO, making them widely applicable in developing countries.

5.2. Recommendations

From this study it could be recommended that

- DTNB and ATChI are standard reagents commonly used for colorimetric determination of pesticides, but are sensitive to light. Therefore, further research is needed to improve their stability and hence the shelf life of the paper-device.
- It is important to keep prepared μ-PADs in a cold environment when storing the device for a long period of time to maintain its performance.
- The natural enzyme-based (acetylcholinesterase) colorimetric sensing technique has drawbacks such as high-cost and low stability to harsh environments. In this regard, metal organic frameworks (MOFs) can either act as the biomimetic catalysts to mimic enzymatic activities. Therefore, synchronizing biomimetic MOFs, with μ-PADs should be explored in the future for the development more cost effective and stable sensor for environmental monitoring of OP and CM pesticides.

REFERENCES

Abe, K., Suzuki, K. and Citterio, D., 2008. Inkjet-printed microfluidic multianalyte chemical sensing paper. Analytical chemistry, 80(18): 6928-6934.

Adkins, J.A., 2016. The development of paper-based microfluidic devices for environmental and food quality analysis, Colorado State University.

Ahmadvand, M., Sereshti, H. and Parastar, H., 2015. Chemometric-based determination of polycyclic aromatic hydrocarbons in aqueous samples using ultrasound-assisted emulsification microextraction combined to gas chromatography–mass spectrometry. Journal of Chromatography A, 1413: 117-126.

Aidil, M.S., Sabullah, M.K., Halmi, M.I., Sulaiman, R., Shukor, M.S., Shukor, M.Y., Shaharuddin, N.A., Syed, M.A. and Syahir, A., 2013. Assay for heavy metals using an inhibitive assay based on the acetylcholinesterase from Pangasius hypophthalmus (Sauvage, 1878). Fresenius Environ Bull, 22(12): 3572-6.

Akiyama, Y., Yoshioka, N. and Tsuji, M., 2002. Determination of ten sulfonyl urea herbicides in unpolished rice by solid-phase extraction cleanup and LC-diode array detection. Food Hygiene and Safety Science (Shokuhin Eiseigaku Zasshi), 43(2): 99-103.

Aktar, W., Sengupta, D. and Chowdhury, A., 2009. Impact of pesticides use in agriculture: their benefits and hazards. Interdisciplinary toxicology, 2(1): 1-12.

Alahmad, W., Uraisin, K., Nacapricha, D. and Kaneta, T., 2016. A miniaturized chemiluminescence detection system for a microfluidic paper-based analytical device and its application to the determination of chromium (III). Analytical Methods, 8(27): 5414-5420.

Albero, B., Sánchez-Brunete, C. and Tadeo, J.L., 2005. Multiresidue determination of pesticides in juice by solid-phase extraction and gas chromatography–mass spectrometry. Talanta, 66(4): 917-924.

Ali, M.M., Aguirre, S.D., Xu, Y., Filipe, C.D., Pelton, R. and Li, Y., 2009. Detection of DNA using bioactive paper strips. Chemical Communications(43): 6640-6642.

Alkasir, R.S., Rossner, A. and Andreescu, S., 2015. Portable colorimetric paper-based biosensing device for the assessment of bisphenol A in indoor dust. Environmental science & technology, 49(16): 9889-9897.

Amiri, A., 2016. Solid-phase microextraction-based sol–gel technique. TrAC Trends in Analytical Chemistry, 75: 57-74.

Anastassiades, M., Lehotay, S.J., Štajnbaher, D. and Schenck, F.J., 2003. Fast and easy multiresidue method employing acetonitrile extraction/partitioning and "dispersive solid-phase extraction" for the determination of pesticide residues in produce. Journal of AOAC international, 86(2): 412-431.

Andraščíková, M. and Hrouzková, S., 2016. Fast preconcentration of pesticide residues in oilseeds by combination of QuEChERS with dispersive liquid–liquid microextraction followed by gas chromatography-mass spectrometry. Food Analytical Methods, 9(8): 2182-2193.

Andrić, P., Meyer, A.S., Jensen, P.A. and Dam-Johansen, K., 2010. Reactor design for minimizing product inhibition during enzymatic lignocellulose hydrolysis: I. Significance and mechanism of cellobiose and glucose inhibition on cellulolytic enzymes. Biotechnology advances, 28(3): 308-324.

Apilux, A., Isarankura-Na-Ayudhya, C., Tantimongcolwat, T. and Prachayasittikul, V., 2015. based acetylcholinesterase inhibition assay combining a wet system for organophosphate and carbamate pesticides detection. Excli Journal, 14: 307.

Arduini, F., Ricci, F., Bourais, I., Amine, A., Moscone, D. and Palleschi, G., 2005. Extraction and detection of pesticides by cholinesterase inhibition in a two-phase system: A strategy to avoid heavy metal interference. Analytical letters, 38(11): 1703-1719.

Arunachalam, R. and Annadurai, G., 2011. Optimized response surface methodology for adsorption of dyestuff from aqueous solution. Journal of environmental science and technology, 4(1): 65-72.

Asensio-Ramos, M., Hernández-Borges, J., Borges-Miquel, T.M. and Rodríguez-Delgado, M.Á., 2011a. Ionic liquid-dispersive liquid–liquid microextraction for the simultaneous determination of pesticides and metabolites in soils using high-performance liquid chromatography and fluorescence detection. Journal of Chromatography A, 1218(30): 4808-4816.

Asensio-Ramos, M., Ravelo-Pérez, L.M., González-Curbelo, M.Á. and Hernández-Borges, J., 2011b. Liquid phase microextraction applications in food analysis. Journal of Chromatography A, 1218(42): 7415-7437.

Assefa, G., 2011. Pesticide use in Ethiopia. Ministry of Agriculture, Addis Ababa.

Atwood, D. and Paisley-Jones, C., 2017. Pesticides industry sales and usage: 2008–2012 market estimates. US Environmental Protection Agency, Washington, DC, 20460.

Aysal, P., Ambrus, Á., Lehotay, S.J. and Cannavan, A., 2007. Validation of an efficient method for the determination of pesticide residues in fruits and vegetables using ethyl acetate for extraction. Journal of Environmental Science and Health, Part B, 42(5): 481-490.

Badawy, M.E. and El-Aswad, A.F., 2014. Bioactive paper sensor based on the acetylcholinesterase for the rapid detection of organophosphate and carbamate pesticides. International Journal of Analytical Chemistry, 2014.

Bagheri, A.R., Ghaedi, M., Asfaram, A., Jannesar, R. and Goudarzi, A., 2017. Design and construction of nanoscale material for ultrasonic assisted adsorption of dyes: application of derivative spectrophotometry and experimental design methodology. Ultrasonics sonochemistry, 35: 112-123.

Baltussen, E., Cramers, C. and Sandra, P., 2002. Sorptive sample preparation–a review. Analytical and bioanalytical chemistry, 373(1): 3-22.

Ban, T., Kawaizumi, F., Nii, S. and Takahashi, K., 2000. Study of drop coalescence behavior for liquid–liquid extraction operation. Chemical engineering science, 55(22): 5385-5391.

Barr, M.C., Rowehl, J.A., Lunt, R.R., Xu, J., Wang, A., Boyce, C.M., Im, S.G., Bulović, V. and Gleason, K.K., 2011. Direct monolithic integration of organic photovoltaic circuits on unmodified paper. Advanced Materials, 23(31): 3500-3505.

Bedassa, T., Gure, A. and Megersa, N., 2017. The QuEChERS analytical method combined with low density solvent based dispersive liquid–liquid microextraction for quantitative extraction of multiclass pesticide residues in cereals. Bulletin of the Chemical Society of Ethiopia, 31(1): 1-15.

Berijani, S., Assadi, Y., Anbia, M., Hosseini, M.-R.M. and Aghaee, E., 2006. Dispersive liquid–liquid microextraction combined with gas chromatography-flame photometric detection:

very simple, rapid and sensitive method for the determination of organophosphorus pesticides in water. Journal of Chromatography A, 1123(1): 1-9.

Beshana, S., Hussen, A., Leta, S. and Kaneta, T., 2022a. Dispersive liquid–liquid microextraction coupled with microfluidic paper-based analytical device for the determination of organophosphate and carbamate pesticides in the water sample. Analytical Sciences: 1-9.

Beshana, S., Hussen, A., Leta, S. and Kaneta, T., 2022b. Microfluidic Paper Based Analytical Devices for the Detection of Carbamate Pesticides. Bulletin of Environmental Contamination and Toxicology: 1-8.

Bezerra, M.A., Santelli, R.E., Oliveira, E.P., Villar, L.S. and Escaleira, L.A., 2008. Response surface methodology (RSM) as a tool for optimization in analytical chemistry. Talanta, 76(5): 965-977.

Birch, N.C. and Stickle, D.F., 2003. Example of use of a desktop scanner for data acquisition in a colorimetric assay. Clinica chimica acta, 1(333): 95-96.

Bolzan, C.M., Caldas, S.S., Guimarães, B.S. and Primel, E.G., 2015a. Dispersive liquid-liquid microextraction with liquid chromatography-tandem mass spectrometry for the determination of triazine, neonicotinoid, triazole and imidazolinone pesticides in mineral water samples. Journal of the Brazilian Chemical Society, 26: 1902-1913.

Bolzan, C.M., Caldas, S.S., Soares, B.M. and Primel, E.G., 2015b. Dispersive liquid–liquid microextraction for the preconcentration of multiple classes of pesticides in water. Analytical Letters, 48(17): 2754-2772.

Box, G.E. and Draper, N.R., 1987. Empirical model-building and response surfaces. John Wiley & Sons.

Box, G.E., Hunter, J.S. and Hunter, W.G., 2005. Statistics for experimenters: design, innovation, and discovery, 2. Wiley-Interscience New York.

Brondi, S.d., De MacEdo, A., Vicente, G. and Nogueira, A., 2011. Evaluation of the QuEChERS method and gas chromatography–mass spectrometry for the analysis pesticide residues in water and sediment. Bulletin of Environmental Contamination and Toxicology, 86(1): 18-22.

Bruns, R.E., Scarminio, I.S. and de Barros Neto, B., 2006. Statistical design-chemometrics. Elsevier.

Bruzewicz, D.A., Reches, M. and Whitesides, G.M., 2008. Low-cost printing of poly (dimethylsiloxane) barriers to define microchannels in paper. Analytical chemistry, 80(9): 3387-3392.

Bursić, V., Vuković, G., Zeremski, T., Marinković, D., Gvozdenac, S., Popović, A. and Petrović, A., 2016. Advantages and disadvantages of active carbon in QuEChERS sample preparation method for pesticide residues. Biotechnology, 20: 191.

Cacho, J., Campillo, N., Viñas, P. and Hernández-Córdoba, M., 2018. In situ ionic liquid dispersive liquid-liquid microextraction coupled to gas chromatography-mass spectrometry for the determination of organophosphorus pesticides. Journal of Chromatography A, 1559: 95-101.

Caglayan, M.G., Sheykhi, S., Mosca, L. and Anzenbacher, P., 2016. Fluorescent zinc and copper complexes for detection of adrafinil in paper-based microfluidic devices. Chemical Communications, 52(53): 8279-8282.

Cai, L., Xu, C., Lin, S., Luo, J., Wu, M. and Yang, F., 2014. A simple paper-based sensor fabricated by selective wet etching of silanized filter paper using a paper mask. Biomicrofluidics, 8(5): 056504.

Cai, Y., Cai, Y.e., Shi, Y., Liu, J., Mou, S. and Lu, Y., 2007. A liquid–liquid extraction technique for phthalate esters with water-soluble organic solvents by adding inorganic salts. Microchimica Acta, 157(1-2): 73-79.

Candioti, L.V., De Zan, M.M., Cámara, M.S. and Goicoechea, H.C., 2014. Experimental design and multiple response optimization. Using the desirability function in analytical methods development. Talanta, 124: 123-138.

Carrilho, E., Martinez, A.W. and Whitesides, G.M., 2009a. Understanding wax printing: a simple micropatterning process for paper-based microfluidics. Analytical chemistry, 81(16): 7091-7095.

Carrilho, E., Phillips, S.T., Vella, S.J., Martinez, A.W. and Whitesides, G.M., 2009b. Paper microzone plates. Analytical chemistry, 81(15): 5990-5998.

Carter-Franklin, J.N., Victa, C., McDonald, P. and Fahrner, R., 2007. Fragments of protein A eluted during protein A affinity chromatography. Journal of Chromatography A, 1163(1-2): 105-111.

Cate, D.M., Adkins, J.A., Mettakoonpitak, J. and Henry, C.S., 2014. Recent developments in paper-based microfluidic devices. Analytical chemistry, 87(1): 19-41.

Ceylan, H., Kubilay, S., Aktas, N. and Sahiner, N., 2008. An approach for prediction of optimum reaction conditions for laccase-catalyzed bio-transformation of 1-naphthol by response surface methodology (RSM). Bioresource technology, 99(6): 2025-2031.

Chauhan, N., Narang, J. and Pundir, C., 2011. Immobilization of rat brain acetylcholinesterase on ZnS and poly (indole-5-carboxylic acid) modified Au electrode for detection of organophosphorus insecticides. Biosensors and Bioelectronics, 29(1): 82-88.

Chen, C., Li, Y., Chen, M., Chen, Z. and Qian, Y., 2009. Organophosphorus pesticide residues in milled rice (Oryza sativa) on the Chinese market and dietary risk assessment. Food Additives & Contaminants: Part A, 26(3): 340-347.

Chen, H., Chen, R. and Li, S., 2010. Low-density extraction solvent-based solvent terminated dispersive liquid–liquid microextraction combined with gas chromatography-tandem mass spectrometry for the determination of carbamate pesticides in water samples. Journal of Chromatography A, 1217(8): 1244-1248.

Chen, L., Yin, L., Song, F., Liu, Z., Zheng, Z., Xing, J. and Liu, S., 2013. Determination of pesticide residues in ginseng by dispersive liquid–liquid microextraction and ultra high performance liquid chromatography–tandem mass spectrometry. Journal of Chromatography B, 917: 71-77.

Chen, X., Yu, S., Yang, L., Wang, J. and Jiang, C., 2016. Fluorescence and visual detection of fluoride ions using a photoluminescent graphene oxide paper sensor. Nanoscale, 8(28): 13669-13677.

Cheng, C.M., Martinez, A.W., Gong, J., Mace, C.R., Phillips, S.T., Carrilho, E., Mirica, K.A. and Whitesides, G.M., 2010. Paper-based ELISA. Angewandte Chemie International Edition, 49(28): 4771-4774.

Cheng, J.-Y., Yen, M.-H., Wei, C.-W., Chuang, Y.-C. and Young, T.-H., 2005. Crack-free direct-writing on glass using a low-power UV laser in the manufacture of a microfluidic chip. Journal of Micromechanics and Microengineering, 15(6): 1147.

Cui, J., Lisak, G., Strzalkowska, S. and Bobacka, J., 2014. Potentiometric sensing utilizing paper-based microfluidic sampling. Analyst, 139(9): 2133-2136.

Cunha, S. and Fernandes, J., 2011. Multipesticide residue analysis in maize combining acetonitrile-based extraction with dispersive liquid–liquid microextraction followed by gas chromatography–mass spectrometry. Journal of Chromatography A, 1218(43): 7748-7757.

Cunningham, J.C., Brenes, N.J. and Crooks, R.M., 2014. Paper electrochemical device for detection of DNA and thrombin by target-induced conformational switching. Analytical chemistry, 86(12): 6166-6170.

Dăneţ, A.F., Bucur, B., Cheregi, M.-C., Badea, M. and Şerban, S., 2003. Spectrophotometric determination of organophosphoric insecticides in a FIA system based on AChE inhibition. Analytical letters, 36(1): 59-73.

Danzer, T. and Schwedt, G., 1996. Chemometric methods for the development of a biosensor system and the evaluation of inhibition studies with solutions and mixtures of pesticides and heavy metals Part 1. Development of an enzyme electrodes system for pesticide and heavy metal screening using selected chemometric methods. Analytica chimica acta, 318(3): 275-286.

Darreh-Shori, T. and Soininen, H., 2010. Effects of cholinesterase inhibitors on the activities and protein levels of cholinesterases in the cerebrospinal fluid of patients with Alzheimer's disease: a review of recent clinical studies. Current Alzheimer Research, 7(1): 67-73.

Dawson, A.H., Eddleston, M., Senarathna, L., Mohamed, F., Gawarammana, I., Bowe, S.J., Manuweera, G. and Buckley, N.A., 2010. Acute human lethal toxicity of agricultural pesticides: a prospective cohort study. PLoS medicine, 7(10).

De Alwis, G.H., Needham, L.L. and Barr, D.B., 2006. Measurement of human urinary organophosphate pesticide metabolites by automated solid-phase extraction, post extraction derivatization, and gas chromatography–tandem mass spectrometry. Journal of Chromatography B, 843(1): 34-41.

de Pinho, G.P. and Neves, A.A., 2010. Maria Eliana Lopes Ribeiro de Queiroz, et al. Optimization of the liquid-liquid extraction method and low temperature purification (LLE-LTP) for pesticide residue analysis in honey samples by gas chromatography. Food Control, 21(10): 1307-1311.

Dehghani, M.H., Faraji, M., Mohammadi, A. and Kamani, H., 2017. Optimization of fluoride adsorption onto natural and modified pumice using response surface methodology: isotherm, kinetic and thermodynamic studies. Korean Journal of Chemical Engineering, 34(2): 454-462.

Dejaegher, B., Dumarey, M., Capron, X., Bloomfield, M.S. and Vander Heyden, Y., 2007. Comparison of Plackett–Burman and supersaturated designs in robustness testing. Analytica chimica acta, 595(1-2): 59-71.

del Castillo, M.L.R., Rodríguez-Valenciano, M., Flores, G. and Blanch, G.P., 2019. New method based on Solid Phase Microextraction and Multidimensional gas chromatography-mass spectrometry to determine pesticides in strawberry jam. LWT, 99: 283-290.

Demeestere, K., Dewulf, J., De Witte, B. and Van Langenhove, H., 2007. Sample preparation for the analysis of volatile organic compounds in air and water matrices. Journal of chromatography A, 1153(1-2): 130-144.

Dos Santos, E.O., Gonzales, J.O., Ores, J.C., Marube, L.C., Caldas, S.S., Furlong, E.B. and Primel, E.G., 2019. Sand as a solid support in ultrasound-assisted MSPD: A simple, green and low-cost method for multiresidue pesticide determination in fruits and vegetables. Food chemistry, 297: 124926.

Dou, M., Sanjay, S.T., Benhabib, M., Xu, F. and Li, X., 2015. Low-cost bioanalysis on paper-based and its hybrid microfluidic platforms. Talanta, 145: 43-54.

Du, D., Huang, X., Cai, J. and Zhang, A., 2007. Amperometric detection of triazophos pesticide using acetylcholinesterase biosensor based on multiwall carbon nanotube–chitosan matrix. Sensors and Actuators B: Chemical, 127(2): 531-535.

Dungchai, W., Chailapakul, O. and Henry, C.S., 2009. Electrochemical detection for paper-based microfluidics. Analytical chemistry, 81(14): 5821-5826.

Dungchai, W., Chailapakul, O. and Henry, C.S., 2011. A low-cost, simple, and rapid fabrication method for paper-based microfluidics using wax screen-printing. Analyst, 136(1): 77-82.

Dušek, M., Jandovská, V., Čermák, P., Mikyška, A. and Olšovská, J., 2016. A novel approach for identification of biologically active phenolic compounds in complex matrices using hybrid quadrupole-orbitrap mass spectrometer: A promising tool for testing antimicrobial activity of hops. Talanta, 156: 209-217.

EC, 2005. Commission Regulation (EC) No 396/2005 of 23 February 2005 on maximum residue levels of pesticides in or on food and feed of plant and animal origin. Official Journal of European Union L, 70: 1-16.

Eldridge, B.F., 2008. Pesticide application and safety training for applicators of public health pesticides. Vector-Borne Disease Section, Center for Infectious Diseases California Department of Public Health.

Ellman, G.L., 1959. Tissue sulfhydryl groups. Archives of biochemistry and biophysics, 82(1): 70-77.

Elsharkawy, M., Schutzius, T.M. and Megaridis, C.M., 2014. Inkjet patterned superhydrophobic paper for open-air surface microfluidic devices. Lab on a Chip, 14(6): 1168-1175.

Evans, E., Gabriel, E.F.M., Coltro, W.K.T. and Garcia, C.D., 2014. Rational selection of substrates to improve color intensity and uniformity on microfluidic paper-based analytical devices. Analyst, 139(9): 2127-2132.

Farajzadeh, M.A., Djozan, D., Mogaddam, M.A. and Bamorowat, M., 2011. Extraction and preconcentration technique for triazole pesticides from cow milk using dispersive liquid–liquid microextraction followed by GC-FID and GC-MS determinations. Journal of separation science, 34(11): 1309-1316.

Farajzadeh, M.A., Goushjuii, L., Djozan, D. and Mohammadi, J.K., 2012. Dispersive liquid–liquid microextraction combined with gas chromatography for extraction and determination of class 1 residual solvents in pharmaceuticals. Journal of separation science, 35(8): 1027-1035.

Farajzadeh, M.A., Khoshmarram, L. and Sheykhizadeh, S., 2014a. A review on application of microextraction techniques for analysis of chemical compounds and metal ions in foodstuffs. Analytical and Bioanalytical Chemistry Research, 1(1): 1-19.

Farajzadeh, M.A., Sohrabi, H. and Mohebbi, A., 2019. Combination of modified QuEChERS extraction method and dispersive liquid–liquid microextraction as an efficient sample preparation approach for extraction and preconcentration of pesticides from fruit and vegetable samples. Food Analytical Methods, 12(2): 534-543.

Farajzadeh, M.A., Sorouraddin, S.M. and Mogaddam, M.R.A., 2014b. Liquid phase microextraction of pesticides: a review on current methods. Microchimica Acta, 181(9-10): 829-851.

Farré, M., Pérez, S., Gonçalves, C., Alpendurada, M. and Barceló, D., 2010. Green analytical chemistry in the determination of organic pollutants in the aquatic environment. TrAC Trends in Analytical Chemistry, 29(11): 1347-1362.

Fernández-Ramos, M.D., Ogunneye, A., Babarinde, N., Erenas, M. and Capitán-Vallvey, L.F., 2020. Bioactive microfluidic paper device for pesticide determination in waters. Talanta, 218: 121108.

Ferreira, S.C., Bruns, R., Ferreira, H., Matos, G., David, J., Brandão, G., da Silva, E.P., Portugal, L., Dos Reis, P. and Souza, A., 2007. Box-Behnken design: an alternative for the optimization of analytical methods. Analytica chimica acta, 597(2): 179-186.

Filippou, O., Bitas, D. and Samanidou, V., 2017. Green approaches in sample preparation of bioanalytical samples prior to chromatographic analysis. Journal of Chromatography B, 1043: 44-62.

Fishel, F.M. and Ferrell, J.A., 2010. Managing pesticide drift. EDIS, 2010(7).

Fontana, A.R. and Bottini, R., 2016. QuEChERS Method for the Determination of 3-Alkyl-2-Methoxypyrazines in Wines by Gas Chromatography-Mass Spectrometry. Food Analytical Methods, 9(12): 3352-3359.

Friedman, M., 1973. Chemistry and biochemistry of the sulfhydryl group in amino acids, peptides and proteins.

Funes-Huacca, M., Wu, A., Szepesvari, E., Rajendran, P., Kwan-Wong, N., Razgulin, A., Shen, Y., Kagira, J., Campbell, R. and Derda, R., 2012. Portable self-contained cultures for phage and bacteria made of paper and tape. Lab on a Chip, 12(21): 4269-4278.

Galindo Padilha, G.A., Ko, J., Jung, J.J. and de Mattos Neto, P.S.G., 2022. Transformer-Based Hybrid Forecasting Model for Multivariate Renewable Energy. Applied Sciences, 12(21): 10985.

Gambacorta, G., Faccia, M., Lamacchia, C., Di Luccia, A. and La Notte, E., 2005. Pesticide residues in tomato grown in open field. Food control, 16(7): 629-632.

Gelsomino, A., Petrovičová, B., Tiburtini, S., Magnani, E. and Felici, M., 1997. Multiresidue analysis of pesticides in fruits and vegetables by gel permeation chromatography followed by gas chromatography with electron-capture and mass spectrometric detection. Journal of chromatography A, 782(1): 105-122.

Germany, P., 2012. Pesticides and health hazards facts and figures, Hamburg, Germany.

Ghani, S.B.A., Alhewairini, S.S. and Hrouzková, S., 2018. A fast and easy QuEChERS-DLLME method combined with GC-MS for ethion and bifenthrin residues determination and study of their dissipation dynamics in palm dates. Food Analytical Methods, 11(12): 3542-3550.

Goel, A. and Aggarwal, P., 2007. Pesticide poisoning. National medical journal of India, 20(4): 182.

Gong, J., Guan, Z. and Song, D., 2013. Biosensor based on acetylcholinesterase immobilized onto layered double hydroxides for flow injection/amperometric detection of organophosphate pesticides. Biosensors and Bioelectronics, 39(1): 320-323.

González-Curbelo, M.Á., Lehotay, S.J., Hernández-Borges, J. and Rodríguez-Delgado, M.Á., 2014. Use of ammonium formate in QuEChERS for high-throughput analysis of pesticides in food by fast, low-pressure gas chromatography and liquid chromatography tandem mass spectrometry. Journal of Chromatography A, 1358: 75-84.

Guillette, L.J. and Iguchi, T., 2012. Life in a contaminated world. Science, 337(6102): 1614-1615.

Hadjmohammadi, M.R., Fatemi, M.H. and Shakeri, P., 2012. Developing an alcoholic-assisted dispersive liquid–liquid microextraction for extraction of pentachlorophenol in water. Journal of separation science, 35(23): 3375-3380.

Hamed, A.M., Moreno-González, D., Gámiz-Gracia, L. and García-Campaña, A.M., 2017. Evaluation of a new modified QuEChERS method for the monitoring of carbamate residues in high-fat cheeses by using UHPLC–MS/MS. Journal of separation science, 40(2): 488-496.

Hamilton, D., Ambrus, A., Dieterle, R., Felsot, A., Harris, C., Holland, P., Katayama, A., Kurihara, N., Linders, J. and Unsworth, J., 2003. Regulatory limits for pesticide residues in water (IUPAC Technical Report). Pure and Applied Chemistry, 75(8): 1123-1155.

Han, D. and Row, K.H., 2012. Trends in liquid-phase microextraction, and its application to environmental and biological samples. Microchimica Acta, 176(1-2): 1-22.

Hao, T.J. and Sulaiman, A., 2019. Comparison between Univariate and Multivariate Optimisations on Wet Digestion of Almond Nuts Prior To Determination of Magnesium. eProceedings Chemistry, 4(1).

Harris, N., Hill, M., Beeby, S., Shen, Y., White, N., Hawkes, J. and Coakley, W., 2003. A silicon microfluidic ultrasonic separator. Sensors and Actuators B: Chemical, 95(1-3): 425-434.

He, P.J., Katis, I.N., Eason, R.W. and Sones, C.L., 2015a. Laser-based patterning for fluidic devices in nitrocellulose. Biomicrofluidics, 9(2): 026503.

He, Q., Ma, C., Hu, X. and Chen, H., 2013. Method for fabrication of paper-based microfluidic devices by alkylsilane self-assembling and UV/O3-patterning. Analytical chemistry, 85(3): 1327-1331.

He, Y., Wu, W.-b. and Fu, J.-z., 2015b. Rapid fabrication of paper-based microfluidic analytical devices with desktop stereolithography 3D printer. Rsc Advances, 5(4): 2694-2701.

Hennion, M.-C., 1999. Solid-phase extraction: method development, sorbents, and coupling with liquid chromatography. Journal of chromatography A, 856(1-2): 3-54.

Hercegová, A., Dömötörová, M., Kružlicová, D. and Matisová, E., 2006. Comparison of sample preparation methods combined with fast gas chromatography–mass spectrometry for ultratrace analysis of pesticide residues in baby food. Journal of separation science, 29(8): 1102-1109.

Herrera-Herrera, A.V., Asensio-Ramos, M., Hernández-Borges, J. and Rodríguez-Delgado, M.Á., 2010. Dispersive liquid-liquid microextraction for determination of organic analytes. TrAC Trends in Analytical Chemistry, 29(7): 728-751.

Hodgson, E., 2004. A textbook of modern toxicology. John Wiley & Sons.

Hossain, S.Z., Luckham, R.E., McFadden, M.J. and Brennan, J.D., 2009. Reagentless bidirectional lateral flow bioactive paper sensors for detection of pesticides in beverage and food samples. Analytical chemistry, 81(21): 9055-9064.

Hu, C., Bai, X., Wang, Y., Jin, W., Zhang, X. and Hu, S., 2012. Inkjet printing of nanoporous gold electrode arrays on cellulose membranes for high-sensitive paper-like electrochemical oxygen sensors using ionic liquid electrolytes. Analytical chemistry, 84(8): 3745-3750.

Hussain, S., Siddique, T., Saleem, M., Arshad, M. and Khalid, A., 2009. Impact of pesticides on soil microbial diversity, enzymes, and biochemical reactions. Advances in agronomy, 102: 159-200.

Hyötyläinen, T. and Riekkola, M.-L., 2008. Sorbent-and liquid-phase microextraction techniques and membrane-assisted extraction in combination with gas chromatographic analysis: A review. Analytica chimica acta, 614(1): 27-37.

Ince, M. and Ince, O.K., 2019. Heavy metal removal techniques using response surface methodology: Water/wastewater treatment. Biochemical Toxicology-Heavy Metals and Nanomaterials.

Ismail, A., Araújo, M.O., Chagas, C.L., Griveau, S., D'Orlyé, F., Varenne, A., Bedioui, F. and Coltro, W.K., 2016. Colorimetric analysis of the decomposition of S-nitrosothiols on paper-based microfluidic devices. Analyst, 141(22): 6314-6320.

Izmailov, N. and Shraiber, M., 1938. A drop-chromatographic method of analysis and its applications to pharmacy. Farmatsiya, 3: 1-7.

Izquierdo, A., Tena, M., de Castro, M.L. and Valcarcel, M., 1996. Supercritical fluid extraction of carbamate pesticides from soils and cereals. Chromatographia, 42(3-4): 206-212.

Jaffrezic-Renault, N., 2001. New trends in biosensors for organophosphorus pesticides. Sensors, 1(2): 60-74.

Jarujamrus, P., Tian, J., Li, X., Siripinyanond, A., Shiowatana, J. and Shen, W., 2012. Mechanisms of red blood cells agglutination in antibody-treated paper. Analyst, 137(9): 2205-2210.

Jayaraj, R., Megha, P. and Sreedev, P., 2016. Organochlorine pesticides, their toxic effects on living organisms and their fate in the environment. Interdisciplinary toxicology, 9(3-4): 90-100.

Jayawardane, B.M., Wongwilai, W., Grudpan, K., Kolev, S., Heaven, M., Nash, D. and McKelvie, I., 2014. Evaluation and application of a paper-based device for the determination of reactive phosphate in soil solution. Journal of environmental quality, 43(3): 1081-1085.

Jenkins, G., Wang, Y., Xie, Y.L., Wu, Q., Huang, W., Wang, L. and Yang, X., 2015. Printed electronics integrated with paper-based microfluidics: new methodologies for next-generation health care. Microfluidics and Nanofluidics, 19(2): 251-261.

Jia, C., Zhu, X., Chen, L., He, M., Yu, P. and Zhao, E., 2010. Extraction of organophosphorus pesticides in water and juice using ultrasound-assisted emulsification–mixroextraction. Journal of separation science, 33(2): 244-250.

Jiang, Y., Hao, Z., He, Q. and Chen, H., 2016. A simple method for fabrication of microfluidic paper-based analytical devices and on-device fluid control with a portable corona generator. RSC advances, 6(4): 2888-2894.

Jimidar, M., Niemeijer, N., Peeters, R. and Hoogmartens, J., 1998. Robustness testing of a liquid chromatography method for the determination of vorozole and its related compounds in oral tablets. Journal of pharmaceutical and biomedical analysis, 18(4-5): 479-485.

Jin, L., Hao, Z., Zheng, Q., Chen, H., Zhu, L., Wang, C., Liu, X. and Lu, C., 2020. A facile microfluidic paper-based analytical device for acetylcholinesterase inhibition assay utilizing organic solvent extraction in rapid detection of pesticide residues in food. Analytica chimica acta, 1100: 215-224.

Jing, X., Wang, H., Huang, X., Chen, Z., Zhu, J. and Wang, X., 2021. Digital image colorimetry detection of carbaryl in food samples based on liquid phase microextraction coupled with a microfluidic thread-based analytical device. Food Chemistry, 337: 127971.

Jokerst, J.C., Adkins, J.A., Bisha, B., Mentele, M.M., Goodridge, L.D. and Henry, C.S., 2012. Development of a paper-based analytical device for colorimetric detection of select foodborne pathogens. Analytical chemistry, 84(6): 2900-2907.

Kampioti, A.A., da Cunha, A.C.B., de Alda, M.L. and Barceló, D., 2005. Fully automated multianalyte determination of different classes of pesticides, at picogram per litre levels in water, by on-line solid-phase extraction–liquid chromatography–electrospray–tandem mass spectrometry. Analytical and Bioanalytical Chemistry, 382(8): 1815-1825.

Kataoka, H., 2003. New trends in sample preparation for clinical and pharmaceutical analysis. TrAC Trends in Analytical Chemistry, 22(4): 232-244.

Kavruk, M., Özalp, V.C. and Öktem, H.A., 2013. Portable bioactive paper-based sensor for quantification of pesticides. Journal of Analytical Methods in Chemistry, 2013.

Kevan, P.G., 1999. Pollinators as bioindicators of the state of the environment: species, activity and diversity, Invertebrate Biodiversity as Bioindicators of Sustainable Landscapes. Elsevier, pp. 373-393.

Khodadoust, S. and Ghaedi, M., 2013. Optimization of dispersive liquid–liquid microextraction with central composite design for preconcentration of chlordiazepoxide drug and its determination by HPLC-UV. Journal of separation science, 36(11): 1734-1742.

Kim, H.J., Kim, Y., Park, S.J., Kwon, C. and Noh, H., 2018. Development of colorimetric paper sensor for pesticide detection using competitive-inhibiting reaction. BioChip Journal, 12(4): 326-331.

Kim, K.-H., Kabir, E. and Jahan, S.A., 2017. Exposure to pesticides and the associated human health effects. Science of the Total Environment, 575: 525-535.

Kocúrová, L., Balogh, I.S., Šandrejová, J. and Andruch, V., 2012. Recent advances in dispersive liquid–liquid microextraction using organic solvents lighter than water. A review. Microchemical Journal, 102: 11-17.

Kok, F.N., Bozoglu, F. and Hasirci, V., 2002. Construction of an acetylcholinesterase–choline oxidase biosensor for aldicarb determination. Biosensors and Bioelectronics, 17(6-7): 531-539.

Krężel, A., Leśniak, W., Jeżowska-Bojczuk, M., Młynarz, P., Brasuñ, J., Kozłowski, H. and Bal, W., 2001. Coordination of heavy metals by dithiothreitol, a commonly used thiol group protectant. Journal of inorganic biochemistry, 84(1-2): 77-88.

Krieger, R., 2001. Handbook of Pesticide Toxicology: Principles and Agents, 1. Academic press.

Kukla, A., Kanjuk, N., Starodub, N. and Shirshov, Y.M., 1999. Multienzyme electrochemical sensor array for determination of heavy metal ions. Sensors and Actuators B: Chemical, 57(1-3): 213-218.

Kvíčalová, M., Doubravová, P., Jobánek, R., Jokešová, M., Očenášková, V., Süssenbeková, H. and Svobodová, A., 2012. Application of different extraction methods for the determination of selected pesticide residues in sediments. Bulletin of environmental contamination and toxicology, 89(1): 21-26.

Lambropoulou, D.A. and Albanis, T.A., 2007a. Liquid-phase micro-extraction techniques in pesticide residue analysis. Journal of biochemical and biophysical methods, 70(2): 195-228.

Lambropoulou, D.A. and Albanis, T.A., 2007b. Methods of sample preparation for determination of pesticide residues in food matrices by chromatography–mass spectrometry-based techniques: a review. Analytical and Bioanalytical Chemistry, 389(6): 1663-1683.

Lee, M.-G., Patil, V., Na, Y.-C., Lee, D.S., Lim, S.H. and Yi, G.-R., 2018. Highly stable, rapid colorimetric detection of carbaryl pesticides by azo coupling reaction with chemical pre-treatment. Sensors and Actuators B: Chemical, 261: 489-496.

Lee, S.-J., Mehler, L., Beckman, J., Diebolt-Brown, B., Prado, J., Lackovic, M., Waltz, J., Mulay, P., Schwartz, A. and Mitchell, Y., 2011. Acute pesticide illnesses associated with off-target pesticide drift from agricultural applications: 11 States, 1998–2006. Environmental health perspectives, 119(8): 1162-1169.

Lehotay, S., 2007. AOAC official method 2007.01 pesticide residues in foods by acetonitrile extraction and partitioning with Magnesium Sulfate. Journal of AOAC International, 90(2): 485-520.

Lehotay, S.J., Kok, A.d., Hiemstra, M. and Bodegraven, P.v., 2005a. Validation of a fast and easy method for the determination of residues from 229 pesticides in fruits and vegetables using

gas and liquid chromatography and mass spectrometric detection. Journal of AOAC International, 88(2): 595-614.

Lehotay, S.J., Maštovská, K. and Yun, S.J., 2005b. Evaluation of two fast and easy methods for pesticide residue analysis in fatty food matrixes. Journal of AOAC International, 88(2): 630-638.

Lei, K.F., Lee, K.-F. and Yang, S.-I., 2012. Fabrication of carbon nanotube-based pH sensor for paper-based microfluidics. Microelectronic Engineering, 100: 1-5.

Lesueur, C., Gartner, M., Mentler, A. and Fuerhacker, M., 2008. Comparison of four extraction methods for the analysis of 24 pesticides in soil samples with gas chromatography–mass spectrometry and liquid chromatography–ion trap–mass spectrometry. Talanta, 75(1): 284-293.

Li, J., Sun, M., Chang, Q., Hu, X., Kang, J. and Fan, C., 2017. Determination of pesticide residues in teas via QuEChERS combined with dispersive liquid–liquid microextraction followed by gas chromatography–tandem mass spectrometry. Chromatographia, 80(9): 1447-1458.

Li, J., Wang, Y.-B., Li, K.-Y., Cao, Y.-Q., Wu, S. and Wu, L., 2015a. Advances in different configurations of solid-phase microextraction and their applications in food and environmental analysis. TRAC Trends in Analytical Chemistry, 72: 141-152.

Li, M., Cao, R., Nilghaz, A., Guan, L., Zhang, X. and Shen, W., 2015b. "Periodic-table-style" paper device for monitoring heavy metals in water. Analytical chemistry, 87(5): 2555-2559.

Li, M., Li, Y. and Mao, L., 2007. Application of single drop microextraction in the determination of phthalate esters in food by gas chromatography-mass spectrometry. Chinese journal of chromatography, 25(1): 35-38.

Li, Q., Wang, X. and Yuan, D., 2009. Solid-phase extraction of polar organophosphorous pesticides from aqueous samples with oxidized carbon nanotubes. Journal of Environmental Monitoring, 11(2): 439-444.

Li, W., Qian, D., Wang, Q., Li, Y., Bao, N., Gu, H. and Yu, C., 2016. Fully-drawn origami paper analytical device for electrochemical detection of glucose. Sensors and Actuators B: Chemical, 231: 230-238.

Li, X., Ballerini, D.R. and Shen, W., 2012. A perspective on paper-based microfluidics: current status and future trends. Biomicrofluidics, 6(1): 011301.

Li, X., Tian, J., Garnier, G. and Shen, W., 2010a. Fabrication of paper-based microfluidic sensors by printing. Colloids and surfaces B: Biointerfaces, 76(2): 564-570.

Li, X., Tian, J., Nguyen, T. and Shen, W., 2008. Paper-based microfluidic devices by plasma treatment. Analytical chemistry, 80(23): 9131-9134.

Li, X., Tian, J. and Shen, W., 2010b. Progress in patterned paper sizing for fabrication of paper-based microfluidic sensors. Cellulose, 17(3): 649-659.

Li, Y., Dong, F., Liu, X., Xu, J., Li, J., Lu, C., Wang, Y. and Zheng, Y., 2011. Miniaturized liquid–liquid extraction coupled with ultra-performance liquid chromatography/tandem mass spectrometry for determination of topramezone in soil, corn, wheat, and water. Analytical and bioanalytical chemistry, 400(9): 3097-3107.

Liana, D.D., Raguse, B., Gooding, J.J. and Chow, E., 2012. Recent advances in paper-based sensors. sensors, 12(9): 11505-11526.

Liang, J., Wang, Y. and Liu, B., 2012. Paper-based fluoroimmunoassay for rapid and sensitive detection of antigen. RSC Advances, 2(9): 3878-3884.

Liang, L., Su, M., Li, L., Lan, F., Yang, G., Ge, S., Yu, J. and Song, X., 2016. Aptamer-based fluorescent and visual biosensor for multiplexed monitoring of cancer cells in microfluidic paper-based analytical devices. Sensors and Actuators B: Chemical, 229: 347-354.

Lin, T., Li, Z., Song, Z., Chen, H., Guo, L., Fu, F. and Wu, Z., 2016. Visual and colorimetric detection of p-aminophenol in environmental water and human urine samples based on anisotropic growth of Ag nanoshells on Au nanorods. Talanta, 148: 62-68.

Lisowski, P. and Zarzycki, P.K., 2013. Microfluidic paper-based analytical devices (μPADs) and micro total analysis systems (μTAS): development, applications and future trends. Chromatographia, 76(19-20): 1201-1214.

Liu, F. and Zhang, C., 2015. A novel paper-based microfluidic enhanced chemiluminescence biosensor for facile, reliable and highly-sensitive gene detection of Listeria monocytogenes. Sensors and Actuators B: Chemical, 209: 399-406.

Liu, H. and Crooks, R.M., 2011. Three-dimensional paper microfluidic devices assembled using the principles of origami. Journal of the American Chemical Society, 133(44): 17564-17566.

Liu, S., Fan, Y., Gao, K. and Zhang, Y., 2018. Fabrication of Cyclo-olefin polymer-based microfluidic devices using CO2 laser ablation. Materials Research Express, 5(9): 095305.

Liu, W., Kou, J., Xing, H. and Li, B., 2014. based chromatographic chemiluminescence chip for the detection of dichlorvos in vegetables. Biosensors and Bioelectronics, 52: 76-81.

Lord, H. and Pawliszyn, J., 2000. Evolution of solid-phase microextraction technology. Journal of Chromatography A, 885(1-2): 153-193.

Lorenz, E., 2009. Potential health effects of pesticides, AG communications and marketing. Wiley, New York.

Lu, S.-C., Liao, W.-R. and Chen, S.-F., 2018. Quantification of Trans-resveratrol in Red Wines Using QuEChERS Extraction Combined with Liquid Chromatography–Tandem Mass Spectrometry. Analytical Sciences, 34(4): 439-444.

Lundstedt, T., Seifert, E., Abramo, L., Thelin, B., Nyström, Å., Pettersen, J. and Bergman, R., 1998. Experimental design and optimization. Chemometrics and intelligent laboratory systems, 42(1-2): 3-40.

Ma, K., Zhang, J.N., Zhao, M. and He, Y.J., 2012. Accurate analysis of trace earthy-musty odorants in water by headspace solid phase microextraction gas chromatography-mass spectrometry. Journal of separation science, 35(12): 1494-1501.

Ma, L., Wang, Y., Li, H., Peng, F., Qiu, B. and Yang, Z., 2020. Development of QuEChERS-DLLME method for determination of neonicotinoid pesticide residues in grains by liquid chromatography-tandem mass spectrometry. Food chemistry, 331: 127190.

Maejima, K., Tomikawa, S., Suzuki, K. and Citterio, D., 2013. Inkjet printing: an integrated and green chemical approach to microfluidic paper-based analytical devices. RSC advances, 3(24): 9258-9263.

Majid, S., El Rhazi, M., Amine, A. and Brett, C.M., 2002. An amperometric method for the determination of trace mercury (II) by formation of complexes with L-tyrosine. Analytica Chimica Acta, 464(1): 123-133.

Malik, A.K., Kaur, V. and Verma, N., 2006. A review on solid phase microextraction—High performance liquid chromatography as a novel tool for the analysis of toxic metal ions. Talanta, 68(3): 842-849.

Manz, A., Graber, N. and Widmer, H.á., 1990. Miniaturized total chemical analysis systems: a novel concept for chemical sensing. Sensors and actuators B: Chemical, 1(1-6): 244-248.

March, C., Manclús, J., Jiménez, Y., Arnau, A. and Montoya, A., 2009. A piezoelectric immunosensor for the determination of pesticide residues and metabolites in fruit juices. Talanta, 78(3): 827-833.

Marquis, J.K. and Lerrick, A.J., 1982. Noncompetitive inhibition by aluminum, scandium and yttrium of acetylcholinesterase from Electrophorus electricus. Biochemical Pharmacology, 31(7): 1437-1440.

Martinez, A.W., Phillips, S.T., Butte, M.J. and Whitesides, G.M., 2007. Patterned paper as a platform for inexpensive, low-volume, portable bioassays. Angewandte Chemie International Edition, 46(8): 1318-1320.

Martinez, A.W., Phillips, S.T., Nie, Z., Cheng, C.-M., Carrilho, E., Wiley, B.J. and Whitesides, G.M., 2010. Programmable diagnostic devices made from paper and tape. Lab on a Chip, 10(19): 2499-2504.

Martinez, A.W., Phillips, S.T., Whitesides, G.M. and Carrilho, E., 2009. Diagnostics for the developing world: microfluidic paper-based analytical devices. Analytical Chemistry, 82 (1): 3–10.

Martinez, A.W., Phillips, S.T., Wiley, B.J., Gupta, M. and Whitesides, G.M., 2008. FLASH: a rapid method for prototyping paper-based microfluidic devices. Lab on a Chip, 8(12): 2146-2150.

Maštovská, K. and Lehotay, S.J., 2004. Evaluation of common organic solvents for gas chromatographic analysis and stability of multiclass pesticide residues. Journal of Chromatography A, 1040(2): 259-272.

Maya, F. and Ghani, M., 2019. Ordered macro/micro-porous metal-organic framework of type ZIF-8 in a steel fiber as a sorbent for solid-phase microextraction of BTEX. Microchimica Acta, 186(7): 1-8.

McDonald, J.C. and Whitesides, G.M., 2002. Poly (dimethylsiloxane) as a material for fabricating microfluidic devices. Accounts of chemical research, 35(7): 491-499.

Menezes, M.L.d., Felix, G. and Demarchi, A., 1998. On-line extraction and determination of carbofuran in raw milk by direct HPLC injection on an ISRP column. Chromatographia, 47(1-2): 81-83.

Mentele, M.M., Cunningham, J., Koehler, K., Volckens, J. and Henry, C.S., 2012. Microfluidic paper-based analytical device for particulate metals. Analytical chemistry, 84(10): 4474-4480.

Metters, J.P., Houssein, S.M., Kampouris, D.K. and Banks, C.E., 2013. based electroanalytical sensing platforms. Analytical Methods, 5(1): 103-110.

Miliadis, G.E., Tsiropoulos, N.G. and Aplada-Sarlis, P.G., 1999. High-performance liquid chromatographic determination of benzoylurea insecticides residues in grapes and wine using liquid and solid-phase extraction. Journal of Chromatography A, 835(1-2): 113-120.

Morgan, E., 1995. Chemometrics: experimental design, 41. John Wiley & Son Limited.

Muñoz-Leoz, B., Ruiz-Romera, E., Antigüedad, I. and Garbisu, C., 2011. Tebuconazole application decreases soil microbial biomass and activity. Soil Biology and Biochemistry, 43(10): 2176-2183.

Namiesnik, J., Spietelun, A. and Marcinkowski, L., 2015. Green sample preparation techniques for chromatographic determination of small organic compounds. International Journal of Chemical Engineering and Applications, 6(3): 215.

Nemiroski, A., Christodouleas, D.C., Hennek, J.W., Kumar, A.A., Maxwell, E.J., Fernández-Abedul, M.T. and Whitesides, G.M., 2014. Universal mobile electrochemical detector designed for use in resource-limited applications. Proceedings of the National Academy of Sciences, 111(33): 11984-11989.

Nerın, C., Batlle, R., Sartaguda, M. and Pedrocchi, C., 2002. Supercritical fluid extraction of organochlorine pesticides and some metabolites in frogs from National Park of Ordesa and Monte Perdido. Analytica Chimica Acta, 464(2): 303-312.

Nery, E.W. and Kubota, L.T., 2013. Sensing approaches on paper-based devices: a review. Analytical and bioanalytical chemistry, 405(24): 7573-7595.

Nge, P.N., Rogers, C.I. and Woolley, A.T., 2013. Advances in microfluidic materials, functions, integration, and applications. Chemical reviews, 113(4): 2550-2583.

Nie, Z., Deiss, F., Liu, X., Akbulut, O. and Whitesides, G.M., 2010a. Integration of paper-based microfluidic devices with commercial electrochemical readers. Lab on a Chip, 10(22): 3163-3169.

Nie, Z., Nijhuis, C.A., Gong, J., Chen, X., Kumachev, A., Martinez, A.W., Narovlyansky, M. and Whitesides, G.M., 2010b. Electrochemical sensing in paper-based microfluidic devices. Lab on a Chip, 10(4): 477-483.

Nouanthavong, S., Nacapricha, D., Henry, C.S. and Sameenoi, Y., 2016. Pesticide analysis using nanoceria-coated paper-based devices as a detection platform. Analyst, 141(5): 1837-1846.

Nuchtavorn, N. and Macka, M., 2016. A novel highly flexible, simple, rapid and low-cost fabrication tool for paper-based microfluidic devices (μPADs) using technical drawing pens and in-house formulated aqueous inks. Analytica chimica acta, 919: 70-77.

Olkkonen, J., Lehtinen, K. and Erho, T., 2010. Flexographically printed fluidic structures in paper. Analytical chemistry, 82(24): 10246-10250.

WHO, 1999. Food safety issues associated with products from aquaculture: report of a joint FAO/NACA/WHO study group. World Health Organization, Geneve, Switzerland.

Pandey, P., Raizada, R. and Srivastava, L., 2010. Level of organochlorine pesticide residues in dry fruit nuts. Journal of environmental biology, 31(5): 705-707.

Pang, S., Yang, T. and He, L., 2016. Review of surface enhanced Raman spectroscopic (SERS) detection of synthetic chemical pesticides. TrAC Trends in Analytical Chemistry, 85: 73-82.

Pelton, R., 2009. Bioactive paper provides a low-cost platform for diagnostics. TrAC Trends in Analytical Chemistry, 28(8): 925-942.

Peris-Vicente, J., Carda-Broch, S., Esteve-Romero, J., Rambla-Alegre, M., Bose, D., Beltrán-Martinavarro, B., Marco-Peiró, S., Martinavarro-Domínguez, A., Ochoa-Aranda, E. and Chin-Chen, M., 2013. Validation of micellar LC-based methods applied to analyze foodstuffs. Bioanalysis, 5(4): 481-494.

Petryayeva, E. and Algar, W.R., 2013. Proteolytic assays on quantum-dot-modified paper substrates using simple optical readout platforms. Analytical chemistry, 85(18): 8817-8825.

Pimentel, D., 1995. Amounts of pesticides reaching target pests: environmental impacts and ethics. Journal of Agricultural and environmental Ethics, 8(1): 17-29.

Płotka-Wasylka, J., Szczepańska, N., de la Guardia, M. and Namieśnik, J., 2015. Miniaturized solid-phase extraction techniques. TrAC Trends in Analytical Chemistry, 73: 19-38.

Pundir, C. and Malik, A., 2019. Bio-sensing of organophosphorus pesticides: a review. Biosensors and Bioelectronics, 140: 111348.

Pundir, C.S. and Chauhan, N., 2012. Acetylcholinesterase inhibition-based biosensors for pesticide determination: A review. Analytical Biochemistry, 429(1): 19-31.

Qian, G., Wang, L., Wu, Y., Zhang, Q., Sun, Q., Liu, Y. and Liu, F., 2009. A monoclonal antibody-based sensitive enzyme-linked immunosorbent assay (ELISA) for the analysis of the organophosphorous pesticides chlorpyrifos-methyl in real samples. Food Chemistry, 117(2): 364-370.

Rai, S., Singh, A.K., Srivastava, A., Yadav, S., Siddiqui, M.H. and Mudiam, M.K.R., 2016. Comparative evaluation of QuEChERS method coupled to DLLME extraction for the analysis of multiresidue pesticides in vegetables and fruits by gas chromatography-mass spectrometry. Food analytical methods, 9(9): 2656-2669.

Raoul, S., Gremaud, E., Biaudet, H. and Turesky, R.J., 1997. Rapid solid-phase extraction method for the detection of volatile nitrosamines in food. Journal of Agricultural and Food Chemistry, 45(12): 4706-4713.

Rasmussen, K.E. and Pedersen-Bjergaard, S., 2004. Developments in hollow fibre-based, liquid-phase microextraction. TrAC Trends in Analytical Chemistry, 23(1): 1-10.

Rattanarat, P., Dungchai, W., Cate, D.M., Siangproh, W., Volckens, J., Chailapakul, O. and Henry, C.S., 2013. A microfluidic paper-based analytical device for rapid quantification of particulate chromium. Analytica chimica acta, 800: 50-55.

Rattanarat, P., Dungchai, W., Siangproh, W., Chailapakul, O. and Henry, C.S., 2012. Sodium dodecyl sulfate-modified electrochemical paper-based analytical device for determination of dopamine levels in biological samples. Analytica chimica acta, 744: 1-7.

Ravelo-Pérez, L.M., Hernández-Borges, J. and Rodríguez-Delgado, M.Á., 2008. Multi-walled carbon nanotubes as efficient solid-phase extraction materials of organophosphorus pesticides from apple, grape, orange and pineapple fruit juices. Journal of Chromatography A, 1211(1-2): 33-42.

Rejczak, T. and Tuzimski, T., 2015. A review of recent developments and trends in the QuEChERS sample preparation approach. Open Chemistry, 13(1).

Rejczak, T. and Tuzimski, T., 2017. QuEChERS-based extraction with dispersive solid phase extraction clean-up using PSA and ZrO2-based sorbents for determination of pesticides in bovine milk samples by HPLC-DAD. Food chemistry, 217: 225-233.

Reybier, K., Zairi, S., Jaffrezic-Renault, N. and Fahys, B., 2002. The use of polyethyleneimine for fabrication of potentiometric cholinesterase biosensors. Talanta, 56(6): 1015-1020.

Rezaee, M., Assadi, Y., Hosseini, M.-R.M., Aghaee, E., Ahmadi, F. and Berijani, S., 2006. Determination of organic compounds in water using dispersive liquid–liquid microextraction. Journal of Chromatography a, 1116(1-2): 1-9.

Rezaee, M., Yamini, Y. and Faraji, M., 2010. Evolution of dispersive liquid–liquid microextraction method. Journal of Chromatography A, 1217(16): 2342-2357.

Rizzetti, T.M., Kemmerich, M., Martins, M.L., Prestes, O.D., Adaime, M.B. and Zanella, R., 2016. Optimization of a QuEChERS based method by means of central composite design for pesticide multiresidue determination in orange juice by UHPLC–MS/MS. Food Chemistry, 196: 25-33.

Romero-González, R., Frenich, A.G., Vidal, J.M., Prestes, O. and Grio, S., 2011. Simultaneous determination of pesticides, biopesticides and mycotoxins in organic products applying a quick, easy, cheap, effective, rugged and safe extraction procedure and ultra-high performance liquid chromatography–tandem mass spectrometry. Journal of Chromatography A, 1218(11): 1477-1485.

Rosa, A.M., Louro, A.F., Martins, S.A., Inácio, J.o., Azevedo, A.M. and Prazeres, D.M.F., 2014. Capture and detection of DNA hybrids on paper via the anchoring of antibodies with fusions of carbohydrate binding modules and ZZ-domains. Analytical chemistry, 86(9): 4340-4347.

Rosenfeld, T. and Bercovici, M., 2014. 1000-fold sample focusing on paper-based microfluidic devices. Lab on a Chip, 14(23): 4465-4474.

Ruano, J.M., Benoit, V., Aitchison, J.S. and Cooper, J.M., 2000. Flame hydrolysis deposition of glass on silicon for the integration of optical and microfluidic devices. Analytical chemistry, 72(5): 1093-1097.

Ruiz-García, Y., Silva, C.L., Gómez-Plaza, E. and Câmara, J.S., 2016. A powerful analytical strategy based on QuEChERS-dispersive solid-phase extraction combined with ultrahigh pressure liquid chromatography for evaluating the effect of elicitors on biosynthesis of trans-resveratrol in grapes. Food analytical methods, 9(3): 670-679.

Sabullah, M.K., Sulaiman, M.R., Shukor, M.S., Yusof, M.T., Johari, W.L.W., Shukor, M.Y. and Syahir, A., 2015. Heavy metals biomonitoring via inhibitive assay of acetylcholinesterase from Periophthalmodon schlosseri. Rendiconti Lincei, 26(2): 151-158.

Salahi, A., Noshadi, I., Badrnezhad, R., Kanjilal, B. and Mohammadi, T., 2013. Nano-porous membrane process for oily wastewater treatment: optimization using response surface methodology. Journal of Environmental Chemical Engineering, 1(3): 218-225.

Sanchez, R., Vazquez, A., Villén-Altamirano, J. and Villén, J., 2006. Analysis of pesticide residues by on-line reversed-phase liquid chromatography–gas chromatography in the oil from olives grown in an experimental plot. Journal of the Science of Food and Agriculture, 86(1): 129-134.

Sankar, K., Lenisha, D., Janaki, G., Juliana, J., Kumar, R.S., Selvi, M.C. and Srinivasan, G., 2020. Digital image-based quantification of chlorpyrifos in water samples using a lipase embedded paper based device. Talanta, 208: 120408.

Sante, D., 2017. Guidance document on analytical quality control and method validation procedures for pesticide residues and analysis in food and feed SANTE/11813/2017. Bruss. Belg, 46: 31-42.

Sarfraz, J., Tobjork, D., Osterbacka, R. and Linden, M., 2011. Low-cost hydrogen sulfide gas sensor on paper substrates: fabrication and demonstration. IEEE Sensors Journal, 12(6): 1973-1978.

Sarmah, A.K., Müller, K. and Ahmad, R., 2004. Fate and behaviour of pesticides in the agroecosystem—a review with a New Zealand perspective. Soil Research, 42(2): 125-154.

Schwarzenbach, R.P., Escher, B.I., Fenner, K., Hofstetter, T.B., Johnson, C.A., Von Gunten, U. and Wehrli, B., 2006. The challenge of micropollutants in aquatic systems. Science, 313(5790): 1072-1077.

Sedighi, M., Aljlil, S.A., Alsubei, M.D., Ghasemi, M. and Mohammadi, M., 2018. Performance optimisation of microbial fuel cell for wastewater treatment and sustainable clean energy generation using response surface methodology. Alexandria engineering journal, 57(4): 4243-4253.

Seebunrueng, K., Santaladchaiyakit, Y. and Srijaranai, S., 2014. Vortex-assisted low density solvent based demulsified dispersive liquid–liquid microextraction and high-performance liquid chromatography for the determination of organophosphorus pesticides in water samples. Chemosphere, 103: 51-58.

Shabeer, T.A., Girame, R., Utture, S., Oulkar, D., Banerjee, K., Ajay, D., Arimboor, R. and Menon, K., 2018. Optimization of multi-residue method for targeted screening and quantitation of 243 pesticide residues in cardamom (Elettaria cardamomum) by gas chromatography tandem mass spectrometry (GC-MS/MS) analysis. Chemosphere, 193: 447-453.

Shafiee, H., Asghar, W., Inci, F., Yuksekkaya, M., Jahangir, M., Zhang, M.H., Durmus, N.G., Gurkan, U.A., Kuritzkes, D.R. and Demirci, U., 2015. Paper and flexible substrates as materials for biosensing platforms to detect multiple biotargets. Scientific reports, 5: 8719.

Sharifzadeh, M.S., Abdollahzadeh, G., Damalas, C.A. and Rezaei, R., 2018. Farmers' criteria for pesticide selection and use in the pest control process. Agriculture, 8(2): 24.

Shelton, J.F., Geraghty, E.M., Tancredi, D.J., Delwiche, L.D., Schmidt, R.J., Ritz, B., Hansen, R.L. and Hertz-Picciotto, I., 2014. Neurodevelopmental disorders and prenatal residential proximity to agricultural pesticides: the CHARGE study. Environmental health perspectives, 122(10): 1103-1109.

Shostenkot, Y.V., Georgievskii, V. and Levin, M., 2000. History of the discovery of thinlayer chromatography. Journal of Analytical Chemistry, 55(9): 904-905.

Sia, S.K., Linder, V., Parviz, B.A., Siegel, A. and Whitesides, G.M., 2004. An integrated approach to a portable and low-cost immunoassay for resource-poor settings. Angewandte Chemie International Edition, 43(4): 498-502.

Sia, S.K. and Whitesides, G.M., 2003. Microfluidic devices fabricated in poly (dimethylsiloxane) for biological studies. Electrophoresis, 24(21): 3563-3576.

Singh, B. and Mandal, K., 2014. Environmental impact of pesticides belonging to newer chemistry. Biointensive Integrated Pest Management in Horticultural Ecosystems: 152.

Singh, G., Dubey, J.K. and Patyal, S.K., 2016. A study on farmers' knowledge, perception and intensity of approved pesticide use practices/patterns in tomato and cabbage in Himachal Pradesh. International Journal of Farm Sciences, 6(3): 77-83.

Singh, S., Srivastava, A. and Singh, S.P., 2018. Inexpensive, effective novel activated carbon fibers for sample cleanup: application to multipesticide residue analysis in food commodities using a QuEChERS method. Analytical and bioanalytical chemistry, 410(8): 2241-2251.

Snejdarkova, M., Svobodova, L., Nikolelis, D.P., Wang, J. and Hianik, T., 2003. Acetylcholine biosensor based on dendrimer layers for pesticides detection. Electroanalysis: An International Journal Devoted to Fundamental and Practical Aspects of Electroanalysis, 15(14): 1185-1191.

Soldatkin, A., Gorchkov, D., Martelet, C. and Jaffrezic-Renault, N., 1997. New enzyme potentiometric sensor for hypochlorite species detection. Sensors and Actuators B: Chemical, 43(1-3): 99-104.

Sones, C., Katis, I., He, P., Mills, B., Namiq, M., Shardlow, P., Ibsen, M. and Eason, R., 2014. Laser-induced photo-polymerisation for creation of paper-based fluidic devices. Lab on a Chip, 14(23): 4567-4574.

Songjaroen, T., Dungchai, W., Chailapakul, O. and Laiwattanapaisal, W., 2011. Novel, simple and low-cost alternative method for fabrication of paper-based microfluidics by wax dipping. Talanta, 85(5): 2587-2593.

Songok, J., Tuominen, M., Teisala, H., Haapanen, J., Mäkelä, J., Kuusipalo, J. and Toivakka, M., 2014. based microfluidics: fabrication technique and dynamics of capillary-driven surface flow. ACS applied materials & interfaces, 6(22): 20060-20066.

Spietelun, A., Marcinkowski, Ł., de la Guardia, M. and Namieśnik, J., 2014. Green aspects, developments and perspectives of liquid phase microextraction techniques. Talanta, 119: 34-45.

Tadeo, J.L., 2019. Analysis of pesticides in food and environmental samples. CRC Press.

Tankiewicz, M., Fenik, J. and Biziuk, M., 2011. Solventless and solvent-minimized sample preparation techniques for determining currently used pesticides in water samples: A review. Talanta, 86: 8-22.

Tao, H., Chieffo, L.R., Brenckle, M.A., Siebert, S.M., Liu, M., Strikwerda, A.C., Fan, K., Kaplan, D.L., Zhang, X. and Averitt, R.D., 2011. Metamaterials on paper as a sensing platform. Advanced Materials, 23(28): 3197-3201.

Teklu, B.M., 2016. Environmental risk assessment of pesticides in Ethiopia, Thesis submitted in fulfilment of the requirements for the degree of doctor at Wageningen University, Netherl ands .

Terry, S.C., 1975. A gas chromatography system fabricated on a silicon wafer using integrated circuit technology. Stanford University.

Terry, S.C., Jerman, J.H. and Angell, J.B., 1979. A gas chromatographic air analyzer fabricated on a silicon wafer. IEEE transactions on electron devices, 26(12): 1880-1886.

Tolcha, T., Gomoro, K. and Megersa, N., 2021. SALLE combined with LD-DLLME for pesticides analysis in sugar and soil samples. Bulletin of the Chemical Society of Ethiopia, 35(1): 1-16.

Topuz, S., Özhan, G. and Alpertunga, B., 2005. Simultaneous determination of various pesticides in fruit juices by HPLC-DAD. Food Control, 16(1): 87-92.

Trajkovska, S., Mbaye, M., Seye, M.G., Aaron, J., Chevreuil, M. and Blanchoud, H., 2009. Toxicological study of pesticides in air and precipitations of Paris by means of a bioluminescence method. Analytical and bioanalytical chemistry, 394(4): 1099-1106.

Tran-Minh, C., Pandey, P. and Kumaran, S., 1990. Studies on acetylcholine sensor and its analytical application based on the inhibition of cholinesterase. Biosensors and Bioelectronics, 5(6): 461-471.

Vas, G. and Vekey, K., 2004. Solid-phase microextraction: a powerful sample preparation tool prior to mass spectrometric analysis. Journal of mass spectrometry, 39(3): 233-254.

Vickerman, G., 1988. Farm scale evaluation of the long-term effects of different pesticide regimes on the arthropod fauna of winter wheat, Fields methods for the study of environmental effects of pesticides. Symposium, pp. 127-135.

Viñas, P., Campillo, N., López-García, I. and Hernández-Córdoba, M., 2014. Dispersive liquid–liquid microextraction in food analysis. A critical review. Analytical and bioanalytical chemistry, 406(8): 2067-2099.

Viola, I., Ghofraniha, N., Zacheo, A., Arima, V., Conti, C. and Gigli, G., 2013. Random laser emission from a paper-based device. Journal of Materials Chemistry C, 1(48): 8128-8133.

Vogt, C. and Heinig, K., 1999. Trace analysis of surfactants using chromatographic and electrophoretic techniques. Fresenius' journal of analytical chemistry, 363(7): 612-618.

Wang, J.-P., Chen, Y.-Z., Ge, X.-W. and Yu, H.-Q., 2007. Optimization of coagulation–flocculation process for a paper-recycling wastewater treatment using response surface methodology. Colloids and Surfaces A: Physicochemical and Engineering Aspects, 302(1-3): 204-210.

Wang, J., Monton, M.R.N., Zhang, X., Filipe, C.D., Pelton, R. and Brennan, J.D., 2014. Hydrophobic sol–gel channel patterning strategies for paper-based microfluidics. Lab on a Chip, 14(4): 691-695.

Wang, S., Ge, L., Song, X., Yu, J., Ge, S., Huang, J. and Zeng, F., 2012. based chemiluminescence ELISA: lab-on-paper based on chitosan modified paper device and wax-screen-printing. Biosensors and bioelectronics, 31(1): 212-218.

Wang, W., Wu, W.-Y. and Zhu, J.-J., 2010. Tree-shaped paper strip for semiquantitative colorimetric detection of protein with self-calibration. Journal of Chromatography A, 1217(24): 3896-3899.

Wang, Y., Ge, L., Wang, P., Yan, M., Ge, S., Li, N., Yu, J. and Huang, J., 2013. Photoelectrochemical lab-on-paper device equipped with a porous Au-paper electrode and

fluidic delay-switch for sensitive detection of DNA hybridization. Lab on a Chip, 13(19): 3945-3955.

Wang, Y., Liu, H., Wang, P., Yu, J., Ge, S. and Yan, M., 2015. Chemiluminescence excited photoelectrochemical competitive immunosensing lab-on-paper device using an integrated paper supercapacitor for signal amplication. Sensors and Actuators B: Chemical, 208: 546-553.

Wardencki, W., Curyło, J. and Namieśnik, J., 2007. Trends in solventless sample preparation techniques for environmental analysis. Journal of biochemical and biophysical methods, 70(2): 275-288.

Ware, G.W., 1980. Effects of pesticides on nontarget organisms, Residue reviews. Springer, pp. 173-201.

Wei, X., Tian, T., Jia, S., Zhu, Z., Ma, Y., Sun, J., Lin, Z. and Yang, C.J., 2015. Target-responsive DNA hydrogel mediated "stop-flow" microfluidic paper-based analytic device for rapid, portable and visual detection of multiple targets. Analytical chemistry, 87(8): 4275-4282.

Wen, Y., Li, J., Yang, F., Zhang, W., Li, W., Liao, C. and Chen, L., 2013. Salting-out assisted liquid–liquid extraction with the aid of experimental design for determination of benzimidazole fungicides in high salinity samples by high-performance liquid chromatography. Talanta, 106: 119-126.

Whitesides, G.M., 2006. The origins and the future of microfluidics. Nature, 442(7101): 368.

Wiest, L., Buleté, A., Giroud, B., Fratta, C., Amic, S., Lambert, O., Pouliquen, H. and Arnaudguilhem, C., 2011. Multi-residue analysis of 80 environmental contaminants in honeys, honeybees and pollens by one extraction procedure followed by liquid and gas

chromatography coupled with mass spectrometric detection. Journal of Chromatography A, 1218(34): 5743-5756.

Xia, Y., Cheng, M., Guo, F., Wang, X. and Cheng, J., 2012. In-syringe demulsified dispersive liquid–liquid microextraction and high performance liquid chromatography–mass spectrometry for the determination of trace fungicides in environmental water samples. Analytica chimica acta, 724: 47-53.

Xia, Y., Si, J. and Li, Z., 2016. Fabrication techniques for microfluidic paper-based analytical devices and their applications for biological testing: A review. Biosensors and Bioelectronics, 77: 774-789.

Xin-Ran, W., Bo-Wei, L., Hui-Yan, Y. and Ling-Xin, C., 2015. An ion imprinted polymers grafted paper-based fluorescent sensor based on quantum dots for detection of Cu2+ ions. Chinese Journal of Analytical Chemistry, 43(10): 1499-1504.

Yadav, I.C. and Devi, N.L., 2017. Pesticides classification and its impact on human and environment. Environmental Science and Engineering, 6: 140-158.

Yadav, I.C., Devi, N.L., Syed, J.H., Cheng, Z., Li, J., Zhang, G. and Jones, K.C., 2015. Current status of persistent organic pesticides residues in air, water, and soil, and their possible effect on neighboring countries: a comprehensive review of India. Science of the Total Environment, 511: 123-137.

Yafia, M., Shukla, S. and Najjaran, H., 2015. Fabrication of digital microfluidic devices on flexible paper-based and rigid substrates via screen printing. Journal of Micromechanics and Microengineering, 25(5): 057001.

Yamada, K., Henares, T.G., Suzuki, K. and Citterio, D., 2015. Paper-based inkjet-printed microfluidic analytical devices. Angewandte Chemie International Edition, 54(18): 5294-5310.

Yetisen, A.K., Akram, M.S. and Lowe, C.R., 2013. based microfluidic point-of-care diagnostic devices. Lab on a Chip, 13(12): 2210-2251.

Yilmaz, E. and Soylak, M., 2016. Latest trends, green aspects, and innovations in liquid-phase--based microextraction techniques: a review. Turkish journal of chemistry, 40(6): 868-893.

Young, R., 2005. Toxicity profiles: toxicity summary for cadmium, risk assessment information system. RAIS, University of Tennessee, USA.

Yu, J., Ge, L., Huang, J., Wang, S. and Ge, S., 2011. Microfluidic paper-based chemiluminescence biosensor for simultaneous determination of glucose and uric acid. Lab on a Chip, 11(7): 1286-1291.

Zang, D., Ge, L., Yan, M., Song, X. and Yu, J., 2012. Electrochemical immunoassay on a 3D microfluidic paper-based device. Chemical Communications, 48(39): 4683-4685.

Zhang, L., Liu, S., Cui, X., Pan, C., Zhang, A. and Chen, F., 2012. A review of sample preparation methods for the pesticide residue analysis in foods. Open Chemistry, 10(3): 900-925.

Zhang, Y., Zhou, C., Nie, J., Le, S., Qin, Q., Liu, F., Li, Y. and Li, J., 2014. Equipment-free quantitative measurement for microfluidic paper-based analytical devices fabricated using the principles of movable-type printing. Analytical chemistry, 86(4): 2005-2012.

Zhou, I., Bramble, F.Q., Devine, T.J. and Norwood, G.I., 1996. Determination of bensulfuron methyl in rice and crayfish by liquid chromatography with a column-and eluant-switching system and UV detection. Journal of AOAC International, 79(3): 791-796.

Zhou, J., Xu, J.-J., Cong, J.-M., Cai, Z.-X., Zhang, J.-S., Wang, J.-L. and Ren, Y.-P., 2018. Optimization for quick, easy, cheap, effective, rugged and safe extraction of mycotoxins and veterinary drugs by response surface methodology for application to egg and milk. Journal of Chromatography A, 1532: 20-29.

Zhou, Q., Wang, G. and Xie, G., 2013. Dispersive liquid-phase microextraction in combination with HPLC for the enrichment and rapid determination of benzoylurea pesticides in environmental water samples. Journal of separation science, 36(14): 2323-2329.

Zygler, A., Wasik, A. and Namieśnik, J., 2010. Retention behaviour of some high-intensity sweeteners on different SPE sorbents. Talanta, 82(5): 1742-1748.

6. ANNEX

Annex 1. Table for robustness of the method observed by varying the concentration and volume, and image capturing time

Parameters variation	Mean color intensity	Difference %RSD from optimal condition
Concentration AChE (U mL^{-1}) variation		
8.73	44.5	0.68
9*	44.8*	
9.27	43.98	1.85
Concentration ATChI (mM) variation		
3.88	44.4	0.90
4*	44.8*	
4.12	44.7	0.22
Concentration DTNB (mM) variation		
2.91	44.25	1.23
3*	44.8*	
3.09	44.85	0.11
Volume AChE (µL) variation		
1.46	44.59	0.47
1.5*	44.8*	
1.54	44.43	0.83
Volume ATChI (µL)(E)		
1.94	43.98	1.84
2*	44.8*	
2.06	44.62	0.40
Volume DTNB (µL) variation		
1.94	44.33	1.05
2*	44.8*	
2.06	44.56	0.54
Image capturing time (min) variation		
4.85	44.33	1.05
5*	44.8*	
5.15	44.83	0.07

Annex 2. Table for experimental runs and response for concentration optimization

Exp. runs	A	B	C	Mean color intensity	
				Observed	Predicted
1	1	1	3	46.75	46.62
2	12	1	3	45.34	44.85
3	1	5	3	37.18	37.68
4	12	5	3	46.69	46.82
5	1	3	1	42.56	42.10
6	12	3	1	47.02	46.93
7	1	3	5	39.54	39.64
8	12	3	5	41.72	42.18
9	6.5	1	1	46.33	46.92
10	6.5	5	1	38.47	38.44
11	6.5	1	5	38.28	38.32
12	6.5	5	5	40.42	39.83
13(C)	6.5	3	3	39.87	40.23
14(C)	6.5	3	3	40.70	40.23
15(C)	6.5	3	3	40.13	40.23

Annex 3. Table for experimental runs and response for volume optimization

Exp. runs	D	E	F	Mean color intensity	
				Observed	Predicted
1	0.5	0.5	1.5	32.95	32.77
2	2.5	0.5	1.5	45.39	45.80
3	0.5	2.5	1.5	49.8	49.39
4	2.5	2.5	1.5	53.21	53.39
5	0.5	1.5	0.5	34.47	35.12
6	2.5	1.5	0.5	43.23	43.29
7	0.5	1.5	2.5	35.07	35.01
8	2.5	1.5	2.5	44.54	43.89
9	1.5	0.5	0.5	37.71	37.24
10	1.5	2.5	0.5	51.87	51.63
11	1.5	0.5	2.5	39.53	39.77
12	1.5	2.5	2.5	49.11	49.58
13(C)	1.5	1.5	1.5	50.04	49.21
14(C)	1.5	1.5	1.5	48.43	49.21
15(C)	1.5	1.5	1.5	49.17	49.21

Annex 4. Table for the experimental runs, observed and predicted inhibition percentage in DLLME

					Inhibition percentage	
Run	A	B	C	D	Observed	Predicted
1	30	0.2	6	5	47.3	48.8
2	70	0.2	6	5	46.2	44.0
3	30	0.7	6	5	58.4	60.7
4	70	0.7	6	5	52.4	50.9
5	50	0.45	2	0	42.6	44.4
6	50	0.45	10	0	55.8	57.3
7	50	0.45	2	10	61.6	60.2
8	50	0.45	10	10	39.2	37.5
9	30	0.45	6	0	56.4	54.6
10	70	0.45	6	0	61.3	63.2
11	30	0.45	6	10	70.3	68.5
12	70	0.45	6	10	43.3	45.3
13	50	0.2	2	5	38.9	37.3
14	50	0.7	2	5	55.3	53.7
15	50	0.2	10	5	37.5	39.4
16	50	0.7	10	5	39.8	41.7
17	30	0.45	2	5	35.0	36.4
18	70	0.45	2	5	75.2	76.6
19	30	0.45	10	5	80.7	78.9
20	70	0.45	10	5	25.9	24.2
21	50	0.2	6	0	34.4	33.0
22	50	0.7	6	0	65.1	62.9
23	50	0.2	6	10	49.8	51.5
24	50	0.7	6	10	39.2	40.3
25(C)	50	0.45	6	5	84.3	86.3
26(C)	50	0.45	6	5	87.1	86.3
27(C)	50	0.45	6	5	87.3	86.3

Annex 5. Table for experimental runs and inhibition percentage for the CCD in QuEChERS-DLLME

Runs	A	F	G	Inhibition percentage (%)	
				Observed	Predicted
1	5	150	5	36.3	35.98
2	10	150	5	57.73	57.75
3	5	300	5	31.06	32.41
4	10	300	5	36.3	36.20
5	5	150	10	26.07	26.29
6	10	150	10	55.63	54.40
7	5	300	10	28.31	28.42
8	10	300	10	38.12	38.56
9	5	225	7.5	22.4	21.04
10	10	225	7.5	36.12	36.99
11	7.5	150	7.5	34.01	35.32
12	7.5	300	7.5	27.4	25.61
13	7.5	225	5	24.8	23.85
14	7.5	225	10	19.72	20.18
15(C)	7.5	225	7.5	20.87	21.38
16(C)	7.5	225	7.5	21.99	21.38
17(C)	7.5	225	7.5	20.3	21.38

C: Center point.*Significant ($p < 0.05$), Adjusted $R^2 = 0.984$, $Q^2 = 0.939$ and $R^2 = 0.993$.

Annex 6. Calibration curve obtained by univariate optimization approach

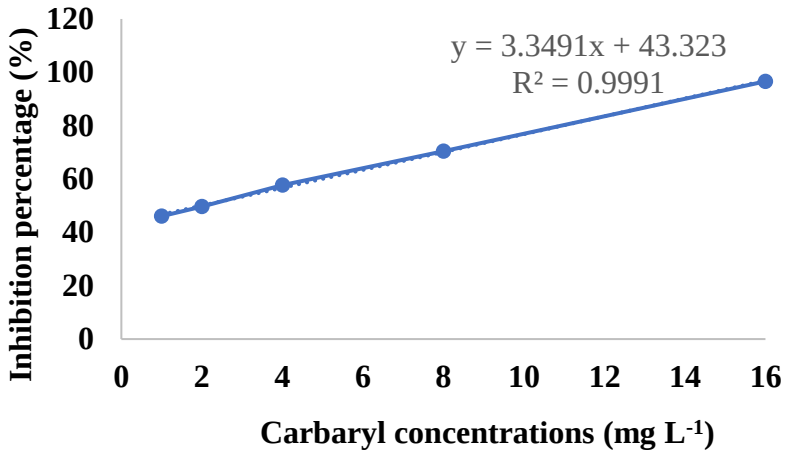

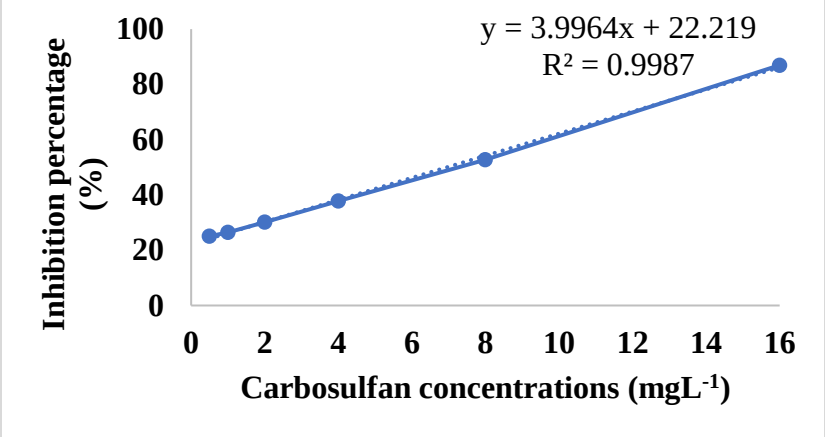

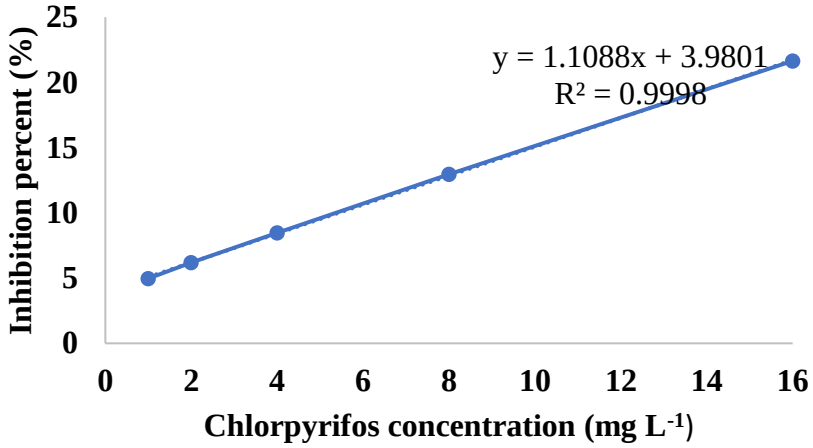

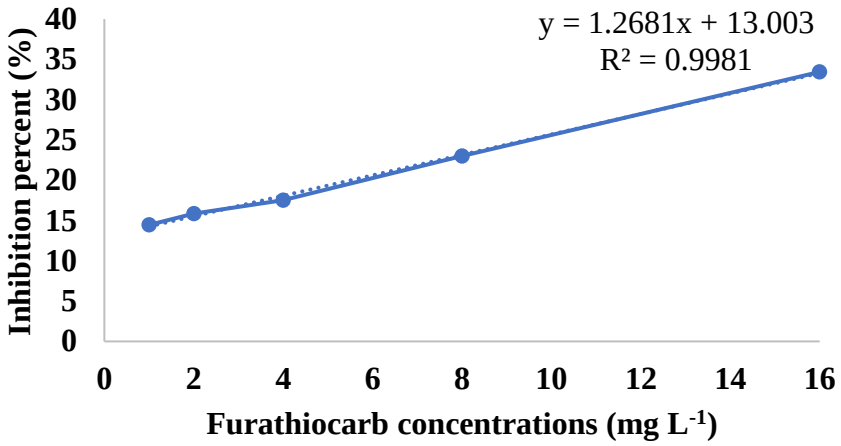
y = 1.2681x + 13.003
R² = 0.9981
Inhibition percent (%)
40
35
30
25
20
15
10
5
0
0
2
4
6
8
10
12
14
16
Furathiocarb concentrations (mg L-1)

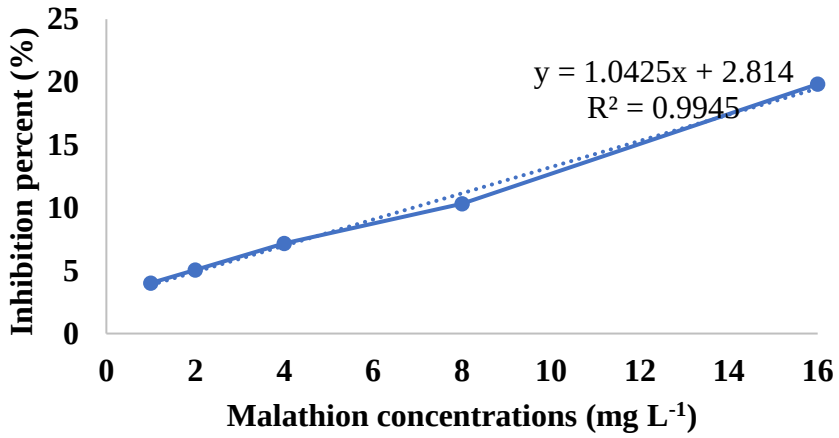
y = 1.0425x + 2.814
R² = 0.9945
Inhibition percent (%)
25
20
15
10
5
0
0
2
4
6
8
10
12
14
16
Malathion concentrations (mg L-1)

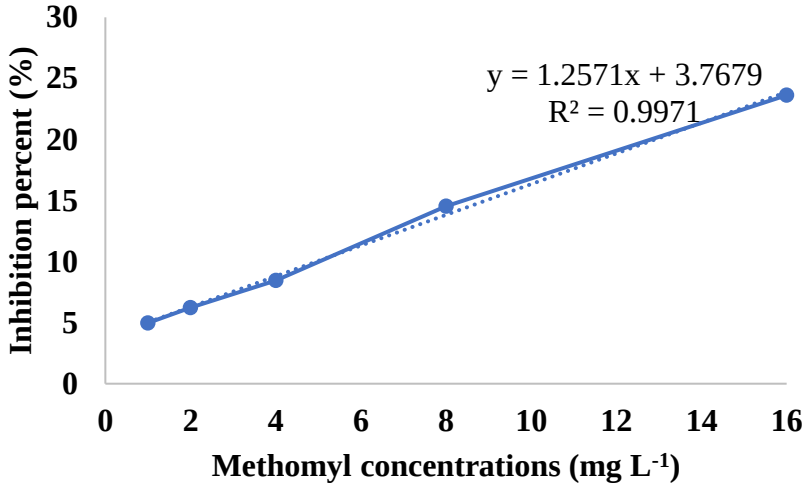
y = 1.2571x + 3.7679
R² = 0.9971
Inhibition percent (%)
30
25
20
15
10
5
0
0
2
4
6
8
10
12
14
16
Methomyl concentrations (mg L-1)

Annex 7. Calibration curve obtained by multivariate optimization approach

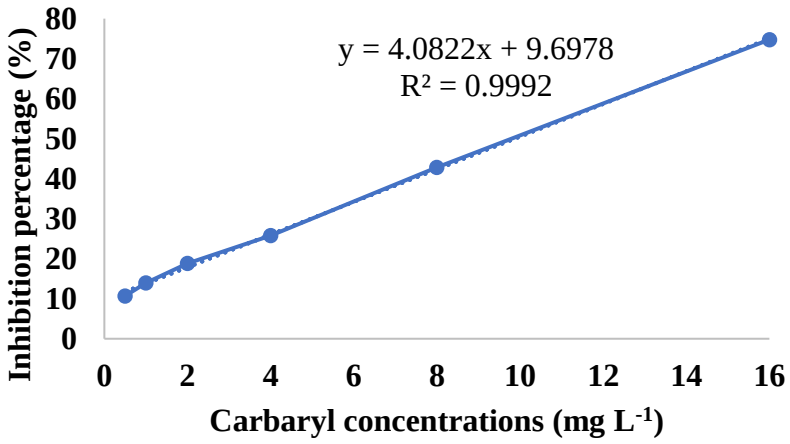

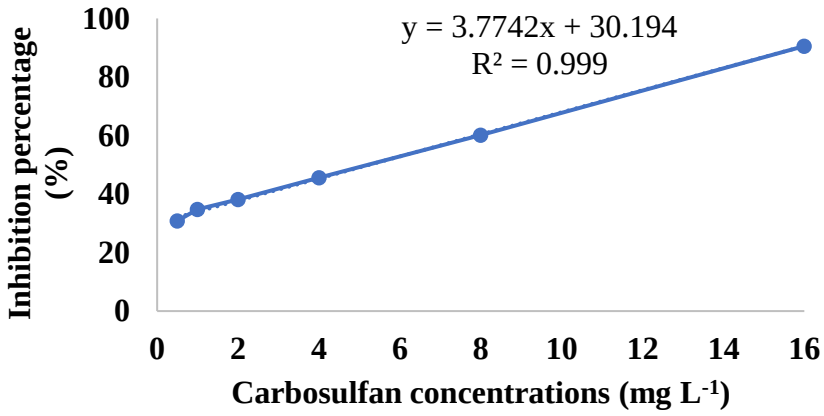

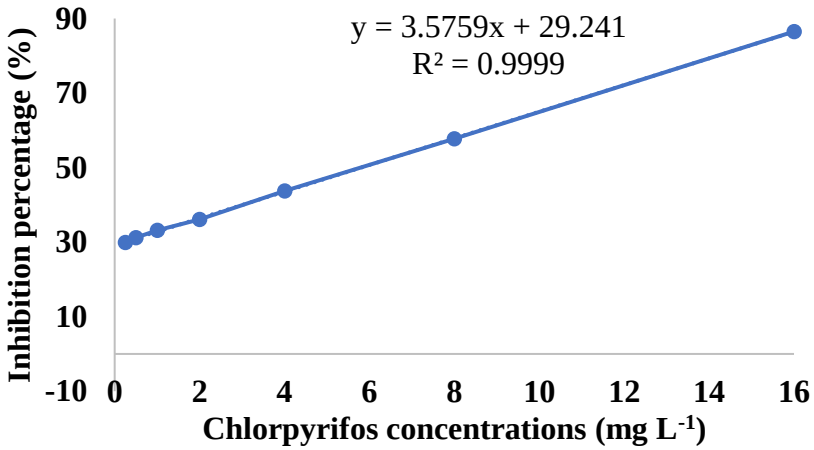

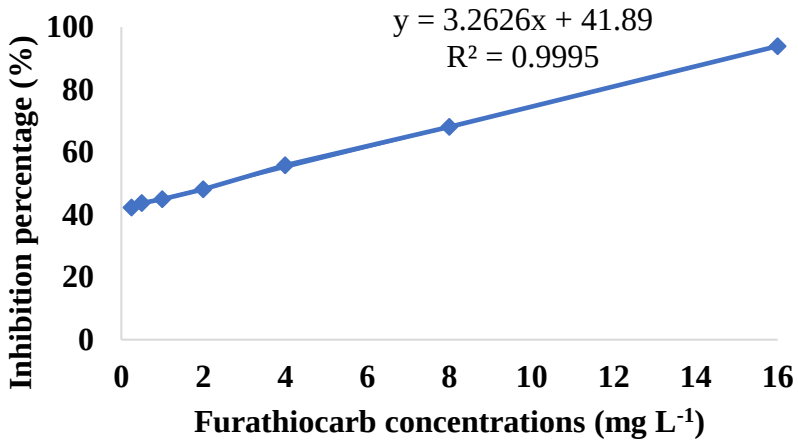
y = 3.2626x + 41.89
R² = 0.9995
Inhibition percentage (%)
100
80
60
40
20
0
0
2
4
6
8
10
12
14
16
Furathiocarb concentrations (mg L-1)

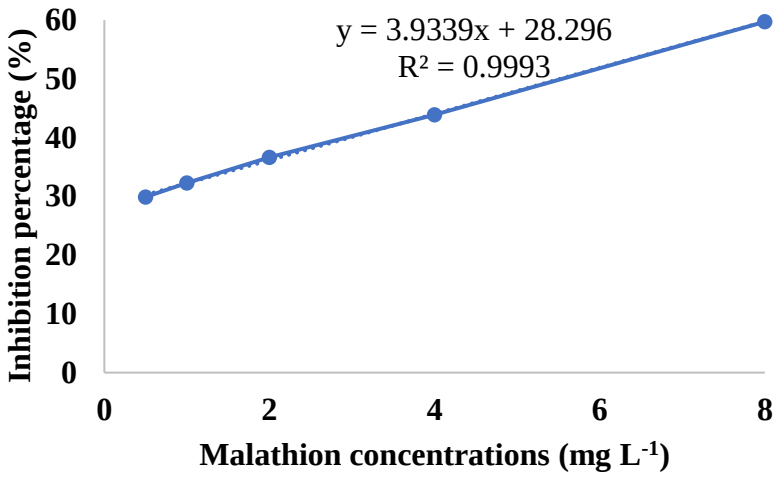
y = 3.9339x + 28.296
R² = 0.9993
Inhibition percentage (%)
60
50
40
30
20
10
0
0
2
4
6
8
Malathion concentrations (mg L-1)

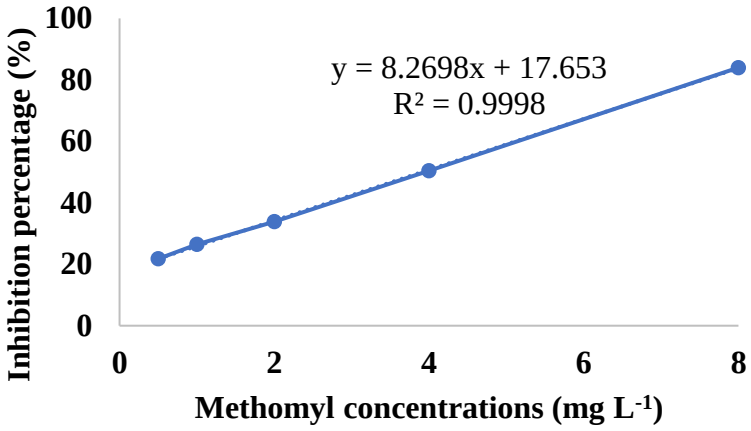
y = 8.2698x + 17.653
R² = 0.9998
Inhibition percentage (%)
100
80
60
40
20
0
0
2
4
6
8
Methomyl concentrations (mg L-1)

Annex 8. Calibration curve obtained by DLLME techniques

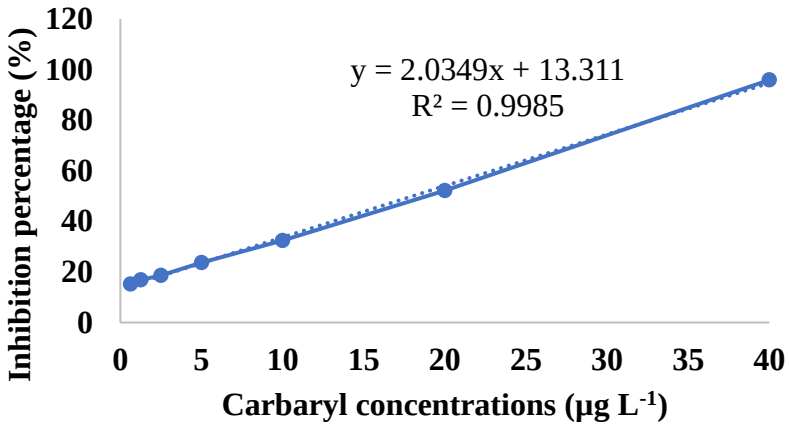

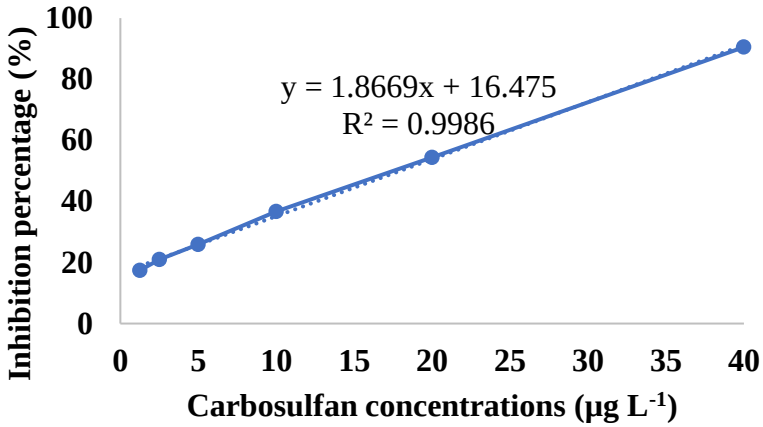

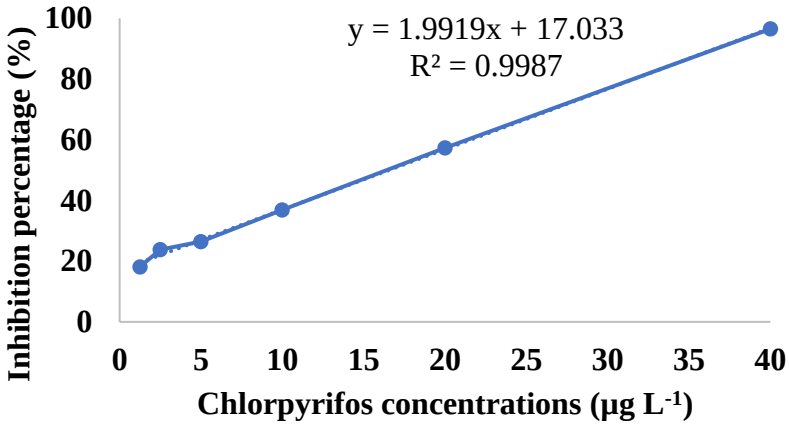

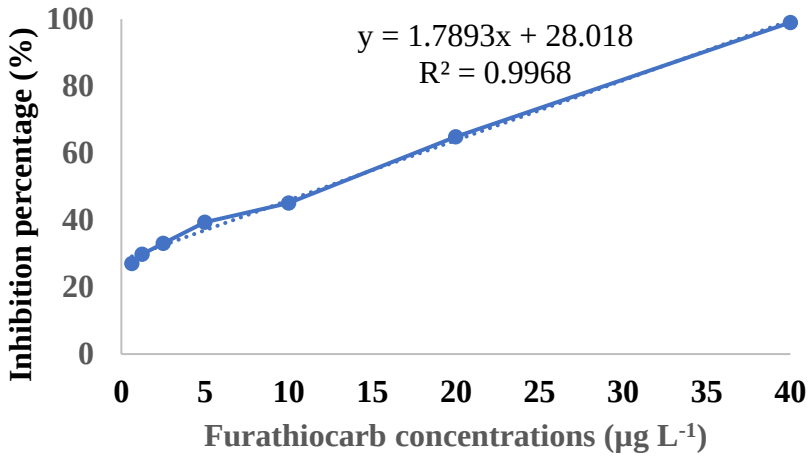
y = 1.7893x + 28.018
R² = 0.9968
Inhibition percentage (%)
100
80
60
40
20
0
0
5
10
15
20
25
30
35
40
Furathiocarb concentrations (µg L-1)

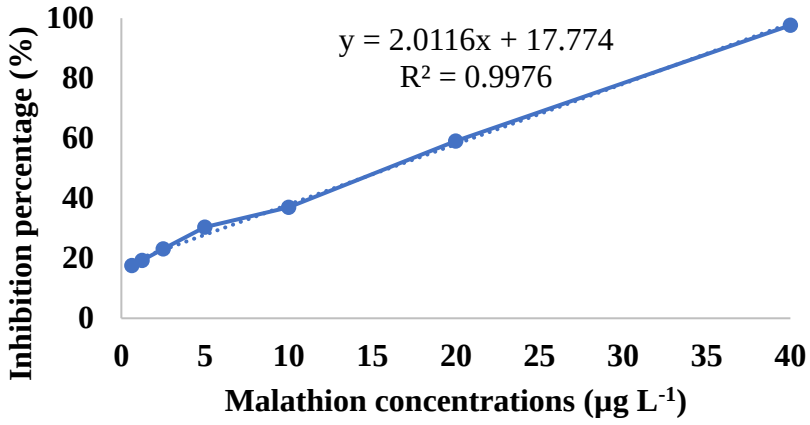
y = 2.0116x + 17.774
R² = 0.9976
Inhibition percentage (%)
100
80
60
40
20
0
0
5
10
15
20
25
30
35
40
Malathion concentrations (µg L-1)

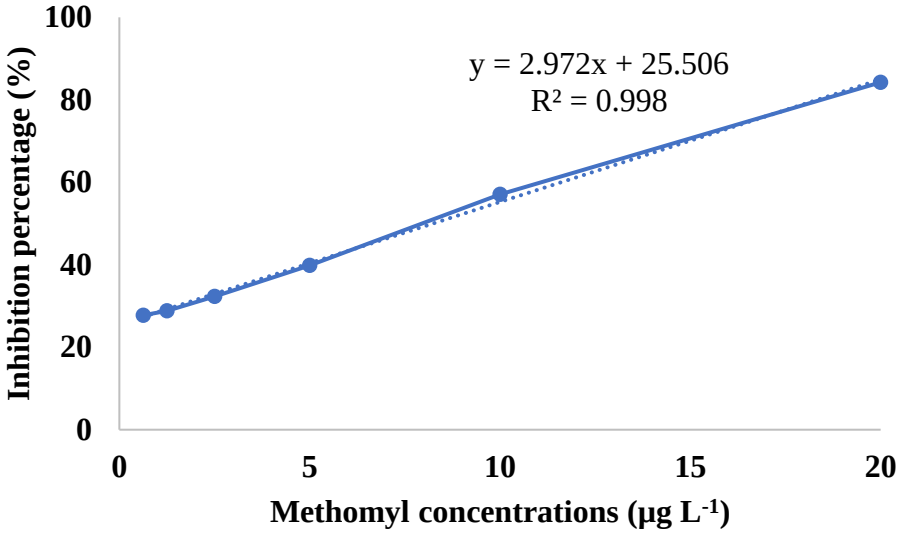
y = 2.972x + 25.506
R² = 0.998
Inhibition percentage (%)
100
80
60
40
20
0
0
5
10
15
20
Methomyl concentrations (µg L-1)

Annex 9. Calibration curve obtained by QuEChERS-DLLME techniques

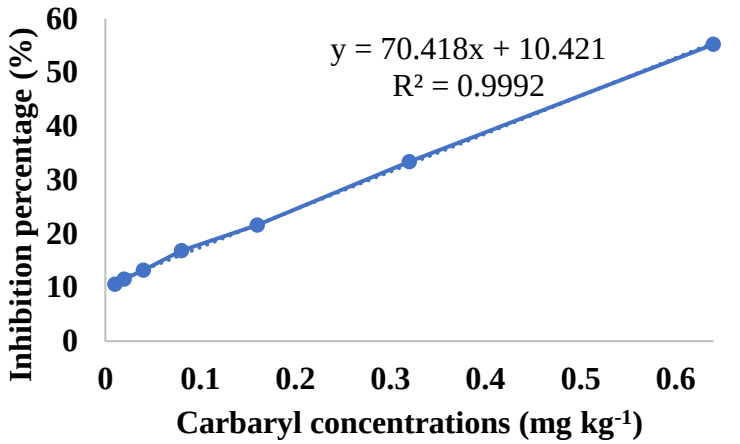

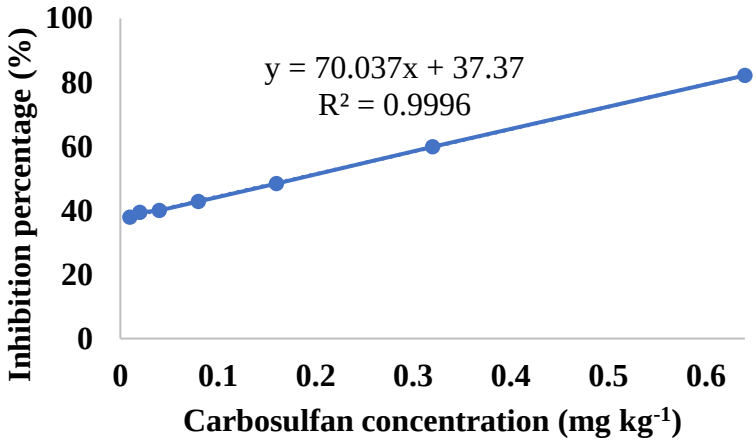

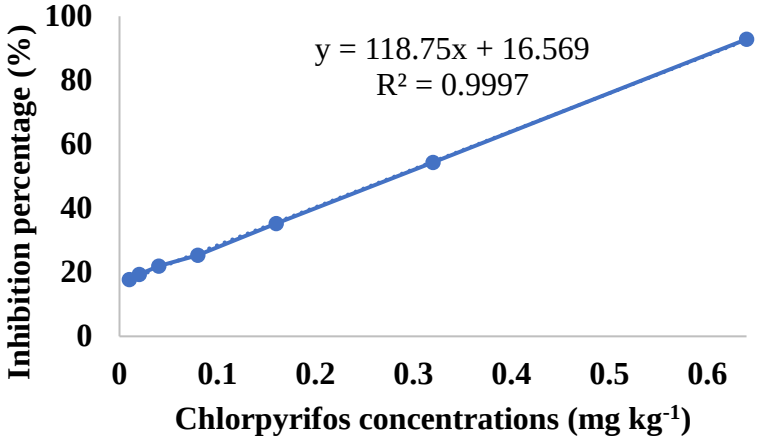

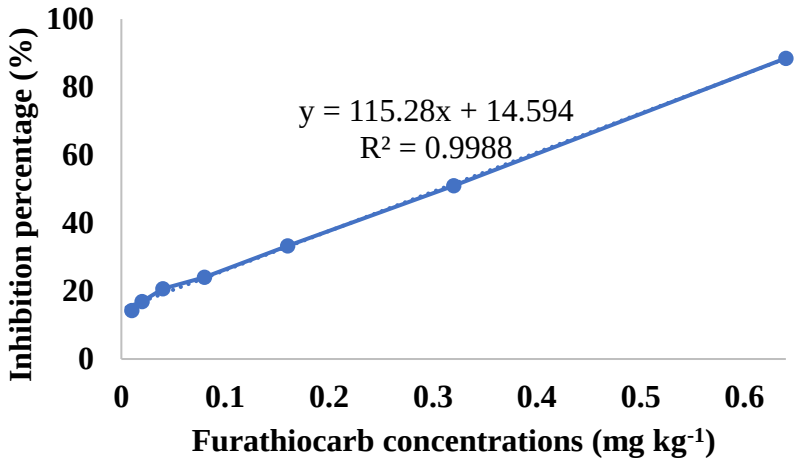
y = 115.28x + 14.594
R² = 0.9988
Inhibition percentage (%)
100
80
60
40
20
0
0
0.1
0.2
0.3
0.4
0.5
0.6
Furathiocarb concentrations (mg kg-1)

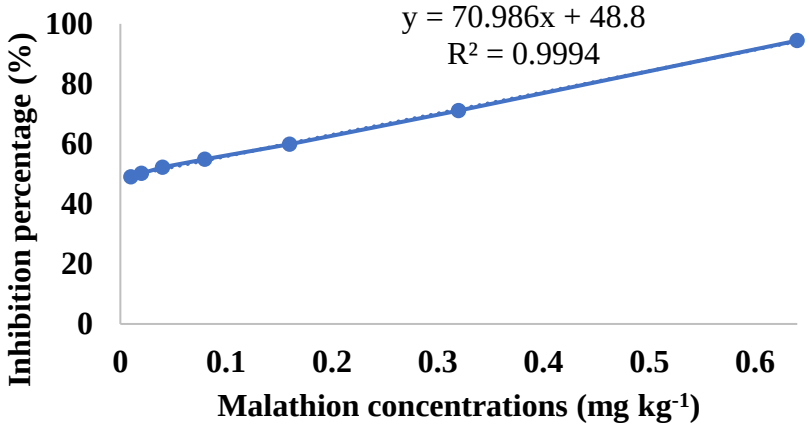
y = 70.986x + 48.8
R² = 0.9994
Inhibition percentage (%)
100
80
60
40
20
0
0
0.1
0.2
0.3
0.4
0.5
0.6
Malathion concentrations (mg kg-1)

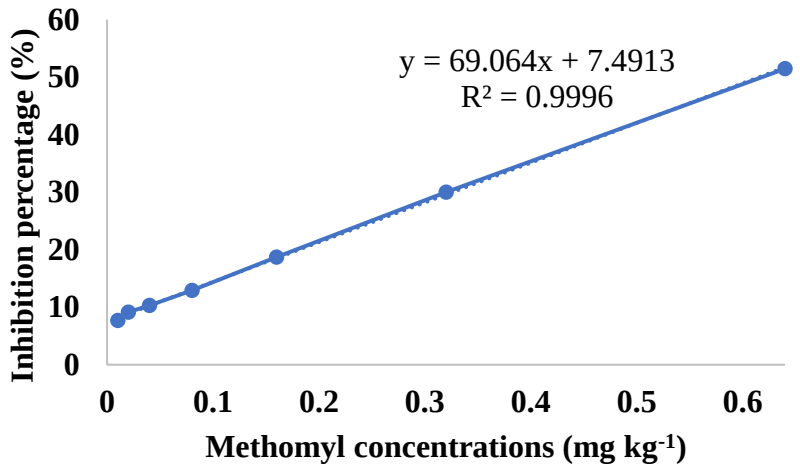
y = 69.064x + 7.4913
R² = 0.9996
Inhibition percentage (%)
60
50
40
30
20
10
0
0
0.1
0.2
0.3
0.4
0.5
0.6
Methomyl concentrations (mg kg-1)

Annex 10. List of publications

Beshana, S., Hussen, A., Leta, S. and Kaneta, T., 2022a. Dispersive liquid–liquid microextraction coupled with microfluidic paper-based analytical device for the determination of organophosphate and carbamate pesticides in the water sample. Analytical Sciences: 1-9.

Beshana, S., Hussen, A., Leta, S. and Kaneta, T., 2022b. Microfluidic Paper Based Analytical Devices for the Detection of Carbamate Pesticides. Bulletin of Environmental Contamination and Toxicology: 1-8.

Beshana, S., Hussen, A., Leta, S. and Kaneta, T., Multivariate optimization of operational parameters in microfluidic paper-based analytical devices for the determination of organophosphate and carbamate pesticides. **Accepted July 21, 2022 on Journal of Analytical Chemistry**.

Beshana, S., Hussen, A., Leta, S. and Kaneta, T., Development of QuEChERS-DLLME method for the determination of pesticide residues in lettuce vegetable by microfluidic paper-based analytical device. **Submitted to Chemical Papers**